NTNU

Norwegian University of
Science and Technology

Composite Hydrogels of Alginate and Cellulose Nanofibrils

A study of mechanical properties

Ina Sander Pedersen

Chemical Engineering and Biotechnology
Submission date: January 2018
Supervisor: Berit Løkensgard Strand, IBT
Co-supervisor: Olav Aarstad, IBT

Norwegian University of Science and Technology
Department of Biotechnology and Food Science

Preface

The work for this master thesis was carried out in the period between January 2015 and January 2018, at the Norwegian University of Science and Technology (NTNU) in the Department of Biotechnology and Food Science.

This thesis is a continuation of the preceding project on alginate-nanocellulose composites conducted during the autumn of 2014. All previous work done in 2014 are marked as faded columns in the results.

Part of this work has led to the publication of *Mechanical properties of composite hydrogels of alginate and cellulose nanofibrils* in *Polymers* [1]. The published paper is given in its entirety in Appendix E.

Acknowledgements

First, I wish to express my deepest gratitude to my supervisors, Berit Løkensgard Strand and Olav Andreas Aarstad, for their incredible patience, positivity and ability to give me motivation when I had none. I always walked out of our meetings with higher confidence in myself than when I entered.

PFI is recognized for the fibrillation and TEMPO-mediated oxidation of CNF that was used in this project, and for sharing their knowledge and experience in this field. The perky spirit of Ellinor Bævre Heggset was especially appreciated during the short time I spent at PFI.

Senior engineers Wenche Iren Strand and Ann-Sissel Teialeret Ulset are appreciated for their helpful nature, and for making the laboratory an enjoyable place to work. Student adviser Jo Esten Hafsmo is thanked for his guidance and administrative work, and Marianne Kjos at SINTEF Materials and Chemistry for an intriguing introduction to ICP-MS.

Lastly, but not least, I would like to express a warm thanks to my family. To my mother for all her support and believe in me, to my father for making me tough, and to Peter how has been incredible patient throughout this period. But most of all I am grateful to my son Jonathan, for his remarkable ability to remind me of what is important, and for giving me glimpses of sunshine and laughter in the darkest of days.

Abstract

The main focus of this thesis was to attain more information about how alginate - CNF composite hydrogels are affected by each of the two polysaccharides, in order to gain additional knowledge which could be used to manipulate these hydrogels to obtain qualities required for specific biomedical or biotechnological applications.

Firstly, light microscopy was used to examine composite gels of *M. pyrifera* alginate and CNF, both mechanically fibrillated and TEMPO-oxidized. Images of these hydrogels showed that the cellulose filbrils were homogeneously distributed, and no phase separation was observed for either of the two composites that were studied.

Secondly, compression tests were done on three separate composite series with calcium saturated hydrogels of 1% (w/v) alginate, extracted from *D. potatorum, M. pyrifera* and *L. hyperborea* stipe, and increasing amounts (0.00 - 0.75% w/v) of mechanically fibrillated and TEMPO-oxidized CNF. Both types of cellulose fibrils contributed to an increase in resistance against compression at low deformation (Young's modulus) and less gel shrinkage (syneresis) upon saturation, relative to pure Ca-alginates, for all three alginate composites. The largest effect was seen by TEMPO-oxidized CNF.

To examine the impact of polymer charge and increase in total dry matter on gel properties, series of hydrogels with 1% (w/v) *M. pyrifera* alginate and a control polysaccharide, dextran, xanthan, hyaluronic acid or additional alginate, were analysed and compared to the alginate - CNF composites. Young's modulus found for composite gels with TEMPO-oxidized CNF was significantly higher than for the control gels, confirming an effect of CNF beyond the fibril charge and increase in polymer weight alone. Further indication of interaction between alginate and CNF was established by the comparison of pure Ca-alginate gels, TEMPO-oxidized gels and composite gels, as Young's modulus of the composite gels was notably higher than the added values of the two pure gels.

Finally, a series of CNF – alginate composites with various polymer composition was treated with saline solution and tested with regard to volume stability and calcium content. Weight analysis showed that TEMPO-oxidized CNF contributed to more volume stable hydrogels. Inductively coupled plasma mass spectrometry (ICP-MS) was used to determine the calcium content of a selection of composite gels. No significant difference was found between composite gels and pure alginate gels, indicating a more complex explanation than an increase in calcium binding alone.

Sammendrag

Hovedfokuset for denne masteroppgaven var å undersøke hvordan alginate – CNF kompositttgeler påvirkes av hver av de to polysakkaridene. Kunnskap om hver komponents rolle i kompositttsystemet vil være nyttig for å skreddersy slike geler til biomedisinske eller bioteknologiske applikasjoner med krav om spesifikke kvaliteter eller egenskaper.

Lysmikroskopi ble brukt for å studere kompositttgeler av *M. pyrifera* alginate og CNF, både mekanisk fibrillert og TEMPO-oksidert. Mikroskopibildene viste en homogen fordeling av cellulosefibriler i kompositttgeler av begge typene CNF, og ingen faseseparasjon ble observert.

Videre ble kompressjonstester utført på tre separate kompositttserier med kalsiummettede hydrogeler av 1% (w/v) alginat, ekstrahert fra *D. potatorum, M. pyrifera* and *L. hyperborea* stilk, og økende konsentrasjoner (0.00 - 0.75% w/v) av mekanisk fibrillert og TEMPO-oksidert CNF. Begge typene cellulosefibriler bidro til en økning i kompressjonsmotstand ved lav deformasjon (Youngs modulus) og mindre reduksjon i gelvolum (synerese) ved metning, relativt til rene Ca-alginat geler, for alle de tre seriene av alginatkompositter. Størst effekt ble observer ved tilsats av TEMPO-oksidert CNF.

For å undersøk effekten av polymerladning og økning i total tørrstoffmengde på gelegenskapene, ble serier med hydrogeler med 1% (w/v) *M. pyrifera* og et kontrollpolysakkarid, dextran, xanthan, hyaluronsyre eller ekstra alginat, analysert og sammenlignet med alginate-CNF kompositttene. Youngs modulus som ble funnet for kompositttgeler med TEMPO-oksidert CNF var betydelig høyere enn for kontrollgelene, noe som bekreftet en effekten av CNF utover fibrilladning og økt polymervekt alene. Ytterligere indikasjon på interaksjoner mellom alginat og CNF ble funnet ved sammenligning av rene Ca-alginat geler, TEMPO-oksiderte CNF geler og kompositttgeler, hvorpå Youngs modulus for kompositttene var markant høyere enn den sammenlagte verdien av de to rene gelene.

Til sist ble en serie med CNF-alginat kompositter, med varierende polymersammensetning, behandlet med NaCl - løsning og testet med tanke på volumstabilitet og kalsiuminnhold. Vektanalysen viste at TEMPO-oksidert CNF bidro til mer volumstabile hydrogeler. ICP-MS ble brukt til å bestemme kalsiuminnholdet til en utvalgt gruppe kompositttgeler. Ingen signifikant forskjell i kalsiumkonsentrasjon ble funnet mellom kompositttgeler og rene alginat geler, noe som peker mot en mer komplisert forklaring enn en økning i kalsiumbindinger alene.

List of abbreviations and symbols

C*	Critical overlap concentration
CNF	Cellulose nanofibrils
DP_n	Average chain length
ϵ	Deformation
E	Young's modulus
EDTA	Ethylenediaminetetraacetic acid
F	Force of compression
FTIR	Fourier transform infrared spectroscopy
G	α-L-guluronic acid
GDL	Glucono δ-lactone
ICP-MS	Inductively coupled plasma mass spectrometry
ITC	Isothermal titration calorimetry
M	β-D-mannuronic acid
M_n	Number average molecular mass
M_w	Weight average molecular mass
$[\eta]$	Intrinsic viscosity
$N_{G>1}$	Average G-block length > 1
$N_{M>1}$	Average M-block length > 1
NMR	Nuclear magnetic resonance spectroscopy
PI	Polydispersity index
SEC-MALS	Size exclusion chromatography with multi-angle light scattering
SEM	Scanning electron microscopy
TEMPO	2,2,6,6-tetramethylpiperidine-1-oxyl
ν	Einstein-Simha viscosity factor

Table of contents

1 Introduction

1.1 Background and aims

In the range of potential biomaterials that can be used to mimic characteristics, such as chemical, electrical and physical factors, of biological tissues, hydrogels are considered very good candidates [2]. Hydrogels are able to retain high amounts of water relative to their dry weight, due to the three-dimensional network achieved upon gelation, and can be casted in to various shapes and sizes [3]. New possibilities in development of advanced biomaterials follow the potential to produce composite hydrogels with tailored functionality for specific biomedical and biotechnological applications [4, 5].

The biocompatibility, renewability, availability and low toxicity of alginates and cellulose nanofibrils (CNF) makes these polysaccharides ideal for biomedical applications, such as tissue engineering. With regard to bioprinting, the combination of alginates beneficial gelling abilities at physiological conditions and the shear thinning properties of CNF make these composites especially appealing [6]. Although the focus on composites of these two materials has increased, mechanical properties of composite hydrogels with various combinations of alginate and CNF has not previously been methodically studied.

In the project preceding this master thesis, composite gels of alginate and nanocellulose were successfully produced and studied with regard to gel properties. In addition, the microstructures of the hydrogels were analysed with the use of scanning electron microscopy (SEM).

As a continuation, the main focus of this thesis was to attain a more detailed knowledge and understanding of the separate role of each of the two components in alginate - CNF composite gels. Information which could be used to manipulate these hydrogels to obtain qualities required for specific applications.

The specific aims were to:

- Further investigate the effect of CNF, both mechanically fibrillated and TEMPO-oxidized, on physical properties of hydrogels with alginate from *Durvillea potatorum*, *Macrocystis pyrifera* and *Laminaria hyperborea* stipe, in terms of resistance against compression at low deformation (Young's modulus), reduction in gel volume upon calcium saturation (syneresis), rupture strength and compressibility (deformation at rupture)

- Compare alginate - CNF composites to control hydrogels, consisting of alginate and other relevant polysaccharides, to attain information on how increased charge and dry matter content impact the gel properties

- Examine the properties of composite gels upon saline exposure, with regard to volume stability and calcium exchange

1.2 Alginates

Alginates are naturally occurring polysaccharides which are mainly found as structural components in marine brown algae (*Phaeophyceae*). The dry plant weight can consist of up to 40% alginate and it is considered to be the main skeletal material in these plants [7]. Alginates are also found in some bacteria where they serve different extracellular purposes [8, 9]. Variability in structure of the different alginates leads to a wide field of application for these polysaccharides, such as wound dressing, bioencapsulation and immobilization of cells, food production, textile printing, paper and water treatments [8, 10]. The ability to retain water and the stabilizing, viscosifying and gelling properties of alginates are the main qualities that account for the wide industrial application of these polysaccharides [11].

1.2.1 Chemical structure and sequence determination

Alginates are linear polysaccharides consisting of the two monomers, β-D-mannuronic acid (M) and α-L-guluronic acid (G), linked together with (1→4) glycosidic linkages as shown in Figure 1.1.

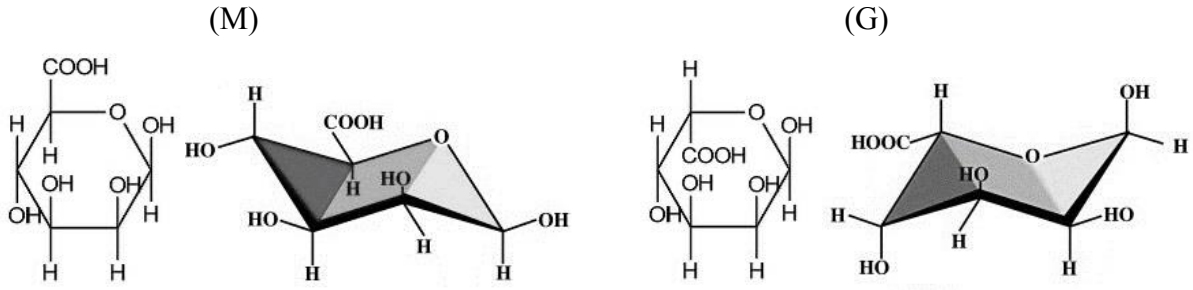

Figure 1.1 Haworth formula and chair conformation of the monomers in alginate, β-D-mannuronic acid (M) and α-L-guluronic acid (G) [12, 13].

The α-L-guluronic acid monomers occurs in $^{1}C_{4}$ conformation and the β-D-mannuronic acid monomers in $^{4}C_{1}$ conformation [14-16]. The distribution of monomers throughout an alginate chain is generally described by three different types of blocks (Figure 1.2), the homopolymeric M- and G-blocks and the alternating MG-blocks. Dependent on the production organism of the alginate, the sequence and composition of the monomers differ widely [8].

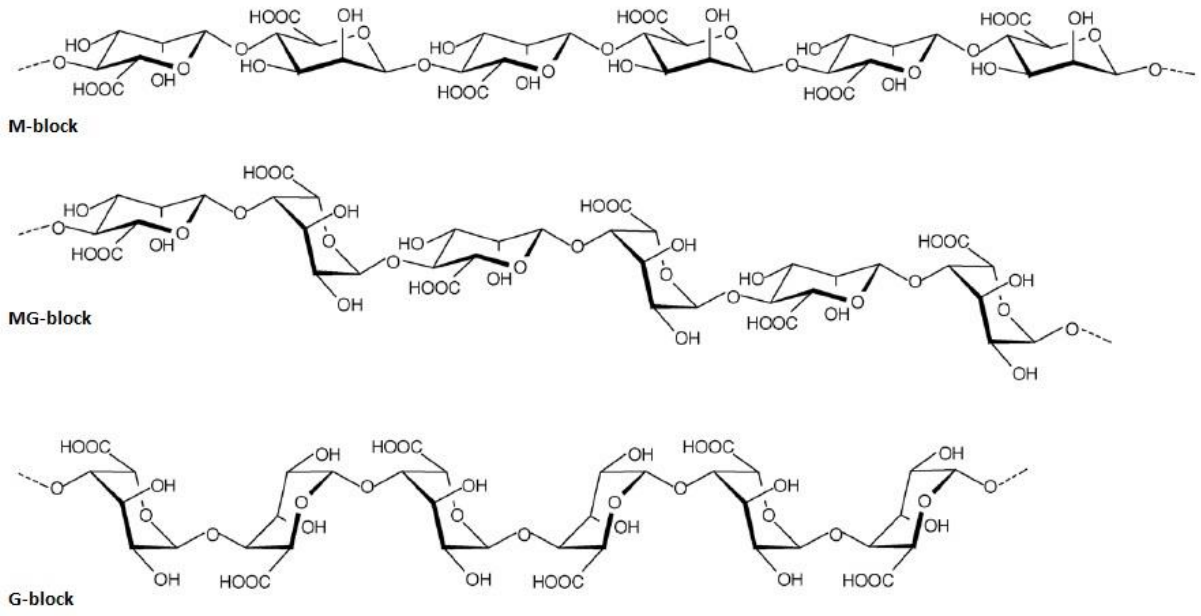

Figure 1.2 An illustration of the different block structures in alginate. The M-block (top) and G-block (bottom) consisting solely of β-D-mannuronic and α-L-guluronic acid respectively, and the alternating MG-block (middle) [17].

Nuclear magnetic resonance (NMR) spectroscopy is typically used to obtain statistics about alginate composition by identifying fractions of monomers (F_G, F_M), diads (F_{GG}, F_{GM}, F_{MG}, F_{MM}) and triads (F_{GGG}, F_{GGM}, F_{GMG}, F_{MGG}, F_{MGM}, F_{GMM}, F_{MMG}, F_{MMM}) [18, 19]. In turn, these fractions are used to calculate different parameters which provide information about the polysaccharide of interest, such as average length of G- and M-blocks ($N_{G>1}$ and $N_{M>1}$) [10, 20]. However, it follows from the heterogeneous feature of alginates that functional properties given by these average based sequence frequencies only provide partial information about the given alginate sample. Although the actual distribution and block lengths influence alginate characteristics, the average block lengths that can be calculated from equation (1.1) and (1.2) are frequently used and give an adequate estimate of structure-functional properties [18].

$$\bar{N}_{G>1} = \frac{F_G - F_{MGM}}{F_{GGM}} \tag{1.1}$$

$$\bar{N}_{M>1} = \frac{F_M - F_{GMG}}{F_{MMG}} \tag{1.2}$$

To obtain information about the average molecular weight and distribution of an alginate of interest, size exclusion chromatography with multi-angle light scattering (SEC-MALS) is often used. This technique separates dissolved molecules based on their size, and further characterize them by detection of intensity and angle of light scattered by the molecules [8]. Alginates are polydispers due to the fact that the polysaccharide is synthesized by enzymes and partially depolymerized in the extraction process, resulting in the molecular mass heterogeneity. For this reason the molecular mass of an alginate is given as an average of the

molecular mass of the total distribution [11, 18]. The number average (M_n) and weight average (M_w) are most commonly used. With n_i representing the number of molecules with a specific molecular weight M_i, the molecular averages are defined as:

$$\bar{M}_n = \frac{\sum_i n_i M_i}{\sum_i n_i} \quad \textbf{(1.3)}$$

$$\bar{M}_w = \frac{\sum_i n_i M_i^2}{\sum_i n_i M_i} \quad \textbf{(1.4)}$$

Information on molecular mass heterogeneity, called the polydispersity index (PI), can be useful for different applications of alginates, as distribution of molecular mass may influence desired properties. While a monodisperse sample will have PI = 1 and randomly degraded polymers have a PI = 2, higher values indicating a wider distribution are achieved by mixing different alginates [21]. The polydispersity index is defined by the ratio of number- and weight-average molecular mass:

$$PI = \frac{\bar{M}_w}{\bar{M}_n} \quad \textbf{(1.5)}$$

Degree of polymerization, which give the average number of monomer units per chain, can be calculated from equation (1.6), M_0 representing the molecular mass of each monomer [8].

$$\overline{DP}_n = \frac{\bar{M}_n}{M_o} \quad \textbf{(1.6)}$$

Structure and stiffness of chain blocks in alginate are influenced by the monomeric linkages. While the M-blocks are straight due to the presence of diequatorial bonds, the diaxial linkages in G-blocks lead to a shorter and more crooked chain. Alternating between equatorial and axial bonds, MG-blocks have previously been reported to be more flexibility than both M- and G-blocks, with an order of chain block stiffness of: MG<MM<GG [14]. However, a more recent study does not find a significant difference in stiffness expressed as persistence length between MG/MG [22].

The arrangement of monomers further affect the length between charges in each block segment, and thereby influence the polyelectrolytic properties as the linear charge density depends on chain block composition. However, the significant difference between chain blocks with respect to selectivity of divalent ion binding is not explained by electrostatic properties alone [23, 24].

1.2.2 Gel formation

In order to achieve continuous contact between polymer chains in a solution, and thereby making it possible for the chains to interact and entangle, the polymer concentration must exceed a critical overlap concentration (C*). Gel formation may occur, with strong physical or chemical interaction between the molecules, above this concentration as the polymer chains link together and form a continuous network. The gel, which contain large amounts of solvent molecules, are able to behave as a solid substance due to its ability to store energy in the network when force is applied [8]. The critical overlap concentration can be calculated from equation (1.7), where ν and [η] represent the Einstein-Simha viscosity factor and the intrinsic viscosity of the polymer, respectively.

$$C^* = \frac{\nu}{[\eta]} \qquad \textbf{(1.7)}$$

Alginates are known for their ability to form gels, the gel strength however vary with the composition of the alginate. The sequence of monomers, block distribution and molecular size of the alginate all influence the strength of the resulting gel. Alginates with a high content of L-guluronic acid and long average G-blocks form mechanically strong gels with low syneresis [25]. These gels junction zones are formed when ions are introduced to the alginate and arrange themselves in the cavities formed by the zig-zag structured G-block chains [26]. The cavities function as binding sites for divalent ions, giving an ion-alginate structure much like an egg-box, as illustrated in Figure 1.3.

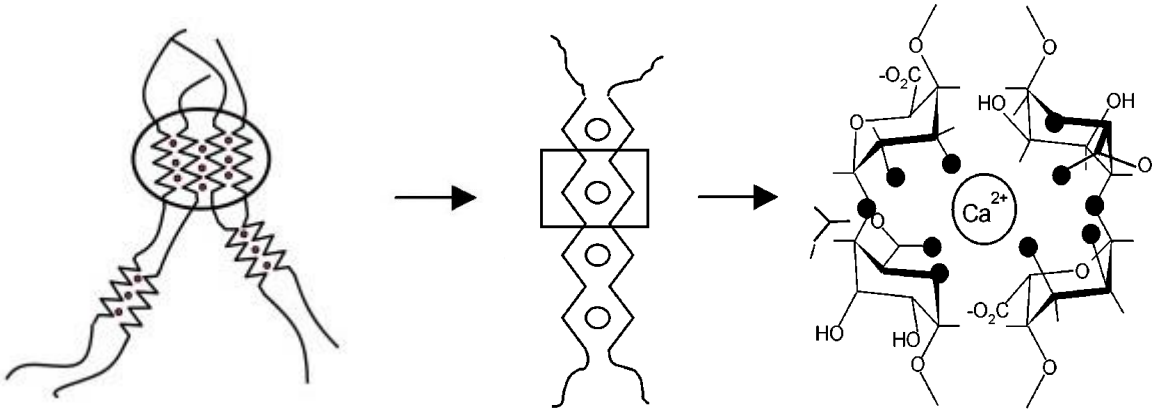

Figure 1.3 An illustration of the formation of junction zones by divalent ions and G-blocks (left), the egg-box model showed for two G-block chains in a calcium-alginate junction zone (middle) and a cavity in the G-block chain with the oxygen atoms involved in the coordination of a calcium ion marked as black circles (right) [27, 28].

In addition to the widely used egg-box model of GG/GG junction, analysis of MG-enriched alginates and strictly alternating alginates have revealed that long MG-blocks serve a contributing role in Ca-alginate gel formation. Alternating sequences are believed to participate in the gelation process by the formation of both MG/MG junctions and mixed GG/MG junctions, and the presence of long MG-blocks has been shown to increase both rupture strength, shrinkage and elasticity [29, 30]. Contrary to the rigid and stable characteristics of gels with long G-blocks and fixed GG/GG junctions, long MG-blocks lead to more flexible gel networks due to a possible "zipping" mechanism of sliding MG/MG junctions when the gel is exposed to stress [18]. The three different junction zones that take part in gel formation of Ca-alginate are illustrated in Figure 1.4.

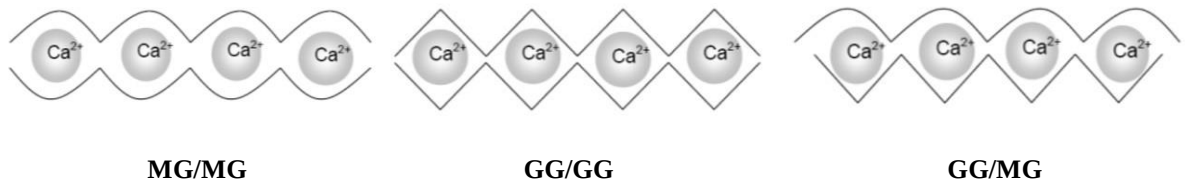

Figure 1.4 The three different Ca^{2+}- junction zones found in alginate. MG/MG junctions consisting of alternating alginate chains (left), GG/GG junctions of chains with long G-blocks (middle) and the mixed GG/MG junctions made up of chains with long G-blocks and alternating alginate chains (right) [29].

Other parameters that influence the mechanical properties of alginate gels are alginate concentration, the type and concentration of gelling ions, the gelling and non-gelling ion ratio and the presence of complexing agents [31, 32]. With the use of internal gelation, a calcium source, e.g. $CaCO_3$, within the alginate solution give a controlled release of Ca^{2+} ions when the pH is lowered by an organic acid, or lactone, and thereby freeing the gelling ions (**Figure 1.5**). Through the limited solubility of the calcium salt source and change in pH the release of gelling ions is usually maintained [32].

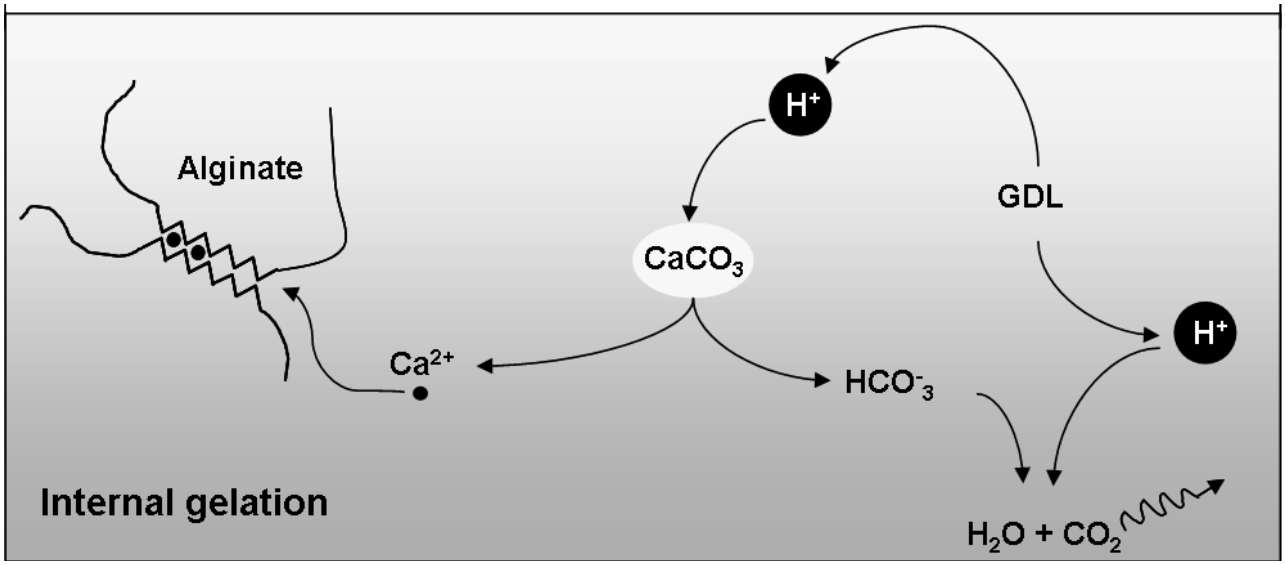

Figure 1.5 Internal gelation of alginate by formation of Ca-alginate junction zones. The addition of glucono-δ-lactone (GDL) to an alginate solution containing an inactive calcium source, in this case $CaCO_3$, cause a reduction in pH which lead to a release of Ca^{2+} ions from $CaCO_3$. The gelation process begins as the released calcium ions form junction zones with the alginate chains [32].

External gelation is a different method, where the alginate solution is dripped into a $CaCl_2$ solution and the calcium ions instantly reacts with the alginate at the surface of the droplet [33]. This results in gel beads and is also called the diffusion method, because the gel is produced as the ions diffuse towards the centre of the droplet. This type of gelation give more inhomogeneous gels with a higher alginate concentration at the droplet surface and is a popular immobilization technique due to its rapid gelling kinetics [32]. Although there are several cations, such as Sr^{2+} and Ba^{2+}, which have a higher affinity towards alginate and give more rigid gels, calcium is widely used due to its non-toxic properties and ability to form stable gels [34].

1.3 Cellulose nanofibrils

Cellulosic materials which have one or more dimensions in the nanometer range are classified as nanocellulose [35]. There are a number of synonyms for nanocellulose, including microfibrillated cellulose (MFC), nanofribrillated cellulose (NFC), cellulose microfibrils (CMF) and cellulose nanofibrils (CNF), which are used interchangeably in the litterature. Cellulose nanofibrils are produsedfrom the linear polymer cellulose, which is the main component of all plant fibers and thereby the most abundant organic polymer in nature (Figure 1.7). The cellulose molecules are build up by repeating units of (1 → 4) linked β-D-glucose monomers (Figure 1.6) and are, in the case of CNF production, usually retreived from wood, sugar beets, potato tuber, hemp and flax [36]. The nanofibrils has an average diameter of 5-60 nm, a length of several micrometers [37] and the size of the fibrils are dependent on pretreatment, plant source and production method [38, 39].

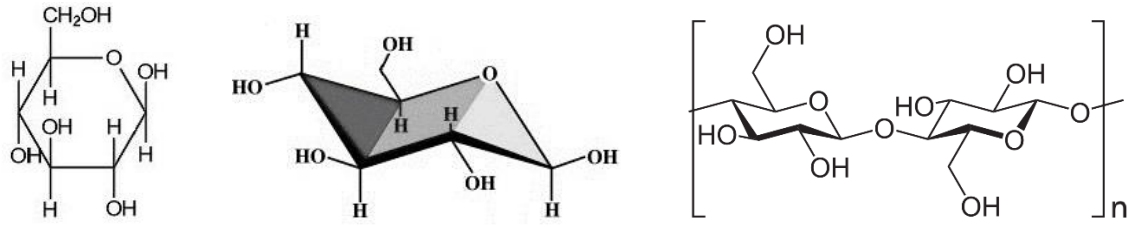

(A) (B) (C)

Figure 1.6 Haworth formula (A) and chair conformation (B) of the monomer in cellulose, β-D-glucose. Structure of the repeating unit of cellulose, (1→4) linked β-D-glucose monomers (C) [36, 38, 40].

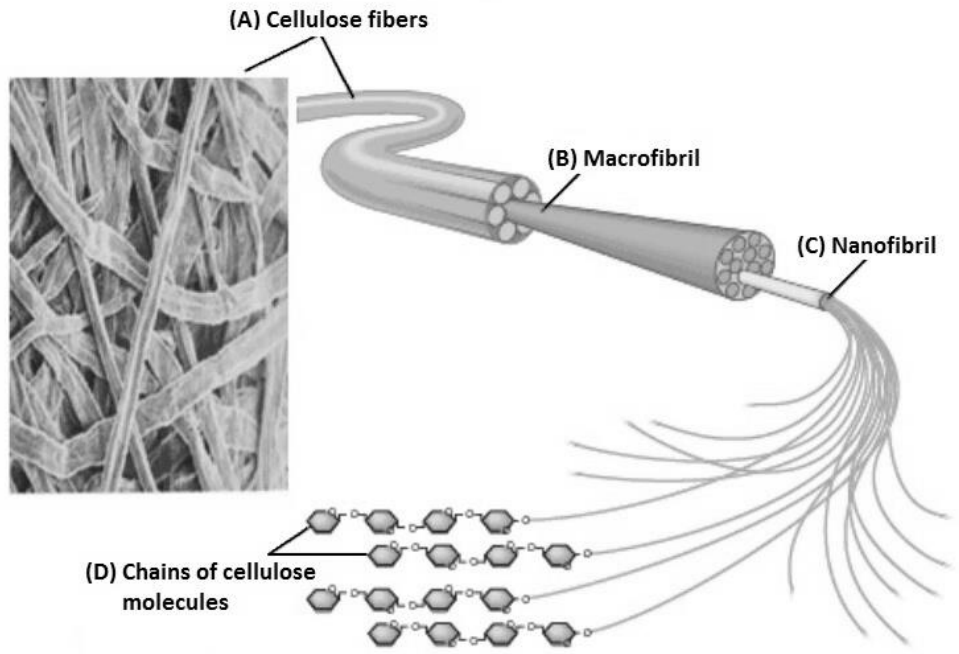

Figure 1.7 Cellulose fibers (A) consist of macrofibrils (B) and nanofibrils (C), which are made up of bundles of cellulose chains (D) with repeating units of (1 → 4) linked β-D-glucose monomers.

1.3.1 Mechanical fibrillation

Homogenization, together with microfluidization and grinding, are the most commonly used methods in production of CNF by mechanical treatment [41]. High pressure homogenization (HPH) was first applied to extract nanofibrils from wood pulp in 1983 by Herrick et al. and Turbak et al. This treatment is considered an efficient method for CNF production, based on its smiplicity, high efficiency and the advantage of no require of organic solvents. The fibrillation of cellulose fibers is achieved by pumping cellulose slurry though a small nozzle at high pressure, and thereby expose the material stream to extreme velocity change. These factors, together with chrusing forces from particle collision, shear forces on the fluid and forces due to changes in velocity in the material stream, cause the cellulose fibers to be fibrillated to nanoscale fibrils [35, 38, 42]. The biggest drawbacks with this method are the amount of energy needed to run the homogenization process, and reoccuring problems with clogging [35, 43]. However, various pretreatment methods can be used to ease the flow through the homogenizer and reduce the use of energy.

1.3.2 TEMPO-mediated oxidation

There is an increasing interest in TEMPO-mediated oxidation as a pretreatment method prior to mechanical processing of cellulose to produce CNF. 2,2,6,6-tetramethylpiperidine-1-oxyl (TEMPO) is a water soluble stable nitroxyl radical that has the ability, in a TEMPO-NaBr-NaClO or TEMPO-NaClO-$NaClO_2$ system, to convert C6 primary hydroxyl groups in cellulose to C6 carboxyl groups [44-46]. Oxidation of cellulose by the two different systems, showed in Figure 1.8, results in a negativly charged fibril surface due to the carboxyl groups. After oxidation the product undergoes gentle mechanical treatment to separate the fibrils, and as a result of the pretreatment it is possible to get fibrils with uniform diameter down to 3-4 nm. This process has an enegy demand about 100-200 times less than the pure mechanical treatment method [45]. The product of this type of oxidation, (1→4)-β-D-polyglucuronate, has the advantage of being easily biodegradable and metabolized by microorganisms in soil [47-50], and might be a good alternative to replace some fossil resources in the future.

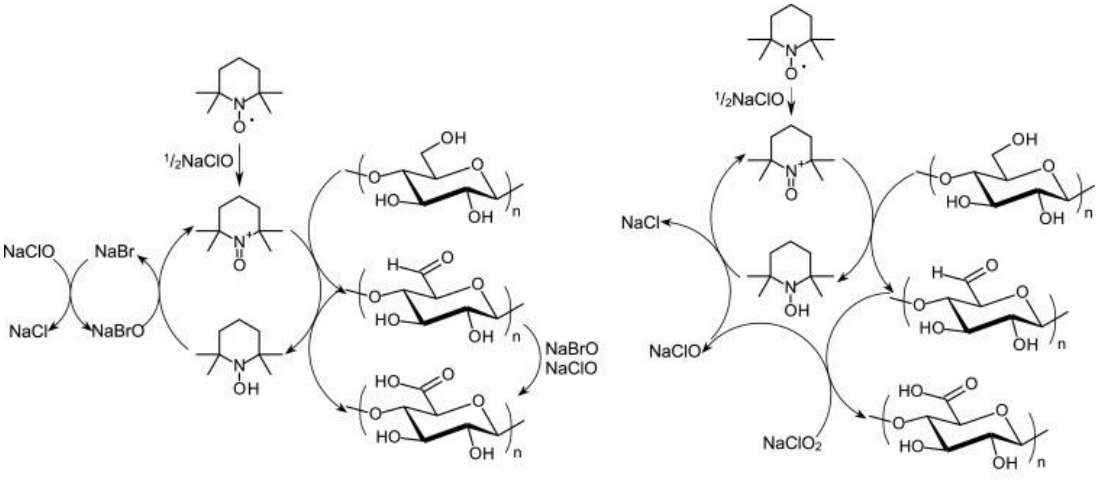

(A) **(B)**

Figure 1.8 The oxidation process of cellulose by a TEMPO-NaBr-NaClO system (A) and a TEMPO-NaClO-$NaClO_2$ system (B). The illustrations show the conversion of a hydroxyl group, on the β-D-glucose monomer of a cellulose chain, to aldehyd and further to a carboxzyl group with TEMPO as a catalyst [51].

1.3.3 Nanocellulose hydrogels

Hydrogels of cellulose nanofibrils can be produced in several ways. The most basic method is by addition of metal cations to carboxylated cellulose nanofibrils. Gelation of CNFs rapidly occur with addition of divalent cations, Ca^{2+}, Zn^{2+} or Cu^{2+}, and trivalent cations, Al^{3+} or Fe^{3+} [52, 53]. The different cations give similar gel formation, however trivalent cations have stronger binding energy and give hydrogels with markedly higher syneresis [53]. The shielding of repulsive charges on cellulose fibrils, by metal-carboxylate bonding, have been proposed as a driving force towards gel formation. As shown in Figure 1.9, this involves interactions between separate fibrils, as well as interchain interactions on the same fibril [53].

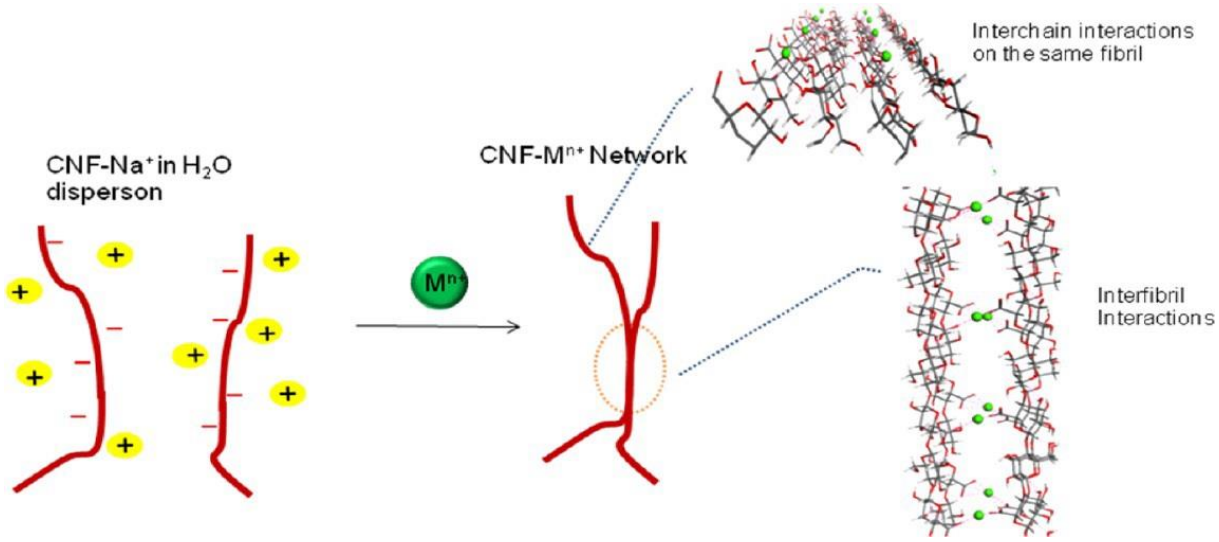

Figure 1.9 The proposed driving force towards gel formation of CNF in the presence of divalent or trivalent metal cations. Interchain interactions and interfibril interactions, crosslinking with metal cations between adjacent cellulose chains on the surface of the same fibril (top right), and between cellulose chains on separate fibrils (bottom right), respectively [53].

More complex methods of gelation include covalent crosslinking. Through reductive amination covalent crosslinking of TEMPO-oxidized CNF with diamines have been used to produce more stable hydrogels [54]. By controlling the conditions of TEMPO-mediated oxidation of CNF it is possible to attain fibrils with aldehyde groups on the surface, which are far more reactive than carboxyl groups with respect to covalent bonding. The aldehyde groups are then able to form Schiff-bases with a primary amine and can further be stabilized by reduction to a secondary amine [55], thus forming covalently linked gels.

1.4 Other polysaccharides

1.4.1 Dextran

Dextrans are polysaccharides that are synthesized from sucrose by some lactic acid bacteria, including certain strains of *Streptococcus* and *Leuconostoc mesenteroides*. These bacteria split sucrose molecules into glucose and fructose, and use the glucose molecules for production of dextran, while the fructose molecules are used in the metabolism of the bacteria itself [8]. The structures of dextrans are built as a primary core, where glucose molecules are linked together with α(1→6) glycosidic linkages to form a linear polymer, and branches of different sizes are attached by α(1→3) glycosidic linkages [56], Figure 1.10. Dextrans varies widely in composition and size, and the positioning and frequency of the branches are dependent on both the environment in which the bacteria grow and the type of producing bacteria. In medical treatments dextrans are used to a great extent as anticoagulants and as substitute for blood plasma, in addition they also have a high diversity of industrial applications.

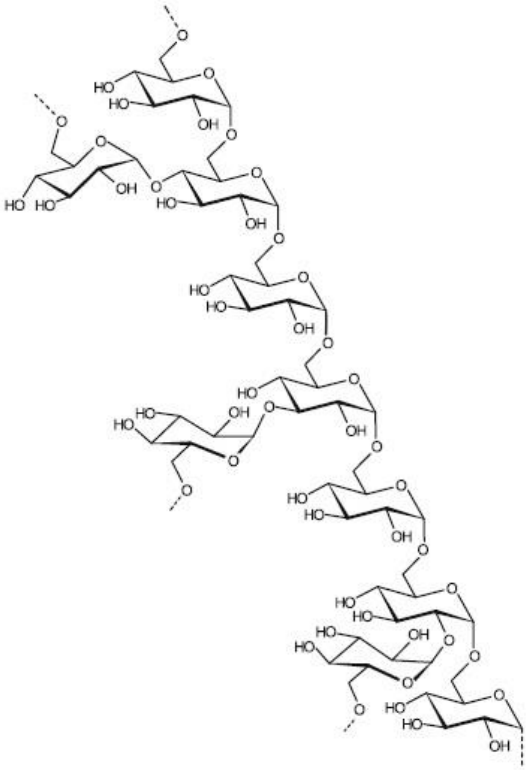

Figure 1.10 An example of a dextran chain with α(1→6) glycosidic linkages in the main chain and points of branching in 2-, 3- and 4-position [57].

1.4.2 Xanthan

The bacterium *Xanthomonas campestris* can produce and secrete xanthan by fermentation of a range of simple sugars. The xanthan function as a protective layer as it surround the cells, shielding them from various environmental stress, and give the bacterium an adhesive effect [58]. The backbone of the polysaccharide is equal to the structure of cellulose, consisting of β-D-glucose units joined together by (1→4) linkages, Figure 1.11. Approximately every other unit of the main chain has a trisaccharide side-chain containing an acetylated α-mannose unit, β-D-glucuronic acid and a pyruvated β-mannose [58-60]. A gel-like network is produced from the formation of junction zones as helical structures of the polymer chains contribute to rigidity. When physical stress is applied these junction zones are quickly disrupted, making the gel instantly fluent. This shear thinning effect is characteristic for xanthan, and as the stress is removed the junction zones are rapidly re-formed, resulting in an immediate gel formation [8, 58, 61]. The presence of ions will markedly affect the conformational change of the helical structures, due to the charged side-chains of the molecule, resulting in a sensitivity to salt [61].

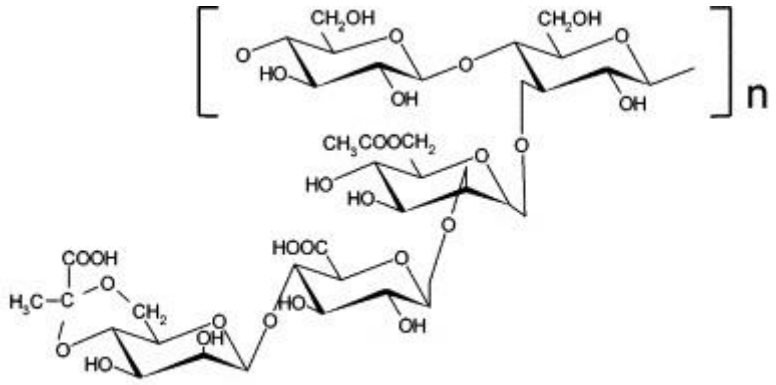

Figure 1.11 Structure of xanthan, β-D-glucose backbone with a side-chain of acetylated α-mannose, β-D-glucuronic acid and a pyruvated β-mannose [62].

Xanthan is used in a wide range of areas, including cosmetics, herbicides, laundry chemicals, textile dyes, agrichemical sprays and food additive. As a food additive xanthan is highly versatile, as its application areas include both stabilization, syneresis inhibition, binding, emulsifying and thickening. The polysaccharide is also used in large quantities by the oil industry for viscosity control of drilling muds due to its pseudoplastic characteristic [8, 61].

1.4.3 Hyaluronic acid

Hyaluronic acid is a polymer of repeating disaccharide units of β-D-N-acetylglucosamin and β-D-glucuronic acid in long chains, with (1→3) and (1→4) glucosidic linkages respectively, as seen in Figure 1.12.

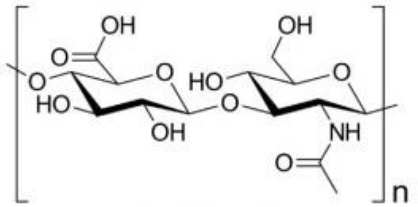

(A) **(B)**

Figure 1.12 Structure of the repeating disaccharide unit of hyaluronic acid, (1→4) linked β-D-glucuronic acid (A) and (1→3) linked β-D-N-acetylglucosamin (B) [63].

Both joint and eye fluid contain the sodium salt of hyaluronic acid, sodium hyaluronate, which act as a lubricant in solution. It is also found in various connective tissue of humans, where it is involved in regulation of cell activity and cell division [8, 64]. The two main methods of industrial production of hyaluronate are bacterial fermentation and extraction from rooster combs [65]. The polymer is widely used in the cosmetic industry, based on the fact that hyaluronate is a natural moisturizer and one of the most shear thinning substances in nature. The polymer is highly suitable for clinical applications, such as joint fluid supplementation and regeneration of surgical wounds, due to its unique properties within viscoelasticity, biocompatibility and non-immunogenicity [66].

1.5 Analytical methods

1.5.1 Physical properties

The mechanical properties of materials can be determined with a variety of methods which may give different results, and it is consequently important to be consistent when choosing characterisation methods and critical when comparing results given by different methods [67]. Young's modulus (E) is often used to define gel strength, as it gives information about the elastic behaviour of a given material. E is defined as the amount of force (F) needed to compress a material with surface area (A) a certain length (Δl) of the total material length (l), as stated in equation (1.8).

$$E = \frac{\frac{F}{A}}{\frac{\Delta l}{l}} \tag{1.8}$$

With a compression test that give a force/deformation curve it is therefore possible to calculate Young's modulus from the initial linear region. Gels made from different alginate types has various degrees of syneresis, shrinkage of the gel due to expulsion of liquid. Syneresis (S) can be calculated from equation (1.9), where W is weight of sample at calcium saturation and W_0 is initial weight of sample.

$$S = \left(1 - \frac{W}{W_o}\right) \cdot 100 \tag{1.9}$$

Syneresis results in increased concentration of alginate per unit volum. As Young's modulus is dependent on the alginate concentration in the gel, the semiempirical relationship stated in equation (1.10) is used so gels with different syneresis can be compared [67, 68].

$$E_{corrected} = E_{measured} \cdot \left(\frac{C_{initial}}{C_{final}}\right)^2 \tag{1.10}$$

Figure 1.13 show an illustration of a typical force/deformation curve. From this curve it is also possible to retrieve other information about the gel in addition to Young's modulus. The curve top show the amount of force needed for the material to rupture and the deformation of the material at this point.

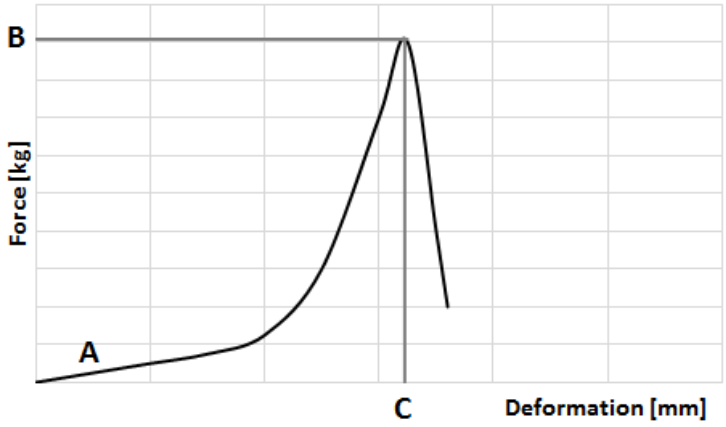

Figure 1.13 An illustration of a typical force/deformation curve with (A) the initial slope used to calculate Young's modulus; (B) the rupture strength; (C) the deformation at rupture.

Hence, the deformation (ϵ) at rupture can be given by equation (1.11) and force at rupture by the force at the same point.

$$\epsilon = \frac{\Delta l}{l} \cdot 100 \tag{1.11}$$

1.5.2 Inductively Coupled Plasma Mass Spectrometry (ICP-MS)

Inductively Coupled Plasma Mass Spectrometry (ICP-MS) is an analytical technique that can be used to detect low concentrations of specific elements in a sample.

The sample is vaporized and presented to an ionizing chamber, consisting of Argon (Ar) plasma produced by an ICP torch. This results in breakage of sample molecules (M) and transfer of charge from the plasma to the sample, as shown in equation (1.12).

$$M + Ar^{+} \rightarrow M^{+} + Ar \tag{1.12}$$

The ions then travel into a high vacuum region consisting of two quadropole analyzers, which function as mass filters, and a collision/reaction cell (CRC) located between them, Figure 1.14. As the ions moves through the first quadropole analyser (Q1) they are separated based on their mass/charge (m/z) ratio. This step removes most of the interfering ions, as only ions with a specific pre-selected m/z ratio are let through to the CRC [69].

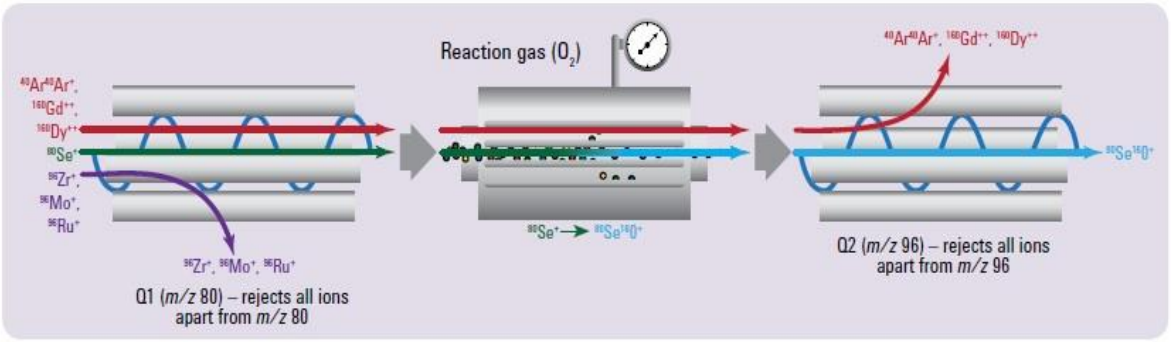

Figure 1.14 A simplified sketch of the three main steps in ICP-MS, two quadropole analyzers (Q_1 and Q_2) with a collision/reaction cell in the middle [69].

The CRC consists of an octopole reaction system (ORS) which can be filled with different gases. The type of gas, or gas-mix, selected is dependent on the element of interest. Selection of a gas that will react with the target element, but not with the other interfering ions, leads to a change in the m/z ratio. Thus, enabling a filtration of the remaining interfering ions in the second quadropole analyser (Q2), by pre-selecting a m/z ratio which only allows ions containing the desired element to pass through to the detector. The ions that are let through are then registered by a detector that reveals the abundance of the element [69].

2 Materials and methods

2.1 Alginate materials

Alginates extracted from *Durvillea potatorum, Macrocystis pyrifera* and *Laminaria hyperborea* stipe were used in this project. The specifics for each of the three alginates are given in Table 2.1.

Table 2.1 An overview of the sequence characteristics of the three alginate types used in this project. Average molecular weight (M_w, [kDa]), average chain length (DP_n) and polydispersity index (PI) were determined from SEC-MALS, while the sequence parameters were calculated from ^{1}H-NMR spectroscopy [70].

Alginate source	M_w (kDa)	DP_n	PI	F_G	F_M	F_{GG}	F_{GM}	F_{MM}	F_{MGM}	F_{GGG}	$N_{G>1}$	[η] (ml/g)	Delivered by
D. pot.	163	470	1.76	0.32	0.68	0.20	0.12	0.56	0.07	0.16	6	1250	FMC Health and Nutrition
M. pyr.	177	460	1.94	0.41	0.59	0.21	0.20	0.40	0.18	0.17	5	960	Sigma-Aldrich
L. hyp. stipe	200	450	2.23	0.67	0.33	0.56	0.11	0.23	0.08	0.52	13	980	FMC Health and Nutrition

2.2 Production of CNF

The CNF suspensions, both mechanically fibrillated and TEMPO-oxidized, used in the experiments were produced and delivered by the Paper and Fibre Research Institute (PFI). The mechanically produced CNF was pretreated by shortening the cellulose fibers in a Claflin mill (1000 kWh/ton for 1 hour), while the oxidized CNF was pretreated with TEMPO and NaClO (2.3 mmol per gram cellulose) as described by Saito et al. [71]. Both types of CNF had a fibril concentration of 1% (w/v) after the pretreatments. The samples were further fibrillated by high pressure homogenization (type *APV Rannie 15 - 12.56* from *SPX Flow Technology*, with a pressure drop of 1000 bar/pass). 5 passes was used for the mechanically fibrillated CNF and 1 pass for the TEMPO-oxidized CNF, resulting in fibril concentrations of 0.886% (w/v) and 0.9% (w/v) respectively. The CNF suspensions were very viscous, especially the oxidized CNF, and for this reason they were weighed throughout the experiment with the assumption of a density equal to water. As shown in Table 2.2, the two treatment methods resulted in different nanocellulose characteristics. Images of the two CNF suspensions are given in Appendix A.

Table 2.2 An overview of characteristics for mechanically produced CNF and TEMPO-oxidized CNF used in this project. All data are previously published in [1, 72].

CNF type	Charge density [mmol/g]	Intrinsic viscosity [η] [ml/g]	Fibril diameter [nm]	Fibril length [µm]	Residual fibres [%]
Mechanically fibrillated	0.1	620	< 100	> 1	1.3
TEMPO-oxidized	0.9	450	< 20	> 1	28.5

2.3 Contol polysaccharides

Dextran, hyaluronic acid and xanthan was used to produce control gels. The average molecular weight, and the suppliers, of these polysaccharides are listed in Table 2.3.

Table 2.3 Average molecular weight (M_w) and distributers of the three control polysaccharides used in this project. High performance liquid chromatography was used to determine the molecular weight of the samples, the data is previously published in [1].

Polysaccharide type	M_w [kDa]	Delivered by
Dextran	2000	Pharmaica AB, Sweden
Hyaluronic acid	870	Novamatrix, Norway
Xanthan	1000	CP Kelco, USA

2.4 Preparation of gel cylinders

Alginate – CNF gels

CNF suspension was weighed out in a blue cap glass bottle (end concentration of 0.00 - 0.75% (w/v)). Alginate powder (450 mg, end concentration of 1% (w/v)) and deionized water (MQ, 30 ml minus amount of CNF used) were then added and left stirring over night. The alginate – CNF composite gels that were made are shown in Table 2.4. In addition, gels with low concentrations of *M. pyr*. alginate were made (Table 2.5).

Table 2.4 Hydrogels were made with alginate from *D. potatorum*, *M. pyrifera* and *L. hyperborea* and nanocellulose, either TEMPO-oxidized or mechanically produced CNF. The x indicates which gels that were made with the three alginates [1 %(w/v)] and different fibril amounts [%(w/v)] of each CNF type.

Alginate		CNF					
Type	Conc. [%(w/v)]	Type	Concentration [%(w/v)]				
			0.00	0.15	0.30	0.50	0.75
D. potatorum							
	1.00	*TEMPO-oxidized*	x	x	x	x	x
	1.00	*Mechanically fibrillated*	-	x	x	x	x
M. pyrifera							
	1.00	*TEMPO-oxidized*	x	x	x	x	x
	1.00	*Mechanically fibrillated*	-	x	x	x	x
L. hyperborea							
	1.00	*TEMPO-oxidized*	x	-	x	-	x
	1.00	*Mechanically fibrillated*	-	-	x	-	x

Table 2.5 Gels made with low amounts of *M. pyrifera* alginate. The alginate concentrations [%(w/v)] that were used are marked with x.

Alginate		
Type	Conc. [%(w/v)]	
	0.10	0.20
M. pyrifera	x	x

Control gels

Control polysaccharide (end concentration of 0.30 - 0.75% (w/v)) and alginate powder (450 mg, end concentration of 1% (w/v)) was weighed out in a blue cap glass bottle. Deionized water (MQ, 30 ml) were then added and left stirring over night. The gels that were made are shown in Table 2.6.

Table 2.6 Control gels were made with alginate from *M. pyrifera* and either dextran, hyaluronic acid, xanthan or additional *M.pyr.* alginate. The x indicates the different concentrations [%(w/v)] of various polysaccharides that were combined with 1% (w/v) *M. pyr.* alginate in the control gels.

Alginate		Control polysaccharide				
Type	**Conc. [%(w/v)]**	**Type**	**Concentration [%(w/v)]**			
			0.15	0.30	0.50	0.75
M. pyrifera						
	1.00	*Additional M. pyrifera*	-	x	-	x
	1.00	*Dextran*	-	x	-	x
	1.00	*Hyaluronic acid*	-	x	-	x
	1.00	*Xanthan*	-	x	-	x

CNF – alginate gels

CNF suspension was weighed out in a blue cap glass bottle (end concentration of 0.00 - 0.75% (w/v)). Alginate powder (end concentration of 0.00 – 0.75% (w/v)) and deionized water (MQ, 30 ml minus amount of CNF used) were then added and left stirring over night. The CNF – alginate composite gels that were made are shown in Table 2.7.

Table 2.7 Gel cylinders with various amount of TEMPO-oxidized CNF and alginate from *M. pyrifera* were made for further analysis, as described in 2.7. The x indicates the concentrations [%(w/v)] of *M. pyr.* alginate that were combined with different amounts of TEMPO-oxidized CNF in these composite gels.

CNF		Alginate				
Type	**Conc. [%(w/v)]**	**Type**	**Concentration [%(w/v)]**			
			0.00	0.20	0.375	0.75
TEMPO-oxidized						
	0.00	*M. pyrifera*	-	-	-	x
	0.375	*M. pyrifera*	-	-	x	-
	0.75	*M. pyrifera*	x	x	x	x

All gel mixtures were then homogenized (type *VDI 12* from *VWR*, 11500 rpm for 5 minutes) to get a uniform suspension, before 25 g was transferred to a flask with suction. After $CaCO_3$ (5 ml, end concentration of 15 mM, particle size 4µm) was added, the solution was degassed using a vacuum suction while stirring for approximately 10 minutes. To start the gelation process GDL (7.5 ml, end concentration of 30 mM) was carefully stirred in, and the mixture was poured into a 24-well tissue culture plate with diameter and height of 16 mm and 18 mm respectively. This resulted in 6-8 gels, and the well plate was left in room temperature for approximately 20h. To achieve Ca^{2+} saturation the gel cylinders were carefully removed from the well plate and put in a solution of $CaCl_2$ and NaCl (800 ml, 50 mM and 200 mM respectively) at 4°C for 24h.

2.5 Measuring gel properties

Height and diameter of the gel cylinders were determined with a digital caliper and each gel was then weighed. The gel properties were measured, as previously described by Aarstad et al. [73], with the use of *TA.XT plus Texture Analyser* from *Stable Micro Systems* (with probe P/35). Force/deformation curves were recorded at 22 ºC and a compression rate of 0.1 mm/s. Young's modulus (E) was calculated from the initial slope of the curve (0.1-0.3 mm) using a 5 kg load cell.

In order to compare the mechanical strength of gels with different degrees of syneresis, the final alginate concentration was calculated and E was corrected using the semiempirical relationship given in equation (1.10). Rupture strength and compression-to-break was measured in a separate experiment using a 5 kg load.

All data was collected and processed with the *Texture Expert Exponent 32* software. Results given by the texture analyser were used to calculate Young's modulus, rupture strength and deformation at rupture. All data from the compression analysis are given in Appendix C and examples of calculations in Appendix D.

2.6 Preparation for light microscopy

Samples for light microscopy (Table 2.8) were prepared as for gel cylinders. The geling solution was pipetted onto objective glass and observed in the light microscope (type *Nikon Eclipse TS100 microscope* with 40x magnification).

Table 2.8 Gel solutions made with alginate from from 1% (w/v) *M. pyrifera* and CNF. The x indicates which concentrations [%(w/v)] of CNF that were used for the microscopy.

Alginate		CNF		
Type	**Conc. [%(w/v)]**	**Type**	**Concentration [%(w/v)]**	
			0.00	0.30
M. pyrifera				
	1.00	*TEMPO-oxidized*	x	x
	1.00	*Mechanically fibrillated*	-	x

2.7 Preparation for ICP-MS

From all six gels shown in Table 2.7 there were cut three pieces with a scalpel. Each of the three pieces were weighed and placed in separate tubes marked with the number 0, 1 and 2. The tube of gel piece 0 were added EDTA (0.5 ml, 100 mM, pH 7), while piece 1 and 2 were washed with NaCl (40 ml, 150 mM). Both gel piece 1 and 2 were weighed after 24 hours in NaCl, before they were put in new tubes. Gel 1 was then added EDTA, while a 24 hour NaCl wash was repeated for gel 2. After completing the final NaCl treatment and weighin, gel piece 2 was added EDTA. Figure 2.1 give an illustration of the gel preparation. All gel pieces were stored in Eppendorf tubes at 4^{o} C after addition of EDTA.

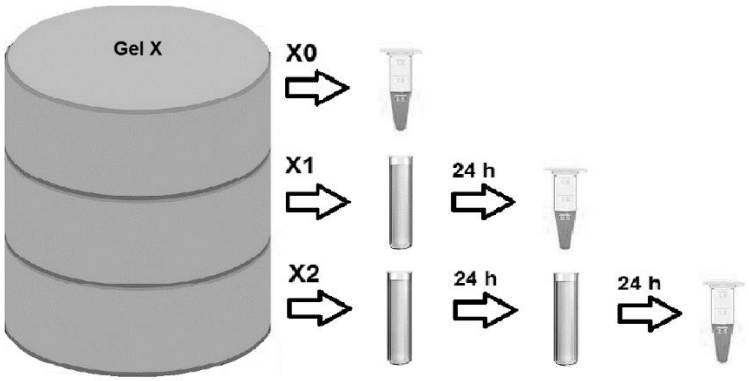

Figure 2.1 Three pieces was cut from each gel and placed in separate tubes marked with gel identification (X) and the number of NaCl treatments for the respective gel piece (0, 1 and 2). The first gel piece was placed directly in an Eppendorf tube and added EDTA (X0). The second and third piece (X1 and X2) were placed in saline solution for 24 hours, once and twice respectively, before the gel pieces were transferred to Eppendorf tubes and added EDTA.

As none of the gels containing TEMPO-oxidized CNF fully dissolved in EDTA, all samples were vortexed (type *Vortex Mixer – Classic* from *VELP Scientifica*) and centrifuged (type *Sorvall Legend XTR Centrifuge* from *Thermo Fisher Scientific*, 2400 rpm for 5 minutes) before they were diluted 100x in 5% HNO_3. Finally the samples were analysed with ICP-MS (type *8800 Triple Quadrupole ICP-MS* with *ASX-520 Autosampler* from *Agilent Technologies*) together with Marianne Kjos at SINTEF Materials and Chemistry, in the department of Biotechnology and Nanomedicine. As internal standards ^{115}In and ^{89}Y were used.

3 Results

Light microscopy was used to investigate the homogeneity of composite gels with 1% alginate and 0.30% CNF, either mechanically fibrillated or TEMPO-oxidized. No phase separation was observed, and the microscopy images showed a homogeneous distribution of cellulose fibrils in the composite gels (Figure 3.1). However, the difference in fibril size between the two CNF types was prominent. While thicker fibrils and low degree of residual fibers was observed in the composite gel with mechanically fibrillated CNF, the composite with TEMPO-oxidized CNF comprised of thin fibrils that was not visible in the light microscopy and a high amount of residual fibers.

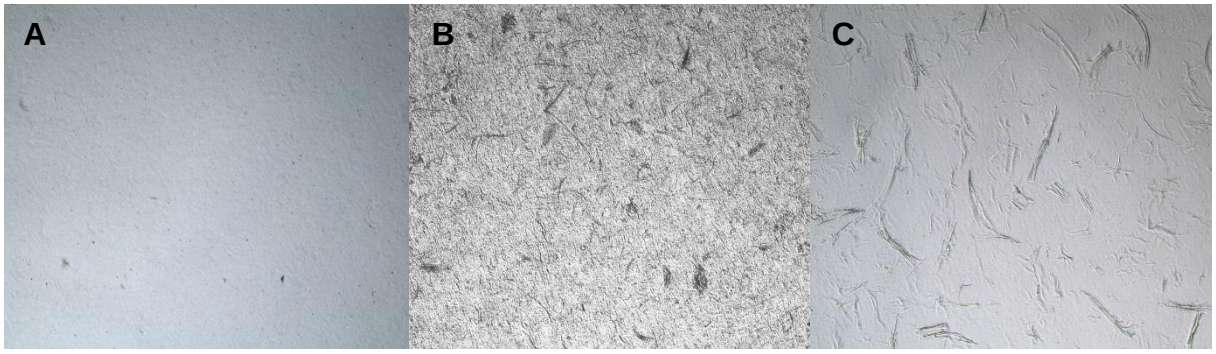

Figure 3.1 Microscopy images with 40x magnification of hydrogels made with 1% (w/v) *M. pyrifera* alginate. The images show a pure Ca-alginate gel (A), a composite gel with 0.30% (w/v) mechanically fibrillated CNF (B) and a composite gel with 0.30% (w/v) TEMPO oxidized CNF (C).

3.1 Alginate gels with cellulose nanofibrils

Calcium saturated composite gels of alginate, extracted from *D. pot.*, *M. pyr.* and *L. hyp.*, and CNF, mechanically fibrillated or TEMPO oxidized, were measured with respect to resistance against compression at low deformation (Young's modulus), synresis, resistance to breakage (rupture strength) and deformation at rupture (Figure 3.2 and Figure 3.3).

An increase in stiffness, shown as Young's modulus in Figure 3.2, was observed with increasing amount of both CNF types in all the different alginate gels. The addition of CNF gave the largest relative effect on Young's modulus in gel samples with the lowest G content, hence the greatest impact was seen in *D. pot.* alginate gels containing 0.75% TEMPO-oxidized CNF. The stiffness in these gel samples was found to be almost 5 times as high as for pure *D. pot.* alginate control gels. Although the increase in stiffness was not as high in the *M. pyr.* alginate gels and the already rigid *L. hyp.* alginate gels, a significant effect was seen. With a Young's modulus of three and two times, respectively, the value of the pure alginate control samples.

The reduction in gel volume after calcium saturation was found to be decreasing with increasing CNF concentration for all alginate gels, as illustrated by syneresis in Figure 3.2. Once again the effect was most prominent in gel samples with low G content. While samples of *M. pyr.* and *L. hyp.* alginate containing 0.75 % TEMPO-oxidized CNF showed a relative decrease in syneresis of 41% and 45%, respectively, the effect on gels with *D. pot.* alginate was far greater. An addition of 0.75 % TEMPO-oxidized CNF in gels of *D. pot.* alginate gave a reduction from 25 % to 7 %, which equals a relative decrease in syneresis of 71%.

The results presented in Figure 3.2 reveals a significant difference in effect of the two types of CNF on both Young's modulus and syneresis, for all the composite gels. Addition of TEMPO-oxidized CNF gave a lager effect than mechanical CNF, both on the gels stiffness and volume after calcium saturation. This can clearly be seen in *D. pot.* alginate samples where the difference is most prominent.

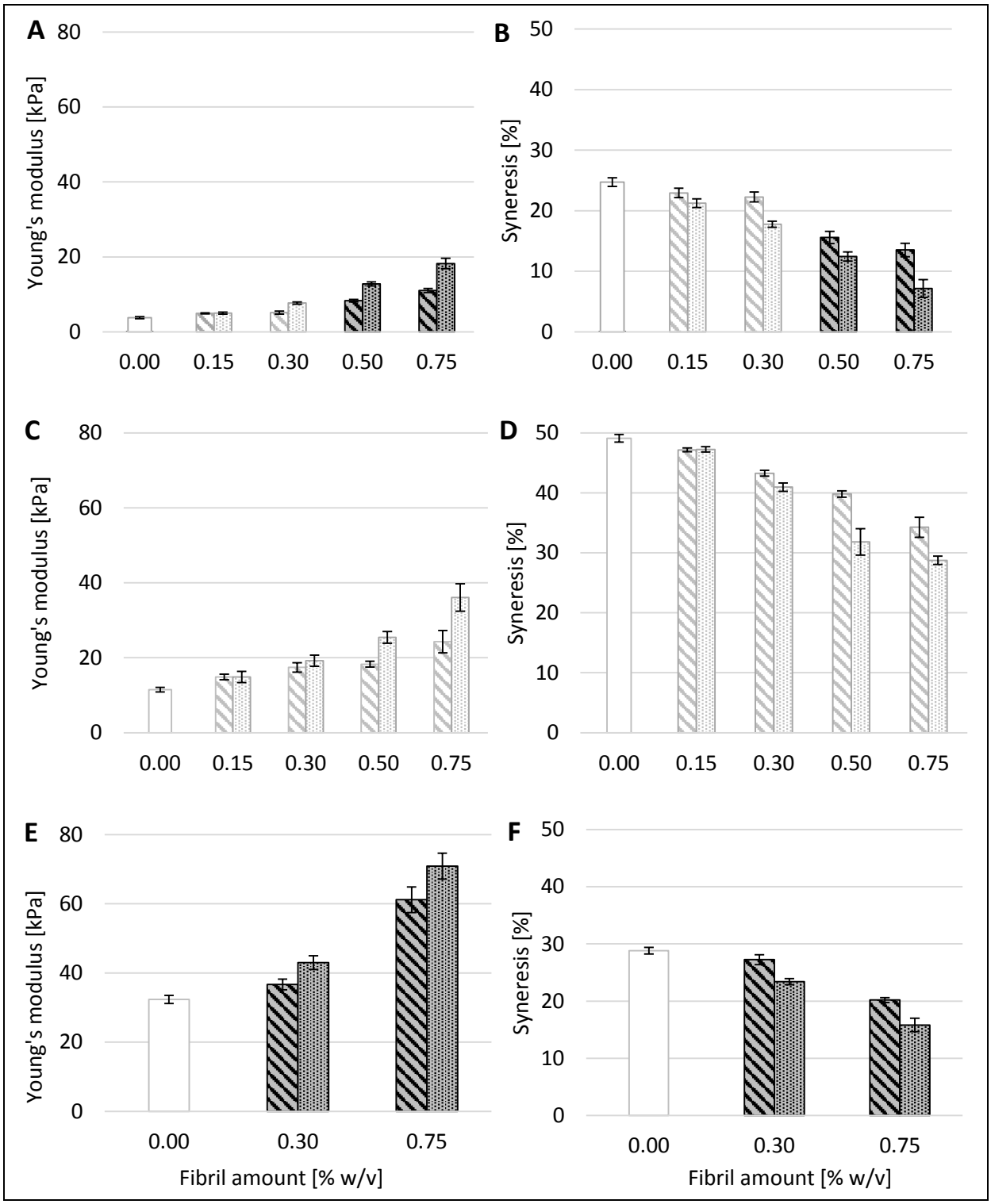

Figure 3.2 Young's modulus [kPa] corrected for concentration and syneresis [%], in right and left charts respectively, for three different 1% (w/v) alginate gels ( ) with addition of mechanically fibrillated ( ) and TEMPO-oxidized CNF ( ). *D. potatorum* (A+B), *M. pyrifera* (C+D) and *L. hyperborea* (E+F). Results obtained from experiments done in the previous project are marked as faded columns. The results are presented as mean of 5-8 gels +/- standard deviation.

Unlike the effect on Young's modulus, no large effect on rupture strength was seen by the addition of CNF to the alginate gels. Small variations could be observed, however no clear trend was found. Gels with alginate from *D. pot.* and *L. hyp.* both showed a slight decrease when low amounts of CNF was added. Contrary to this, high concentrations of CNF gave an increase in rupture strength in *D. pot.* alginate gels and no effect in the *L. hyp.* alginate gels. For *M. pyr.* alginate samples no change was seen with addition of TEMPO-oxidized CNF. However, an increase in rupture strength in gels with the mechanically fibrillated CNF was observed independent of fibril amount.

The distance the gels could be compressed before rupturing was decreasing with increasing concentration of TEMPO-oxidized CNF, shown in Figure 3.3 as a slight reduction in deformation at rupture in all gel samples. The same effect was seen for addition of mechanical CNF to *M. pyr.* alginate gels, while a decrease independent of fibril amount was observed for the two other gel types.

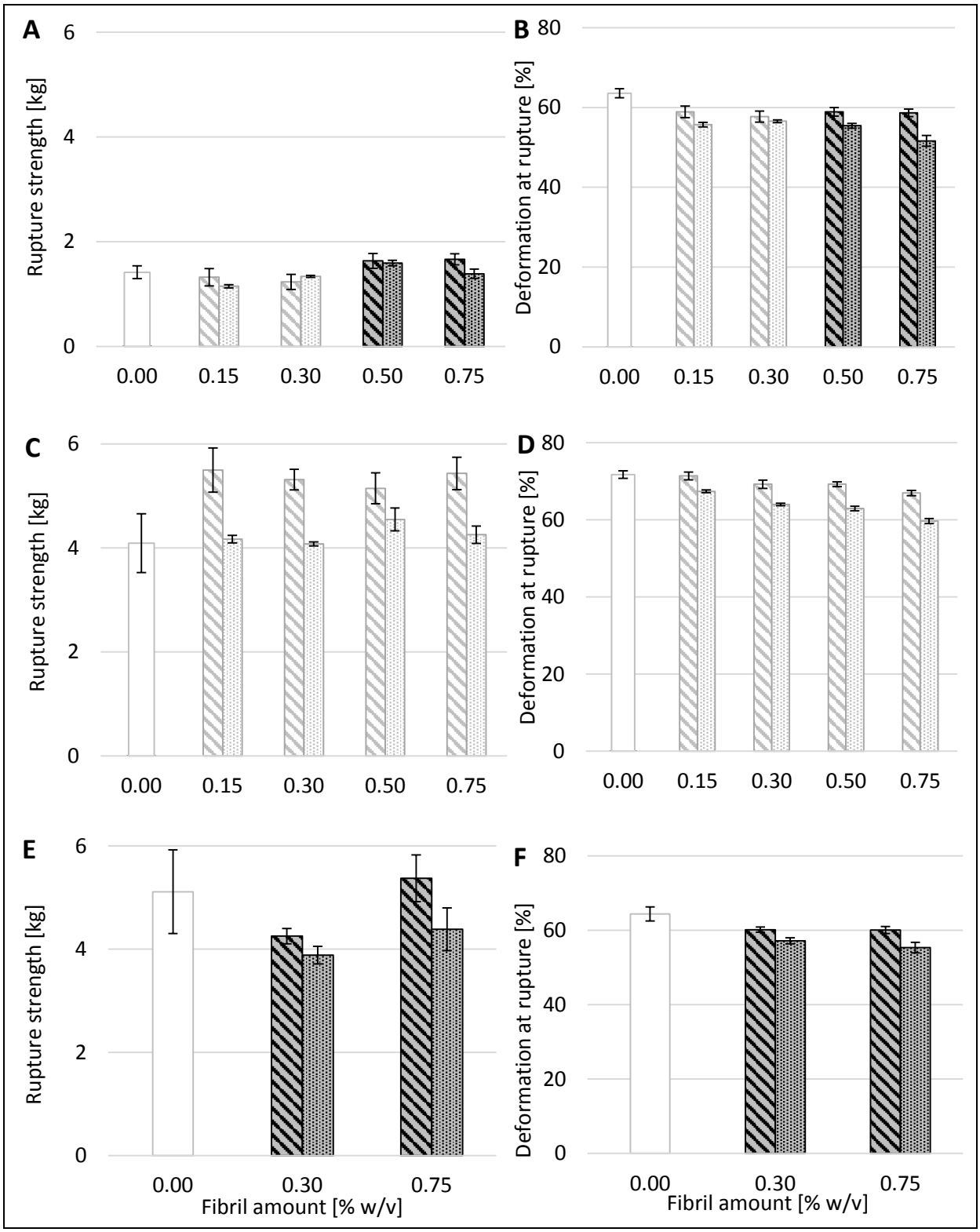

Figure 3.3 Force [kg] applied and deformation [%] registered at gel rupture, in right and left charts respectively, for three different 1% (w/v) alginate gels ( ) with addition of mechanically fibrillated ( ) and TEMPO-oxidized CNF ( ). *D. potatorum* (A+B), *M. pyrifera* (C+D) and *L. hyperborea* (E+F). Results obtained from experiments done in the previous project are marked as faded columns. The results are presented as mean of 5-8 gels +/- standard deviation.

3.2 Alginate gels with other polysaccharides

Gels of *M. pyr.* alginate with addition of either dextran, hyaluronic acid or xanthan were made to investigate filler effect, as well as effect of charge and stiffness of other polysaccharides, on the physical properties of the alginate gels. In addition a set of pure *M. pyr.* alginate gels with corresponding amount of dry matter was made for comparison.

An increase in Young's modulus, relative to pure 1% alginate gels, was seen with addition of both xanthan, mechanically fibrillated CNF and TEMPO oxidized CNF. An effect similar to that of mechanically fibrillated CNF was observed when the alginate concentration alone was increased. However, the highest increase was found in gels with TEMPO oxidized CNF, while addition of dextran and sodium hyaluronate gave no effect on this property.

All polymers was found to reduce gel shrinkage with increasing polymer concentration, shown as syneresis in Figure 3.4 B. The largest effect was seen in gels with xanthan and sodium hyaluronate, with a relative decrease of 46% and 52% respectively, while the smallest effect was observed with addition of dextran, with a relative decrease of only 15%. As with Young's modulus, the impact on syneresis of increased alginate concentration was the same as with addition of mechanically fibrillated CNF.

Addition of TEMPO oxidized CNF did not affect the force needed to rupture the gels, relative to pure 1% alginate gels. However, gels containing oxidized nanofibrils, alongside gels with xanthan, was found to withstand the least amount of compression before rupture, with a relative decrease in deformation upon rupture of 17%. The remaining polymers all showed a slight reduction of the gel deformation at rupture. While addition of sodium hyaluronate and xanthan markedly reduced the gel strength, a slight increase was observed in both gels with mechanically produced CNF and dextran. The increase in concentration from 1% to 1.75% alginate gave more than a two fold increase in rupture strength, a far greater impact than any of the other polymers.

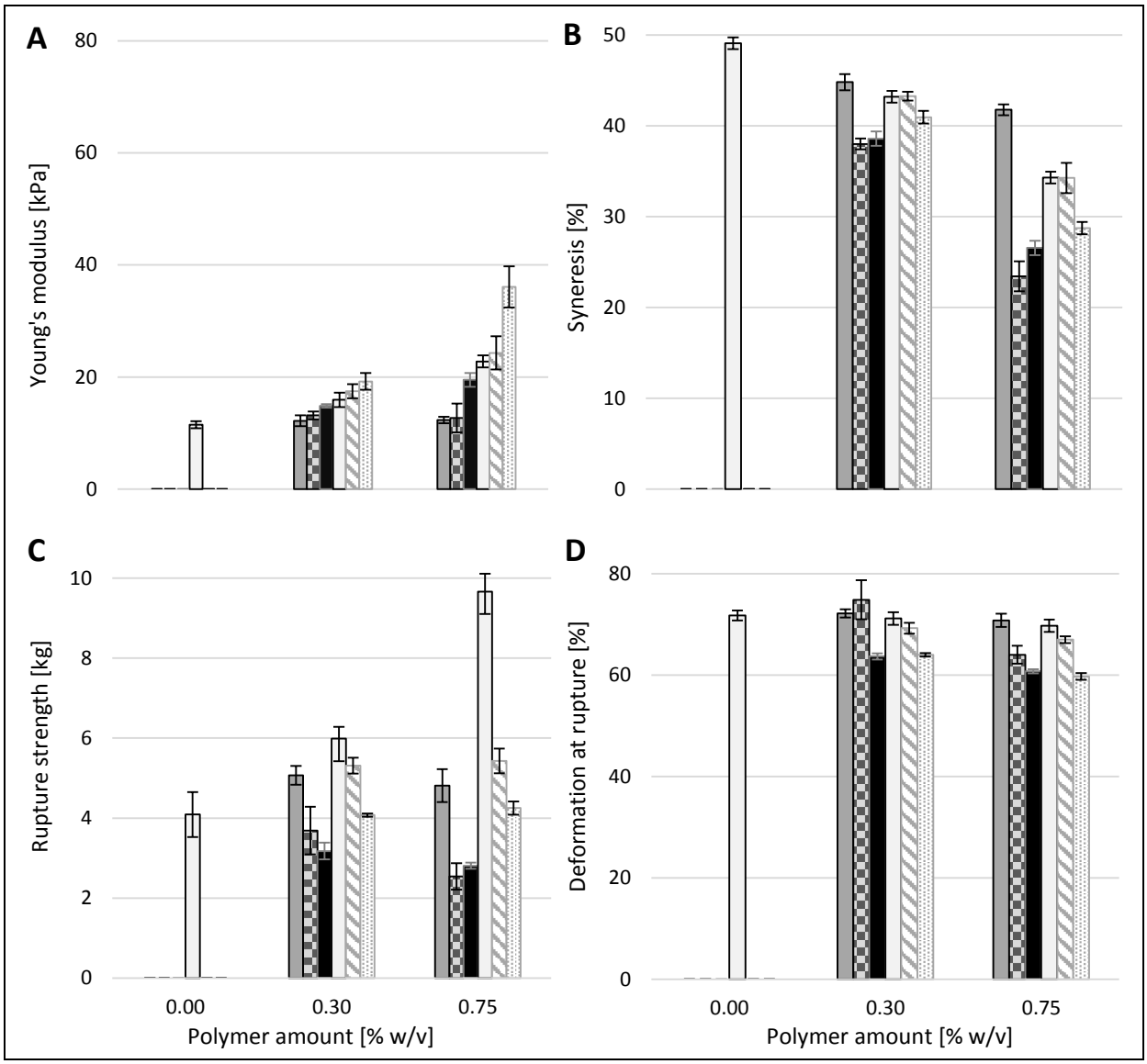

Figure 3.4 Calculated properties of gels made from 1% (w/v) *M. pyrifera* with 0.30% (w/v) and 0.75% (w/v) of dextran ( ), hyaluronic acid ( ), xanthan ( ), mechanically fibrillated CNF ( ), TEMPO-oxidized CNF ( ) and equal amount of additional *M. pyrifera* ( ). Young's modulus corrected for concentration (A), syneresis (B), rupture strength (C) and deformation at rupture (D). Results obtained from experiments done in the previous project are marked as faded columns. The results are presented as mean of 5-8 gels +/- standard deviation.

3.3 TEMPO-oxidized CNF gels with *M. pyrifera* alginate

Composite gels of TEMPO-oxidized CNF and *M. pyr*. alginate were measured with respect to gel stiffness (Young's modulus), volume reduction upon calcium saturation (syneresis), rupture strength and deformation at rupture (Figure 3.5).

As expected, the gel stiffness of TEMPO-oxidized CNF hydrogels was found to increase with addition of alginate. Figure 3.5 show an alginate dependent increase in Young's modulus. No significant difference was seen between gels made of pure 0.750% alginate, pure 0.750% TEMPO-oxidized CNF and the composite comprising 0.375% of each polymer. However, the 0.750/0.750 composite showed a nearly twice as high Young's modulus as the value of the pure hydrogels of each polymer added together. In addition a twofold increase in both alginate and CNF, from composites of 0.375/0.375 to 0.750/0.750, gave more than a threefold increase in gel stiffness.

The gel shrinkage upon calcium saturation, shown as syneresis in Figure 3.5, increased when alginate was present in the gels, relative to gels of pure 0.750% TEMPO-oxidized CNF. From an alginate concentration of 0.375% no further increase in syneresis could be observed in gels when additional alginate was introduced. Although the alginate content after this point was raised by a factor of 2.6 in these composite gels of 0.750% CNF and 1% alginate, the syneresis remained constant at approximately half the value of gels made with pure alginate.

A comparison of composite gels with CNF-alginate composition 0.750/0.375 and 0.375/0.375, hence reducing the CNF concentration by half, showed a change in gel volume reduction from 28.5% to 43%. This equals a relative increase in syneresis of 50%.

No significant difference in rupture strength was seen between pure 0.750% alginate gels and the 0.750/0.750 composite gels, nor between the composite gels with composition of 0.750/0.375 and 0.375/0.375. Hence, no effect on rupture strength was observed with varying concentrations of TEMPO-oxidized CNF. Figure 3.5 show an alginate dependant increase in both rupture strength and deformation, although the 0.375/0.375 composite stand out in the latter as the composite that are able to withstand the most compression before rupture.

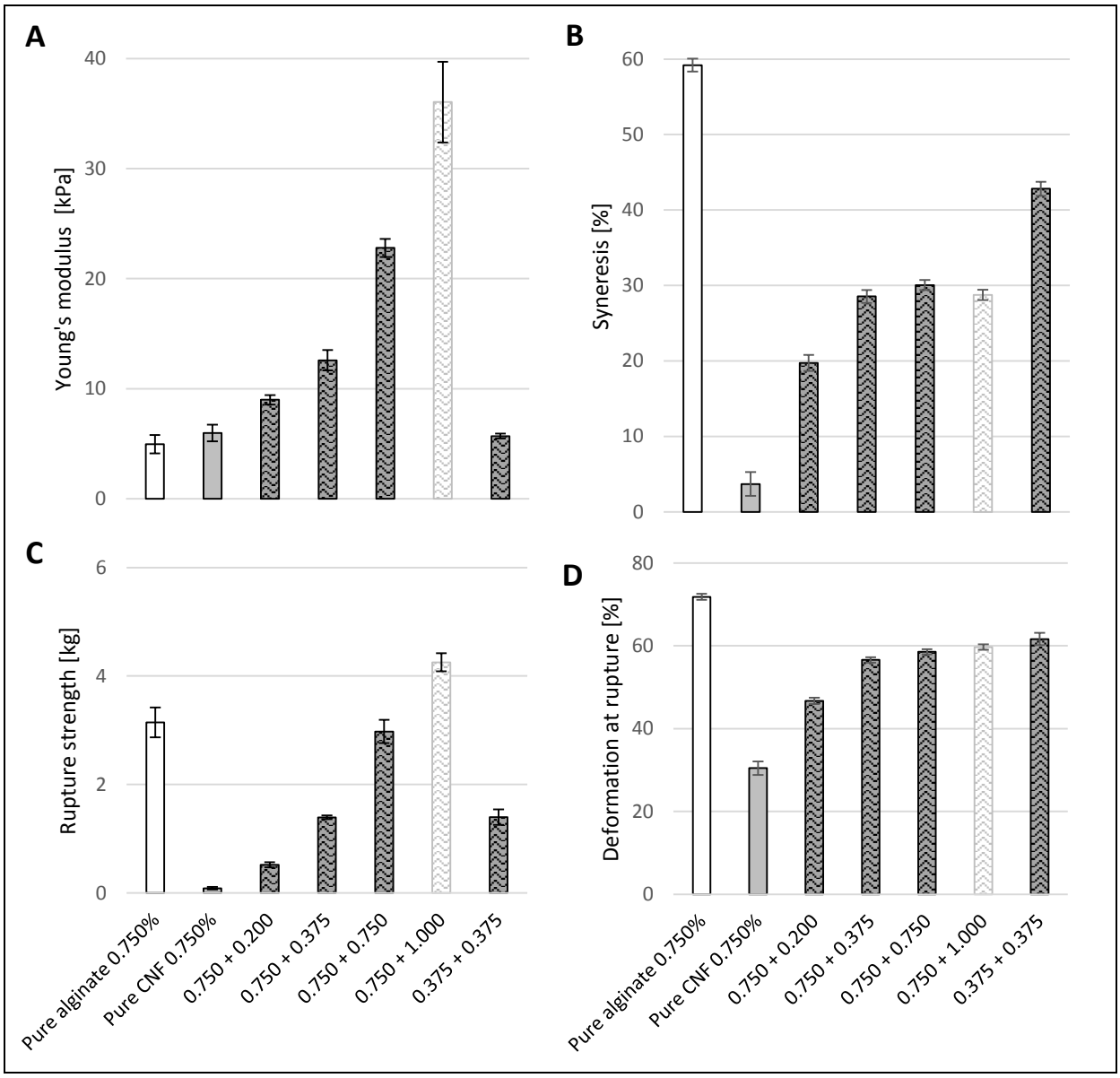

Figure 3.5 Gel properties of gels made from TEMPO-oxidized CNF and different amounts of *M. pyrifera* alginate, presented as [% CNF + % alginate]. The charts represent Young's modulus corrected for concentration (A), syneresis (B), rupture strength (C) and deformation at rupture (D). The results are presented as mean of 5-8 gels +/- standard deviation.

3.4 Critical overlap concentration of *M. pyrifera* alginate

To get an estimate of the critical overlap concentration of *M. pyr*. alginate, the point in which polymer coils start to interact and entangle, pure alginate gels were made with 0.10% and 0.20% *M. pyr.* alginate. The physical properties of these gels were compared to hydrogels of pure 0.75% TEMPO-oxidized CNF and a composite gel of 0.75% CNF and 0.20% *M. pyr*. alginate, shown in Figure 3.6.

Although the product made of 0.10% alginate were not able to maintain their shape after calcium saturation, and for that reason could not be characterized as gels, they were still viable for testing. The high syneresis indicate interaction between the polymer chains and from this that the concentration is above critical overlap concentration. The results are marked as red columns in Figure 3.6 and should be used with caution due to their poor condition.

In contrast, a concentration of 0.20% alginate produced stable hydrogels. Despite the large distinction in appearance between gels of 0.10% and 0.20% *M. pyr.* alginate, the difference in Young's modulus and syneresis for the two hydrogels were not noteworthy. However, the contrast was clearly seen with regard to rupture strength and deformation at rupture (Figure 3.6).

A relative increase in Young's modulus of 43% was seen for the 0.75/0.20 composite gels, compared to the added effect of pure 0.75% CNF and 0.20% alginate gels. While the composite gels shrunk 73% less than pure 0.20% alginate gels, no significant difference in rupture strength was found between composite gels and pure alginate gels. However, a relative decrease in deformation at rupture of 29%, compared to hydrogels of 0.20% alginate, was seen for the composite gels.

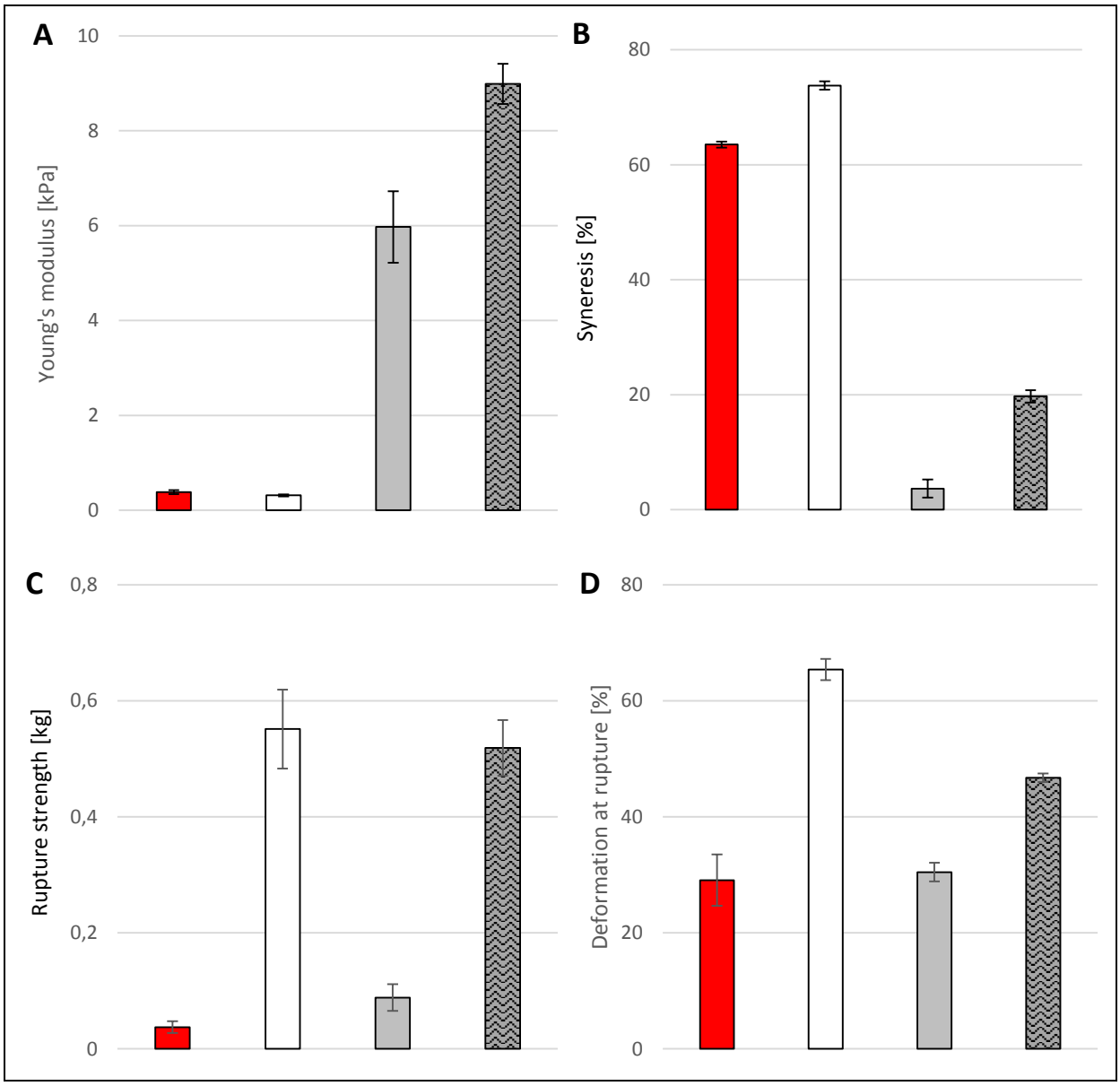

Figure 3.6 Gradient (A), Young's modulus (B), syneresis (C), rupture strength (D) and deformation at rupture (E) for gels made with low concentrations of *M. pyrifera* alginate (0.10% ■ and 0.20% □ w/v), gels made of pure 0.75% (w/v) TEMPO-oxidized CNF (■) and composite gels with 0.75% (w/v) TEMPO-oxidized CNF and 0.20% (w/v) *M. pyrifera* alginate (▩). The results are presented as mean of 5-8 gels +/- standard deviation.

3.5 Gel properties upon saline exposure

To examine the volume stability of the different gels, a treatment with physiological saline solution was done, Figure 3.7. Gels containing TEMPO-oxidized CNF showed significantly less swelling, relative to pure alginate gels where more than a twofold increase in weight could be seen. While the gel volume was found to increase with increasing alginate content, for composite gels of equal concentration of CNF, a decrease in swelling was observed with increasing amount of cellulose fibrils for composite gels with equal concentration of alginate. A syneretic effect was found for the gels made of pure TEMPO-oxidized CNF, resulting in a 15% decrease in gel volume upon exposure to 0.9 % (w/v) NaCl.

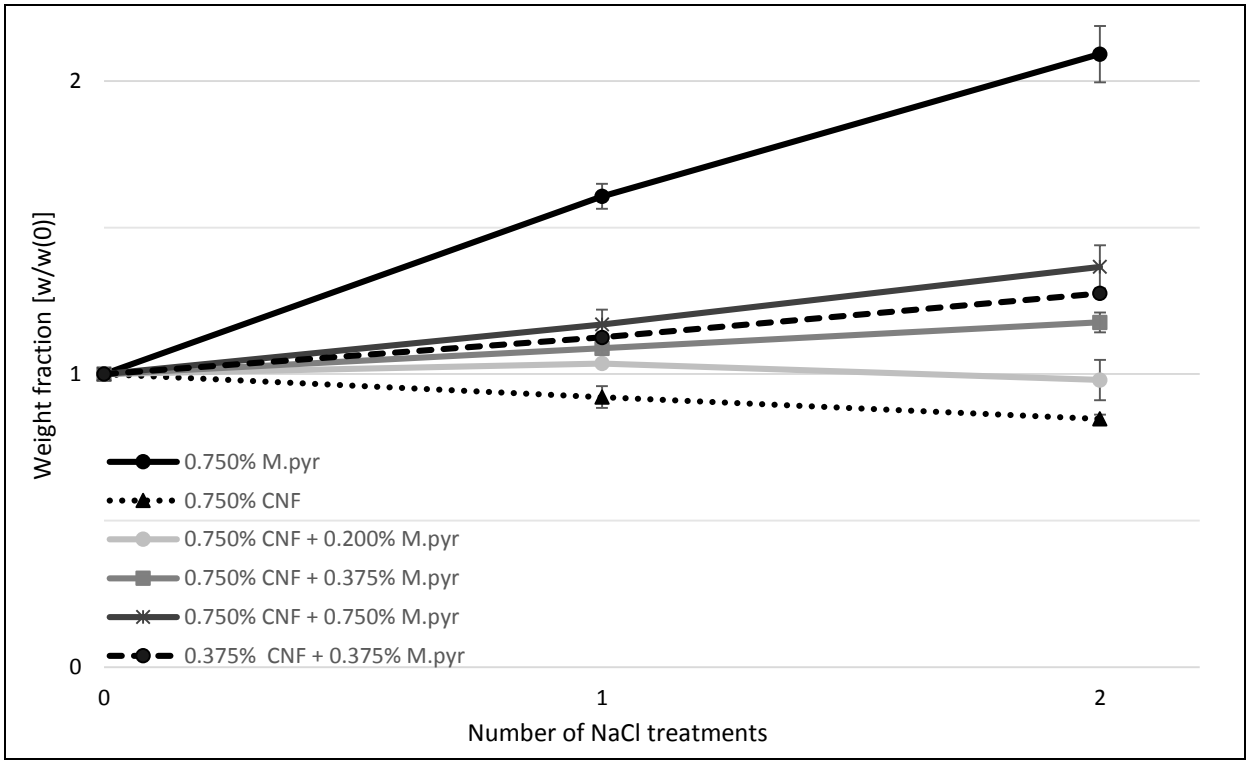

Figure 3.7 Stability of calcium gels, made from various combinations of *M.pyrifera* alginate and TEMPO-oxidized CNF, after treatments with 0.9% (w/v) NaCl. The results are presented as means of 3 gels +/- standard deviation.

Before exposure to the saline solution the highest concentration of calcium was observed in gels made of pure alginate (Figure 3.8). However, after two treatments the same calcium concentration was registered for pure alginate gels and the composite gels with equal alginate content. The gels showed increasing calcium concentration with increasing alginate content and lowest binding to the pure CNF gel.

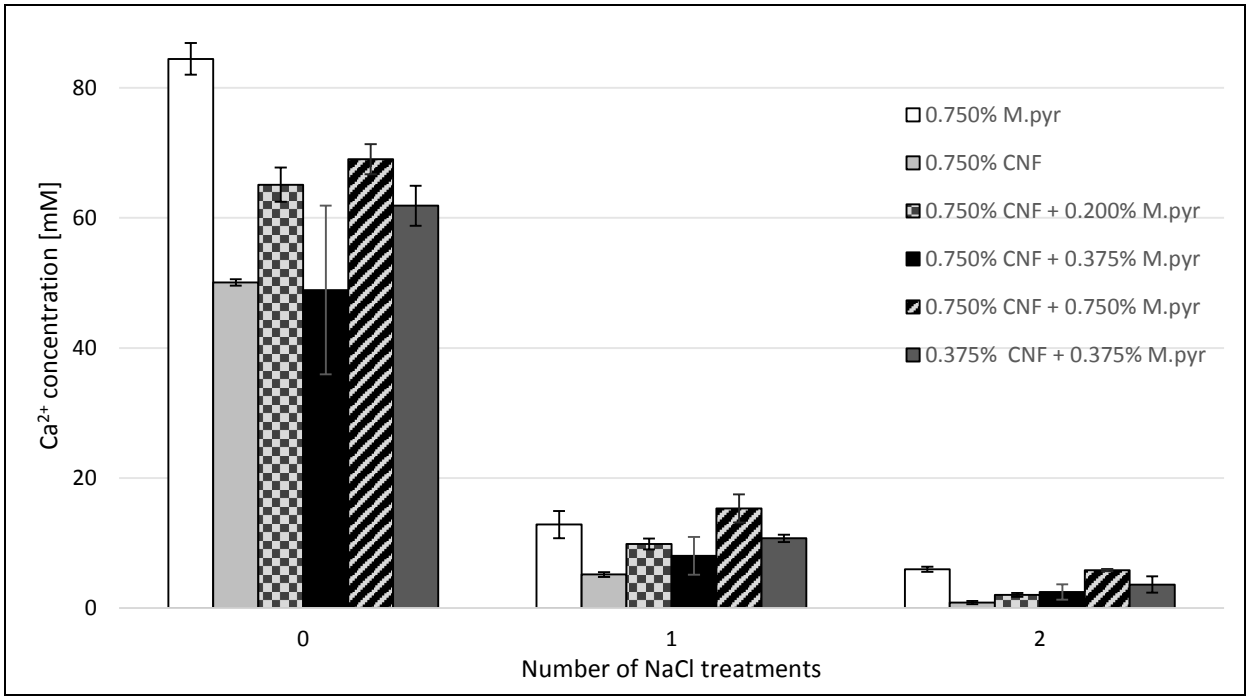

Figure 3.8 Measured calcium concentration in gels, made from various combinations of *M.pyrifera* and TEMPO-oxidized CNF, treated with 0.9% (w/v) NaCl. The results are presented as means of 3 gels +/- standard deviation.

4 Discussion

Gel morphology and homogeneity were examined with light microscopy for composite gels of *M. pyr.* alginate and mechanically fibrillated or TEMPO-oxidized CNF. The images revealed a homogeneous distribution of fibrils and showed no phase separation for either of the composites. This was supported by the images previously taken with scanning electron microscopy (SEM) of gels with the same composition (Appendix B). The structures observed by SEM were tread-like networks, frequently seen with supercritical drying of alginate hydrogels [74]. However, differences were detected in the polymer networks of the composite gels, relative to pure alginate gels. Although the nanofibrils appeared well integrated with alginate, both in composites with mechanically produced and TEMPO-oxidized CNF some fiber structures of substantial size were observed.

While light microscopy of both composite types showed visible strands (Figure 3.1 and Appendix A), TEMPO-oxidized CNF stood out with a high degree of residual fibres. These findings correspond well to fibril characteristics given in Table 2.1, as oxidized fibrils contain close to 30 % residual fibres. The low fibril diameter of TEMPO-oxidized CNF lead to a transparent gel where only the residual fibres could be seen, while the five times thicker fibrils of mechanically produced CNF gave the composite gel a muddy appearance due to the visible fibrils. Both the notable difference in fibril diameter and residual fibres would be expected to influence the mechanical properties of composite gels of alginate and CNF.

4.1 Mechanical properties of composite gels

4.1.1 Young's modulus

The stiffness of the different hydrogels was measured as Young's modulus, which give information on how well a gel resist compression at low deformation. While alginates with a low content of α-L-guluronic acid normally result in softer hydrogels, high G-content in the alginate is known to produce gels that are stiff and rigid [75], due to formation of additional junction zones between G-block chains and calcium ions [25]. Young's modulus found for the pure alginate gels of different G content follow this trend (Figure 3.2), *L. hyp.* stipe alginate resulting in hydrogels with a stiffness of more than 8 times that of gels made with *D.pot.* alginate.

Increased Young's modulus in composite materials, relative to pure alginate films, has previously been shown in nanocellulose-alginate films [76]. This effect on stiffness, with addition of cellulose nanofibrils, was also found for the hydrogels of all three alginates that were studied here. Both addition of mechanically fibrillated and TEMPO-oxidized nanocellulose gave a concentration dependant increase in gel rigidity, although the latter was significantly more efficient (Figure 3.2). The largest effect of nanofibrils was seen in gels made from alginate with lowest G content (*D. pot.*), and showed almost a fivefold increase in Young's modulus upon addition of 0.75% TEMPO CNF.

Control gels comprising alginate with addition of dextran, sodium hyaluronate and xanthan were compared to the alginate-nanocellulose gels, alongside pure *M. pyr*. alginate gels with a total alginate concentration of 1.30% and 1.75% (Figure 3.4). The lack of effect on gel stiffness from both dextran and sodium hyaluronate demonstrated that dry matter content or polymer charge on its own did not impact the Young's modulus. Not surprisingly, gel stiffness was increased in both alginate gels containing xanthan, which can form helical rod-like structures, and pure gels of 1.75% alginate, where the increase in alginate concentration lead to formation of more junction zones. However, the effect of oxidized fibrils was far more prominent, showing that fibril fibers were very efficient in increasing resistance to compression at low degree of deformation.

Pure Ca-gels of *M. pyr*. alginate or pure oxidized CNF displayed the same Young's modulus (Figure 3.5). Increasing gel rigidity was seen with increasing alginate concentration in TEMPO-oxidized CNF gels. For a composite gel where the effect on gel stiffness from the two polymers were independent of each other would give an expectation of a twofold increase in rigidity for a combination of 0.75% alginate and 0.75% TEMPO oxidized CNF. Instead a fourfold increase, relative to pure CNF gels, was found for these gels, indicating that some molecular interactions between cellulose fibrils and alginate occurred in the composites. These results complies with the findings in studies of nanocellulose-alginate films [76, 77], membranes [78] and sponges [79], all in which molecular interactions between alginate and nanocellulose has been shown. The difference in effect of mechanically fibrillated and TEMPO-oxidized nanocellulose on Young's modulus might be explained by the increased number of carboxyl groups and charge on the oxidized fibrils, leading to formation of calcium-carboxylate bonds [53]. The successful production of hydrogels from pure TEMPO-oxidized CNF, forming weak gels without the presence of alginate, as shown here and previously by Dong et al. [80] give further strength to this theory. Stable hydrogels of pure TEMPO-oxidized CNF were in this study seen at considerably lower concentration, with a fibril amount of 0.75%.

Interestingly the Young's modulus of the 0.375/0.375 composite gels was found to be the same as for 0.750/0 composites, only one-fourth of the value of the 0.750/0.750 gels. The different critical overlap concentration of the two polymers, $c^* = 0.5\%$ for CNF (verbal correspondence with Kristin Syverud at PFI) and an estimated $c^* = 0.1 - 0.4\%$ for *M. pyr.* alginate (calculated from equation (1.7) with, $\nu = 1\text{-}4$ for random coils and the intrinsic viscosity given in Table 2.1), may influence this gel feature. A higher polymer concentration than c^* could be needed to achieve an additional combined effect on Young's modulus, and might be a contributing factor to the large increase in stiffness of the 0.750/0.750 composite, in which both CNF and alginate exceed their respective critical concentration. Detailed rheology studies of the critical overlap concentration of both TEMPO-oxidized CNF and *M. pyr*. alginate could provide valuable insight to this composite system.

4.1.2 Syneresis

All three alginates studied gave rise to highly syneretic hydrogels (Figure 3.2). A notably larger shrinkage was seen for gels made of alginate from *M. pyrifera*, with a syneresis as high as 49%, relative to gels made of the two other alginates that were tested. This was expected, as alginates that are rich in MG-blocks are known to have high shrinkage upon calcium saturation [31].

A concentration dependant decrease was seen for all alginate gels with the addition of cellulose nanofibrils (Figure 3.2). This may partly be an effect of long fibrils functioning as support in the elastic alginate gels keeping the gel expanded. The reduction in syneresis was notably higher in gels with TEMPO-oxidized CNF than gels with mechanically produced CNF. This might be due to differences in fibril size and charge of the two CNF types (Table 2.2), as the fibril diameter of the mechanically produced type is approximately five times thicker than the TEMPO-oxidized fibrils, and the charge density of the latter is nine times that of the mechanically fibrillated CNF. Residual fibres may also impact the syneresis, although oxidized CNF contain thinner fibrils, a large amount of residual fibres are present in this CNF solution.

A reduction in syneresis was found with increasing amount of dry matter, for all polymers that were tested. While dextran, a highly flexible molecule without charge, affected the syneresis least, the negatively charged control polymers hyaluronate and xanthan had the same effect as TEMPO-oxidized CNF (Figure 3.4). This indicate that the additional reduction in syneresis caused by TEMPO-oxidized CNF, relative to mechanically fibrillated CNF, may be the result of a higher capacity to contain water due to increased amount of negatively charged carboxyl groups on the surface of the oxidized nanofibrils.

As expected the addition of alginate to hydrogels of TEMPO-oxidized CNF lead to an increase in syneresis relative to pure CNF gels (Figure 3.5). However, as the amount of added alginate reach 0.375% the syneresis leveled out and was not affected by further increase in alginate concentration. Although the syneresis seem to reach a plateau, with respect to alginate content, a reduction of nanofibrils result in additional increase of syneresis (Figure 3.5). Together with the previous arguments, these observations indicate that the syneresis of the composite gels depend on both alginate and CNF up to a certain alginate concentration, in which only variation in CNF concentration affect the volume reduction for the calcium saturated gels.

4.1.3 Rupture strength and deformation at rupture

As expected, hydrogels with *L. hyp.* alginate showed the highest rupture strength of the pure Ca-alginate gels, while the lowest was found for gels with *D. pot.* alginate. The rupture strength of these pure Ca-alginate gels thereby increase with increasing G content (Table 2.1).

Although introduction of cellulose in alginate membranes [78] and nanocrystalline cellulose in alginate films [77] has been reported to increase tensile strength, the same effect was not seen on rupture strength for the composite hydrogels. Although no clear trend was found for the alginate-CNF composite gels, small variations was seen with both CNF types in the composite gels with *D. pot.* alginate and *L. hyp.* alginate, and mechanically produced CNF gave an increase in rupture strength independent of concentration in gels with *M. pyr.* alginate. However, the cellulose concentration in the study done here was not as high as in the previous studies of membranes and films, and an increase in CNF concentration might be necessary to achieve measurable changes in rupture strength. Different preparation processes and cellulose characteristics may also cause the various alginate-cellulose composites to behave dissimilar.

No significant effect was seen on the rupture strength upon the introduction of nanofibrils to the two alginates with lowest and highest G content, however a slight increase in gels of alginate from *M. pyr.* with mechanically produced CNF was observed. A slight reduction in deformation at rupture counterbalance the increase in rupture strength. The alginate from *M. pyr.* contains more MG-blocks than the other alginates (Table 2.1) and the MG-junctions have been shown to tolerate high compression force [81]. A slight increase in rupture strength was also seen for hydrogel samples containing dextran. However, a reduction in rupture strength was caused by both hyaluronate and xanthan (Figure 3.4). As expected, an increase in alginate concentration while keeping CNF at a constant level increased the rupture strength of the composite gels markedly (Figure 3.5).

The same concentration of TEMPO-oxidized CNF was added to hydrogels made from three different alginate concentration, 0.20% (Figure 3.6), 0.75% (Figure 3.5) and 1.00% (Figure 3.3), yet no significant effect on rupture strength was detected at either of the three alginate concentration. This suggest that although the alginate-cellulose interactions influence initial compression resistance, the force that the composite gels can withstand before rupture are determined mainly by the strong junction zones in alginate. This theory is further supported by the extremely low rupture strength of pure gels of 0.750% TEMPO-oxidized CNF (Figure 3.5).

In all three alginates tested there was seen a concentration dependent reduction in deformation at rupture with the presence of TEMPO-oxidized fibrils. Although the same trend was found for *M. pyr.* alginate gels with mechanically produced CNF, the effect was independent of fibril amount in gels of the two remaining alginates. The deformation at rupture decreased with both of the charged control polymers, with xanthan showing the same effect as TEMPO-oxidized CNF, and no change was seen with addition of the flexible dextran.

Similar to syneresis of the TEMPO-oxidized CNF gels the deformation at rupture of the same gels appear to level out after an alginate concentration of 0.375%. From this point the deformation of the gels are mainly dependent on CNF. While the 0.750/0.375 and 0.375/0.375 composite gels showed equal rupture strength, the latter stands out with a rather high deformation at the point of breakage and a low total polymer concentration.

4.2 Gel properties upon saline exposure

4.2.1 Gel stability in saline solution

Ca-alginate gels are known to swell when exposed to saline solution, also for alginate with a high content of guluronic acid [31]. The same effect was found in this study, with more than 100% volume increase of pure *M. pyr.* alginate gels upon the saline treatments. The increase in gel volume is due to the exchange of calcium ions with sodium ions and water. Two sodium ions, together with one water molecule, are needed for every calcium ion to achieve concentration balance inside the hydrogels. This leads to a higher osmotic pressure due to the flow of water in to the gels. A reduction in specific binding of calcium, and thereby a loss of junction zones, in alginates occur as the ions are washed out of the hydrogels and replaced by sodium ions.

Surprisingly all of the different composite gels stayed intact during the two treatments with physiological saline solution and were far more stable than the pure alginate gels. This was also the case for the pure oxidized CNF gels. In fact, the pure CNF gels stand out as the only gel type which shrunk when exposed to NaCl. Although no visual loss of gel was observed, no microscopic detection of leakage was done and low scale loss of gel matter could have occurred. As the charge density of the oxidized CNF is far lower than the alginate there will be a lower amount of calcium in the pure CNF gel, which lead to a lower ionic strength inside the gel. Hence, swelling in these gels is expected to be lower upon saline treatment, due to less flow of water and sodium ions into the gel. A more compact gel structure may be accomplished for the pure oxidized CNF gels upon saline exposure and contribute to the reduced gel volume.

For the composite gels a combined effect was seen, with increasing alginate concentration resulting in increased gel volume and a reduction in swelling was seen with increasing CNF concentration. However, as the composite gels containing 0.75% alginate show considerably less swelling than pure gels of the same alginate concentration, other factors such as steric hindrance might influence the volume stability in addition to difference in ionic strength and specific binding of calcium of the two polysaccharides.

4.2.2 Calcium content in alginate – CNF gels

The registration of calcium after exposure to physiological saline solution showed that an increase in alginate content lead to increase of calcium concentration in the composite gels. As previously mentioned, the increase in Young's modulus of composite gels, relative to pure alginate gels, might be explained by calcium-carboxylate bonds. The expectation of a higher calcium concentration in these gels, relative to pure gels with equal alginate concentration, was however not supported by the measured calcium levels. Surprisingly, the concentration of calcium in the gels were not significantly affected by addition of CNF, and appear to be determined by the alginate concentration. This indicates that the calcium-carboxylate bonds alone are not responsible for the strong influence of nanocellulose fibrils on Young's modulus, and other possible contributing factors should be examined.

Interestingly, a relatively large difference was found between the composite gel of 0.750% CNF and 0.750% alginate and the pure 0.750% alginate gel, prior to saline exposure. In this case the syneresis of the composite gel was found to be approximately half of the syneresis for pure alginate gels, and should thereby be considered an error source on the basis of change in alginate concentration. A similar consequence of syneresis might be relevant when calcium levels of the composites containing 0.375% alginate, and different fibril concentrations, are compared. Although the high values for standard deviation make the data difficult to interpret. As was expected, the gels made of only TEMPO-oxidized CNF showed the lowest amount of calcium upon treatment with saline. However, the initial concentration of calcium was found to be similar to the composite gel of 0.750% CNF and 0.375% alginate.

4.3 Future work

The introduction of CNF in alginate hydrogels was investigated in this study. Although composite gels present increase in Young's modulus, indicating intermolecular interaction between alginate and CNF, further analysis is needed to determine the source of these findings.

An attempt to identify specific calcium binding events, in vacuum dried gels of *M. pyr.* alginate and TEMPO-oxidized CNF, has been done at NTNU by fourier transform infrared spectroscopy (FTIR) characterization [1]. Although the study did not give evidence to support intermolecular interaction between the two polysaccharides, comparison of dried composites and composite hydrogels should be done with caution.

Alternative techniques should be considered for further investigation of alginate – CNF interactions. Isothermal titration calorimetry (ITC) would be relevant in terms of determination of binding affinity and measurement of thermodynamic properties for these composites.

Finally, a detailed study of gelation kinetics, critical overlap concentration of each gel component and rheological behaviour at low concentration might provide valuable information with respect to the role of each polysaccharide in this composite system.

5 Conclusion

In this master thesis, the effect of cellulose nanofibrils on a selection of gel properties for hydrogels made from alginate was investigated in terms of Young's modulus, syneresis, rupture strength, deformation at rupture and finally volume stability.

Light microscopy showed a homogeneous distribution of cellulose fibrils, and no phase separation, in composite gels with both the mechanically fibrillated CNF and the TEMPO-oxidized CNF.

Cellulose nanofibrils contributed to an increase in Young's modulus and reduced the syneresis of hydrogels made with alginate from both *D. potatorum, M. pyrifera* and *L. hyperborea*. The largest effect was seen in composite gels containing TEMPO-oxidized CNF. Analysis of control gels, made of *M. pyr*. alginate and other relevant polysaccharides, did not show the same effect on Young's modulus, confirming that the effect of CNF could not be explained solely by the increase in polymer charge or total dry matter content. Registration of calcium concentration with ICP-MS revealed no increase in calcium concentration for composite gels relative to pure Ca-alginate gels, indicating that calcium binding alone could not explain the high increase in Young's modulus of the composite gels.

TEMPO-oxidized CNF also contributed to volume stability in hydrogels made of *M. pyr.* alginate when the gels were treated with saline solution.

The addition of CNF gave no change in rupture strength relative to pure Ca-alginate gels, and showed that resistance against rupture at large deformations and elastic gel properties are provided mainly by the alginate.

The attained information about the effect of each component in this composite system, on the different gel properties, can be used to manipulate composite materials to fit specific tasks and are highly relevant in areas such as tissue engineering and bioprinting.

References

1. Aarstad O, B. Heggset E, Pedersen I, Bjørnøy S, Syverud K, Strand B: **Mechanical Properties of Composite Hydrogels of Alginate and Cellulose Nanofibrils**. *Polymers* 2017, **9**(8):378.
2. Fisher OZ, Khademhosseini A, Langer R, Peppas NA: **Bioinspired materials for controlling stem cell fate**. *Accounts of chemical research* 2010, **43**(3):419-428.
3. Gaharwar AK, Peppas NA, Khademhosseini A: **Nanocomposite hydrogels for biomedical applications**. *Biotechnology and bioengineering* 2014, **111**(3):441-453.
4. Lowman AM, Dziubla TD, Bures P, Peppas NA: **Structural and dynamic response of neutral and intelligent networks in biomedical environments** In: *Advances in Chemical Engineering.* vol. 29: Academic Press; 2004: 75-130.
5. Peppas NA, Huang Y, Torres-Lugo M, Ward JH, Zhang J: **Physicochemical foundations and structural design of hydrogels in medicine and biology**. *Annual review of biomedical engineering* 2000, **2**:9-29.
6. Markstedt K, Mantas A, Tournier I, Martínez Ávila H, Hägg D, Gatenholm P: **3D Bioprinting Human Chondrocytes with Nanocellulose–Alginate Bioink for Cartilage Tissue Engineering Applications**. *Biomacromolecules* 2015, **16**(5):1489-1496.
7. Painter TJ: **Algal polysaccharides**. [S.l.]: Academic Press; 1983.
8. Smidsrød O, Moe ST: **Biopolymerkjemi**. Trondheim: Tapir; 1995.
9. Govan JR, Fyfe JA, Jarman TR: **Isolation of alginate-producing mutants of Pseudomonas fluorescens, Pseudomonas putida and Pseudomonas mendocina**. *Journal of general microbiology* 1981, **125**(1):217-220.
10. Moe ST, Draget KI, Skjåk-Bræk G, Smidsrød O: **Alginates**. In: *Food Polysaccharides and Their Applications.* Edited by Stephen AM, Philips GO, Williams PA. New York: Marcel Dekker Inc; 2006: 245-286.
11. Draget KI, Smidsrød O, Skjåk-Bræk G: **Alginates from algae.** In: *Biopolymers.* Edited by Vandamme E, De Baets S, Steinbüchel A, vol. 6. Weinheim, Germany: Wiley-VCH Verlag GmbH; 2002: 215-244.
12. Aarstad OA: **Alginate sequencing: block distribution in alginates and its impact on macroscopic properties**, vol. 2013:26. Trondheim: Norges teknisk-naturvitenskapelige universitet; 2013.
13. Atkins ED, Mackie W, Smolko EE: **Crystalline structures of alginic acids**. *Nature* 1970, **225**(5233):626-628.
14. Smidsrød O, Glover RM, Whittington SG: **The relative extension of alginates having different chemical composition**. Amsterdam: Elsevier; 1973.
15. Atkins ED, Nieduszynski IA, Mackie W, Parker KD, Smolko EE: **Structural components of alginic acid. I. The crystalline structure of poly-beta-D-mannuronic acid. Results of x-ray diffraction and polarized infrared studies**. *Biopolymers* 1973, **12**(8):1865-1878.
16. Atkins ED, Nieduszynski IA, Mackie W, Parker KD, Smolko EE: **Structural components of alginic acid. II. The crystalline structure of poly-alpha-L-guluronic acid. Results of x-ray diffraction and polarized infrared studies**. *Biopolymers* 1973, **12**(8):1879-1887.
17. Ballance S, Holtan S, Aarstad OA, Sikorski P, Skjak-Braek G, Christensen BE: **Application of high-performance anion-exchange chromatography with pulsed amperometric detection and statistical analysis to study oligosaccharide**

distributions--a complementary method to investigate the structure and some properties of alginates. *Journal of chromatography A* 2005, **1093**(1-2):59-68.
18. Skjåk-Bræk G, Donati I, Paoletti S: **Alginate Hydrogels: Properties and Applications**. In: *Polysaccharide Hydrogels: Characterization and Biomedical Applications.* Edited by Matricardi P, Alhaique F, Coviello T: Pan Stanford Publishing; 2015: 443-492.
19. Grasdalen H: **High-field, 1H-n.m.r. spectroscopy of alginate: sequential structure and linkage conformations**. *Carbohydrate Research* 1983, **118**:255-260.
20. Grasdalen H, Larsen B, Smisrod O: **13C-n.m.r. studies of monomeric composition and sequence in alginate**. *Carbohydrate Research* 1981, **89**(2):179-191.
21. Draget KI: **Alginates**. In: *Handbook of hydrocolloids.* Edited by Phillips GO, Williams PA, 1st edn. Cambridge: Woodhead Publishing; 2000: 379-395.
22. Vold IM, Kristiansen KA, Christensen BE: **A study of the chain stiffness and extension of alginates, in vitro epimerized alginates, and periodate-oxidized alginates using size-exclusion chromatography combined with light scattering and viscosity detectors**. *Biomacromolecules* 2006, **7**(7):2136-2146.
23. Smidsrød O, Haug A: **Dependence upon uronic acid composition of some ion-exchange properties of alginates**. *Acta Chemica Scandinavica* 1968(22):1989-1997.
24. Haug A, Smidsrød O: **Selectivity of Some Anionic Polymers for Divalent Metal Ions**. *Acta Chemica Scandinavica* 1970(24):843-854.
25. Martinsen A, Skjak-Braek G, Smidsrod O: **Alginate as immobilization material: I. Correlation between chemical and physical properties of alginate gel beads**. *Biotechnology and bioengineering* 1989, **33**(1):79-89.
26. Grant GT, Morris ER, Rees DA, Smith PJC, Thom D: **Biological interactions between polysaccharides and divalent cations: The egg-box model**. *FEBS Letters* 1973, **32**(1):195-198.
27. Braccini I, Perez S: **Molecular basis of C(2+)-induced gelation in alginates and pectins: the egg-box model revisited**. *Biomacromolecules* 2001, **2**(4):1089-1096.
28. Kashima K, Imai M: **Selective diffusion of glucose, maltose, and raffinose through calcium alginate membranes characterized by a mass fraction of guluronate**. *Food and Bioproducts Processing*, **102**:213-221.
29. Donati I, Holtan S, Morch YA, Borgogna M, Dentini M, Skjak-Braek G: **New hypothesis on the role of alternating sequences in calcium-alginate gels**. *Biomacromolecules* 2005, **6**(2):1031-1040.
30. Draget KI, Strand B, Hartmann M, Valla S, Smidsrod O, Skjak-Braek G: **Ionic and acid gel formation of epimerised alginates; the effect of AlgE4**. *International journal of biological macromolecules* 2000, **27**(2):117-122.
31. Mørch YA, Donati I, Strand BL, Skjak-Braek G: **Effect of Ca2+, Ba2+, and Sr2+ on alginate microbeads**. *Biomacromolecules* 2006, **7**(5):1471-1480.
32. Smidsrød O, Draget KI: **Alginate gelation technologies**. In: *Food Colloids: Proteins, Lipids and Polysaccharides.* Edited by Dickinson E, Bergståhl B. Cambridge: The Royal Society of Chemistry; 1997: 279-293.
33. Liu XD, Yu WY, Zhang Y, Xue WM, Yu WT, Xiong Y, Ma XJ, Chen Y, Yuan Q: **Characterization of structure and diffusion behaviour of Ca-alginate beads prepared with external or internal calcium sources**. *Journal of microencapsulation* 2002, **19**(6):775-782.
34. Smidsrød O, Skjåk-Bræk G: **Alginate as immobilization matrix for cells**. *Trends in Biotechnology* 1990, **8**(Supplement C):71-78.

35. Abdul Khalil HP, Davoudpour Y, Islam MN, Mustapha A, Sudesh K, Dungani R, Jawaid M: **Production and modification of nanofibrillated cellulose using various mechanical processes: a review**. *Carbohydrate polymers* 2014, **99**:649-665.
36. Klemm D, Heublein B, Fink HP, Bohn A: **Cellulose: fascinating biopolymer and sustainable raw material**. *Angewandte Chemie (International ed in English)* 2005, **44**(22):3358-3393.
37. Klemm D, Kramer F, Moritz S, Lindstrom T, Ankerfors M, Gray D, Dorris A: **Nanocelluloses: a new family of nature-based materials**. *Angewandte Chemie (International ed in English)* 2011, **50**(24):5438-5466.
38. Lee S-Y, Chun S-J, Kang I-A, Park J-Y: **Preparation of cellulose nanofibrils by high-pressure homogenizer and cellulose-based composite films**. *Journal of Industrial and Engineering Chemistry* 2009, **15**(1):50-55.
39. Svagan AJ, Samir MASA, Berglund LA: **Biomimetic Foams of High Mechanical Performance Based on Nanostructured Cell Walls Reinforced by Native Cellulose Nanofibrils**. *Advanced Materials* 2008, **20**(7):1263-1269.
40. Habibi Y: **Key advances in the chemical modification of nanocelluloses**. *Chemical Society reviews* 2014, **43**(5):1519-1542.
41. Lavoine N, Desloges I, Dufresne A, Bras J: **Microfibrillated cellulose - its barrier properties and applications in cellulosic materials: a review**. *Carbohydrate polymers* 2012, **90**(2):735-764.
42. Nakagaito AN, Yano H: **The effect of morphological changes from pulp fiber towards nano-scale fibrillated cellulose on the mechanical properties of high-strength plant fiber based composites**. *Appl Phys A* 2004, **78**(4):547-552.
43. Siró I, Plackett D: **Microfibrillated cellulose and new nanocomposite materials: a review**. *Cellulose* 2010, **17**(3):459-494.
44. Adam W, Saha-Moller CR, Ganeshpure PA: **Synthetic applications of nonmetal catalysts for homogeneous oxidations**. *Chemical reviews* 2001, **101**(11):3499-3548.
45. Isogai A, Saito T, Fukuzumi H: **TEMPO-oxidized cellulose nanofibers**. *Nanoscale* 2011, **3**(1):71-85.
46. Davis NJ, Flitsch SL: **Selective oxidation of monosaccharide derivatives to uronic acids**. *Tetrahedron Letters* 1993, **34**(7):1181-1184.
47. Konno N, Habu N, Iihashi N, Isogai A: **Purification and characterization of exo-type cellouronate lyase**. *Cellulose* 2008, **15**(3):453-463.
48. Watanabe E, Habu N, Isogai A: **Biodegradation of (1-->3)-beta-polyglucuronate prepared by TEMPO-mediated oxidation**. *Carbohydrate polymers* 2013, **96**(1):314-319.
49. Kato Y, Habu N, Yamaguchi J, Kobayashi Y, Shibata I, Isogai A, Samejima M: **Biodegradation of β-1,4-linked polyglucuronic acid (cellouronic acid)**. *Cellulose* 2002, **9**(1):75-81.
50. Delattre C, Michaud P, Elboutachfaiti R, Courtois B, Courtois J: **Production of oligocellouronates by biodegradation of oxidized cellulose**. *Cellulose* 2006, **13**(1):63-71.
51. Nechyporchuk O, Belgacem MN, Bras J: **Production of cellulose nanofibrils: A review of recent advances**. *Industrial Crops and Products* 2016, **93**(Supplement C):2-25.
52. Zander NE, Dong H, Steele J, Grant JT: **Metal Cation Cross-Linked Nanocellulose Hydrogels as Tissue Engineering Substrates**. *ACS applied materials & interfaces* 2014, **6**(21):18502-18510.

53. Dong H, Snyder JF, Williams KS, Andzelm JW: **Cation-induced hydrogels of cellulose nanofibrils with tunable moduli**. *Biomacromolecules* 2013, **14**(9):3338-3345.
54. Syverud K, Pettersen SR, Draget K, Chinga-Carrasco G: **Controlling the elastic modulus of cellulose nanofibril hydrogels—scaffolds with potential in tissue engineering**. *Cellulose* 2015, **22**(1):473-481.
55. Saito T, Isogai A: **Introduction of aldehyde groups on surfaces of native cellulose fibers by TEMPO-mediated oxidation**. *Colloids and Surfaces A: Physicochemical and Engineering Aspects* 2006, **289**(1):219-225.
56. Dols M, Remaud-Simeon M, Willemot RM, Vignon M, Monsan P: **Characterization of the Different Dextransucrase Activities Excreted in Glucose, Fructose, or Sucrose Medium by Leuconostoc mesenteroides NRRL B-1299**. *Applied and Environmental Microbiology* 1998, **64**(4):1298-1302.
57. Klemm D: **Advances In Polymer Science - Polysaccharides II**. Heidelberg: Springer; 2006.
58. Coultate TP: **FOOD The Chemistry of its Components**, 5th edn. Cambridge: RSC Publishing; 2009.
59. Ielpi L, Couso RO, Dankert MA: **Xanthan cum biosynthesis pyruvic acid acetal residues are transferred from phosphoenolpyruvate to the pentasaccharide-P-P-lipid**. *Biochemical and Biophysical Research Communications* 1981, **102**(4):1400-1408.
60. Jansson P-e, Kenne L, Lindberg B: **Structure of the extracellular polysaccharide from xanthomonas campestris**. *Carbohydrate Research* 1975, **45**(1):275-282.
61. Swings JG, Civerolo EL: **Xanthomonas**. London: Chapman & Hall; 1993.
62. Maruyama Y, Hashimoto W, Mikami B, Murata K: **Crystal Structure of Bacillus sp. GL1 Xanthan Lyase Complexed with a Substrate: Insights into the Enzyme Reaction Mechanism**. *Journal of Molecular Biology* 2005, **350**(5):974-986.
63. Diekjürgen D, Grainger DW: **Polysaccharide matrices used in 3D in vitro cell culture systems**. *Biomaterials* 2017, **141**(Supplement C):96-115.
64. Selyanin MA, Boykov PY, Khabarov VN: **Hyaluronic Acid: Preparation, Properties, Application in Biology and Medicine**. Chichester: John Wiley & Sons; 2015.
65. Kaux J-F, Samson A, Crielaard J-M: **Hyaluronic acid and tendon lesions**. *Muscles, Ligaments and Tendons Journal* 2015, **5**(4):264-269.
66. Necas J, Bartosikova L, Brauner P, Kolar J: **Hyaluronic acid (hyaluronan): a review**. *Veterinarni Medicina* 2008, **53**:397-411.
67. Goodwin JW, Hughes RW: **Rheology for chemists: an introduction**. Cambridge: Royal Society of Chemistry; 2008.
68. Nielsen LE, Landel RF: **Mechanical properties of polymers and composites**, 2nd edn. New York: Marcel Dekker; 1994.
69. Technologies A: **Agilent 8800 Triple Quadrupole ICP-MS**. In. USA: Agilent Technologies; 2015.
70. Aarstad OA, Tondervik A, Sletta H, Skjak-Braek G: **Alginate sequencing: an analysis of block distribution in alginates using specific alginate degrading enzymes**. *Biomacromolecules* 2012, **13**(1):106-116.
71. Saito T, Nishiyama Y, Putaux JL, Vignon M, Isogai A: **Homogeneous suspensions of individualized microfibrils from TEMPO-catalyzed oxidation of native cellulose**. *Biomacromolecules* 2006, **7**(6):1687-1691.
72. B. Heggset E, Chinga Carrasco G, Syverud K: **Temperature stability of nanocellulose dispersions**, vol. 157; 2017.

73. Aarstad O, Strand BL, Klepp-Andersen LM, Skjak-Braek G: **Analysis of G-block distributions and their impact on gel properties of in vitro epimerized mannuronan**. *Biomacromolecules* 2013, **14**(10):3409-3416.
74. Xie M, Olderoy MO, Zhang Z, Andreassen J-P, Strand BL, Sikorski P: **Biocomposites prepared by alkaline phosphatase mediated mineralization of alginate microbeads**. *RSC Advances* 2012, **2**(4):1457-1465.
75. Smidsrød O, Haug A: **Properties of Poly(1,4-hexuronates) in the gel state. II. Comparison of gels of different chemical composition.** *Acta chemica Scandinavica* 1972, **26**:79-88.
76. Sirviö JA, Kolehmainen A, Liimatainen H, Niinimäki J, Hormi OEO: **Biocomposite cellulose-alginate films: Promising packaging materials**. *Food chemistry* 2014, **151**:343-351.
77. Huq T, Salmieri S, Khan A, Khan RA, Le Tien C, Riedl B, Fraschini C, Bouchard J, Uribe-Calderon J, Kamal MR *et al*: **Nanocrystalline cellulose (NCC) reinforced alginate based biodegradable nanocomposite film**. *Carbohydrate polymers* 2012, **90**(4):1757-1763.
78. Yang G, Zhang L, Peng T, Zhong W: **Effects of Ca2+ bridge cross-linking on structure and pervaporation of cellulose/alginate blend membranes**. *J Membr Sci* 2000, **175**(1):53-60.
79. Lin N, Bruzzese C, Dufresne A: **TEMPO-Oxidized Nanocellulose Participating as Crosslinking Aid for Alginate-Based Sponges**. *ACS applied materials & interfaces* 2012, **4**(9):4948-4959.
80. Dong H, Snyder JF, Tran DT, Leadore JL: **Hydrogel, aerogel and film of cellulose nanofibrils functionalized with silver nanoparticles**. *Carbohydrate polymers* 2013, **95**(2):760-767.
81. Mørch YA, Holtan S, Donati I, Strand BL, Skjåk-Bræk G: **Mechanical properties of C-5 epimerized alginates**. *Biomacromolecules* 2008, **9**(9):2360-2368.

APPENDICES

A CNF suspensions

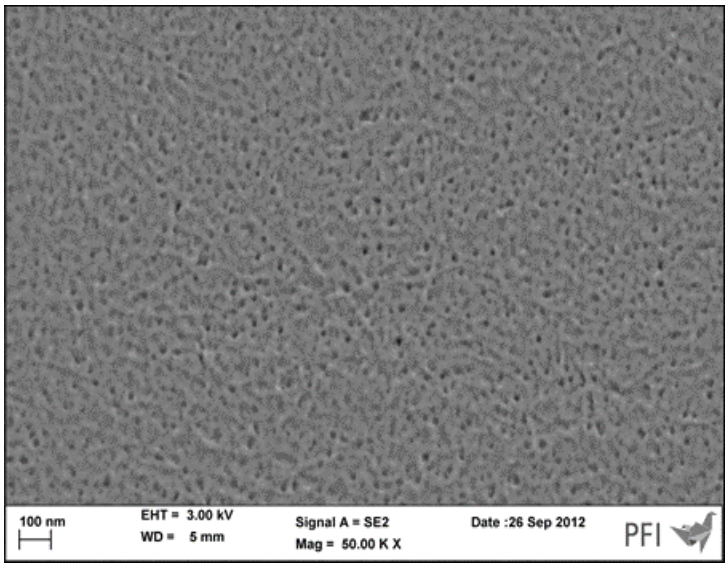

(A) (B)

Figure A.1 - (A) Picture of the TEMPO-oxidized CNF used; (B) SEM image of TEMPO-oxidized CNF, taken by PFI.

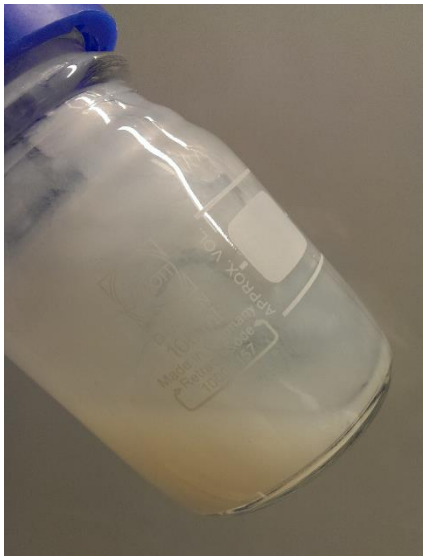

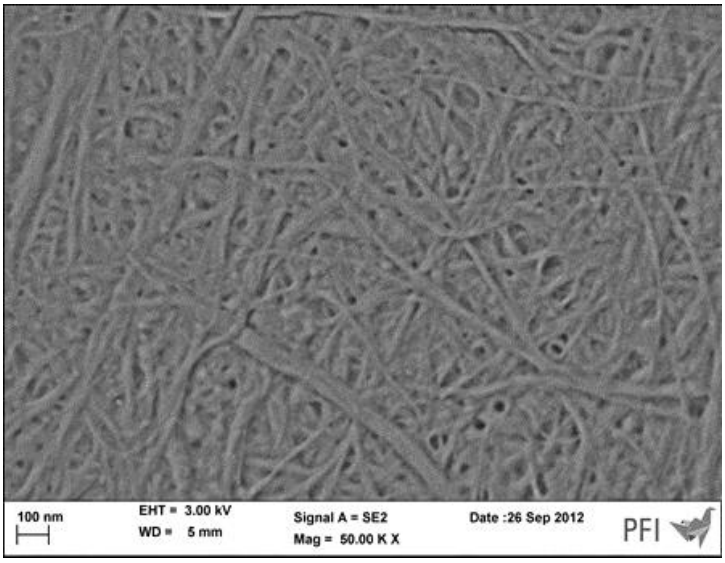

(A) (B)

Figure A.2 - (A) Picture of the mechanical CNF used; (B) SEM image of mechanical CNF, taken by PFI.

B SEM images of alginate – CNF composite gels

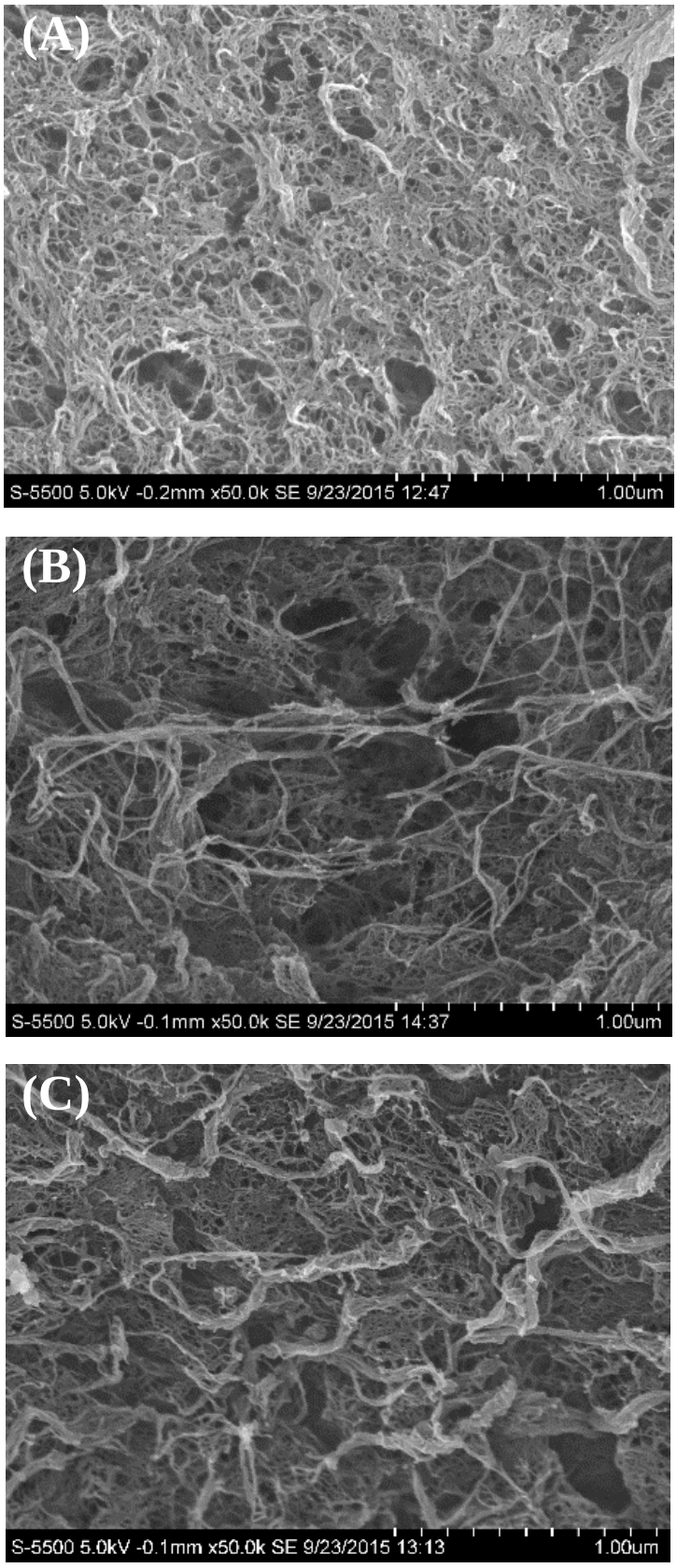

Figure A.3 - SEM images of supercritically dried hydrogels of 1% (w/v) *M. pyrifera* alginate (A), and composite gels with 0.30% mechanically fibrillated CNF (B) and 0.30% TEMPO-oxidized CNF (C).

C Compression analysis of hydrogels

Table A. 1 Raw data for gels with 1% (w/v) *D. potatorum* alginate and composite gels with 1% (w/v) *D. potatorum* alginate and different amounts of TEMPO-oxidized and mechanically fibrillated CNF[%(w/v)]. Height (h), diameter (d), weight (w), gradient, Young's modulus (E), syneresis (S), rupture strength (RS), deformation at rupture (D) and percentage of deformation at rupture (*ϵ*).

		h	*d*	*w*	*Gradient*	*E*	*S*	*RS*	*D*	*ϵ*
Alginate	**n**	**(mm)**	**(mm)**	**(g)**	**(N/m)**	**(Pa)**	**(%)**	**(kg)**	**(mm)**	**(%)**
D. potatorum control	1	16,65	14,45	2,75	69,05	4053,85	23,98	1,68	10,84	65,09
	2	16,60	14,50	2,71	66,06	3728,98	25,08	1,45	10,51	63,34
	3	16,71	14,47	2,74	66,06	3853,65	24,25	1,33	10,49	62,76
	4	16,66	14,58	2,74	60,90	3488,60	24,25	1,45	10,64	63,86
	5	16,56	14,54	2,74	72,47	4148,85	24,25	1,40	10,79	65,13
	6	16,69	14,40	2,67	70,77	3953,53	26,19	1,39	10,42	62,46
	7	16,34	14,52	2,71	66,56	3688,48	25,08	1,26	10,15	62,09
	8	16,48	14,46	2,72	60,50	3434,77	24,81	1,36	10,50	63,70
	9	16,68	14,57	2,74	64,09	3675,09	24,31	1,12	9,67	57,96
Average		**16,60**	**14,50**	**2,72**	**66,55**	**3793,84**	**24,74**	**1,42**	**10,54**	**63,55**
SD		**0,12**	**0,06**	**0,03**	**4,28**	**256,38**	**0,72**	**0,12**	**0,22**	**1,13**
D. potatorum + 0.15% TEMPO-oxidized CNF	1	16,89	14,52	2,84	83,20	5234,18	21,49	1,13	9,31	55,14
	2	16,78	14,68	2,84	85,54	5230,01	21,49	1,19	9,55	56,94
	3	16,93	14,58	2,85	84,59	5327,30	21,21	1,12	9,37	55,36
	4	16,82	14,41	2,80	73,28	4530,89	22,59	1,17	9,30	55,32
	5	16,84	14,59	2,87	78,43	4975,66	20,66	1,13	9,37	55,64
	6	16,83	14,41	2,88	77,36	5063,38	20,38	1,12	9,40	55,84
	7	16,99	14,45	2,86	75,48	4890,78	20,94	1,18	9,46	55,69
Average		**16,87**	**14,52**	**2,85**	**79,70**	**5036,03**	**21,25**	**1,15**	**9,40**	**55,70**
SD		**0,07**	**0,10**	**0,03**	**4,77**	**271,53**	**0,72**	**0,03**	**0,09**	**0,60**
D. potatorum + 0.30% TEMPO-oxidized CNF	1	16,90	14,69	2,96	107,82	7202,86	18,17	1,32	9,46	55,99
	2	16,96	14,75	2,99	114,88	7794,38	17,34	1,34	9,60	56,58
	3	16,96	14,51	2,95	112,84	7701,46	18,45	1,34	9,59	56,55
	4	17,08	14,76	2,99	116,46	7946,87	17,34	1,37	9,70	56,78
	5	17,01	14,50	2,98	112,55	7872,30	17,62	1,32	9,68	56,88
Average		**16,98**	**14,64**	**2,97**	**112,91**	**7703,57**	**17,78**	**1,34**	**9,60**	**56,56**
SD		**0,07**	**0,13**	**0,02**	**3,26**	**294,38**	**0,50**	**0,02**	**0,09**	**0,35**
D. potatorum + 0.50% TEMPO-oxidized CNF	1	17,55	14,63	3,15	171,77	13605,49	12,92	1,57	9,71	55,33
	2	17,63	14,97	3,13	160,58	12049,38	13,47	1,54	9,57	54,28
	3	17,54	14,98	3,17	166,46	12728,95	12,37	1,67	9,79	55,79
	4	17,51	14,80	3,21	159,36	12779,76	11,26	1,59	9,80	55,97
	5	17,48	15,02	3,16	164,58	12396,67	12,64	1,55	9,71	55,55
	6	17,67	15,10	3,18	172,46	13158,21	12,09	1,63	9,84	55,69
Average		**17,56**	**14,92**	**3,17**	**165,87**	**12786,41**	**12,46**	**1,59**	**9,74**	**55,44**
SD		**0,07**	**0,17**	**0,03**	**5,49**	**549,10**	**0,76**	**0,05**	**0,10**	**0,61**
D. potatorum + 0.75% TEMPO-oxidized CNF	1	17,92	15,18	3,42	221,10	19579,12	5,45	1,46	9,50	52,99
	2	18,00	15,03	3,29	210,87	17706,40	9,05	1,42	9,38	52,11
	3	18,16	15,12	3,32	193,20	16468,70	8,22	1,24	9,06	49,89
	4	18,13	15,17	3,39	201,39	17751,68	6,28	1,43	9,55	52,65
	5	18,16	15,07	3,37	222,94	19710,73	6,84	1,38	9,18	50,53
Average		**18,07**	**15,11**	**3,36**	**209,90**	**18243,33**	**7,17**	**1,39**	**9,33**	**51,63**
SD		**0,11**	**0,06**	**0,05**	**12,72**	**1379,94**	**1,45**	**0,09**	**0,21**	**1,35**
D. potatorum + 0.15% mechanically fibrillated CNF	1	16,98	14,47	2,79	82,70	5082,76	22,87	1,35	10,21	60,12
	2	16,64	14,66	2,73	84,80	4764,28	24,53	1,09	9,60	57,70
	3	16,87	14,55	2,78	82,03	4918,60	23,15	1,24	9,88	58,57
	4	16,78	14,61	2,79	80,65	4804,46	22,87	1,47	10,19	60,74
	5	16,89	14,58	2,81	84,38	5153,65	22,32	1,29	10,13	60,00
	6	16,91	14,48	2,79	81,68	4992,37	22,87	1,23	9,86	58,29
	7	16,77	14,25	2,82	74,98	4794,26	22,04	1,59	9,52	56,77
Average		**16,83**	**14,51**	**2,79**	**81,60**	**4930,05**	**22,95**	**1,32**	**9,91**	**58,89**
SD		**0,11**	**0,13**	**0,03**	**3,27**	**152,22**	**0,79**	**0,17**	**0,28**	**1,45**

D. potatorum + *0.30% mechanically fibrillated CNF*	1	16,66	14,07	2,79	83,62	5333,20	22,87	1,12	9,59	57,58
	2	16,85	14,29	2,81	85,66	5433,44	22,32	1,05	9,31	55,27
	3	16,82	14,48	2,78	74,01	4467,04	23,15	1,44	9,81	58,30
	4	16,96	14,24	2,86	82,66	5505,25	20,94	1,31	10,04	59,17
	5	16,91	14,26	2,83	80,36	5210,62	21,76	1,31	9,92	58,68
	6	16,78	14,38	2,80	78,36	4853,35	22,59	1,16	9,60	57,22
Average		**16,83**	**14,29**	**2,81**	**80,78**	**5133,82**	**22,27**	**1,23**	**9,71**	**57,70**
SD		**0,11**	**0,14**	**0,03**	**4,18**	**399,16**	**0,81**	**0,14**	**0,26**	**1,39**
D. potatorum + *0.50% mechanically fibrillated CNF*	1	17,68	14,67	3,08	119,14	9039,36	14,85	1,69	10,53	59,55
	2	17,50	14,59	3,00	112,54	8106,58	17,06	1,50	10,26	58,62
	3	17,54	14,88	3,07	117,18	8517,79	15,13	1,68	10,27	58,56
	4	17,34	14,91	3,00	117,87	8055,43	17,06	1,75	10,42	60,09
	5	17,49	14,65	3,08	109,75	8259,93	14,85	1,44	9,99	57,12
	6	17,66	14,99	3,07	111,72	8056,83	15,13	1,54	10,32	58,46
	7	17,85	14,97	3,07	112,07	8190,94	15,13	1,82	10,72	60,03
Average		**17,58**	**14,81**	**3,05**	**114,32**	**8318,12**	**15,60**	**1,63**	**10,36**	**58,92**
SD		**0,16**	**0,17**	**0,04**	**3,65**	**356,29**	**1,01**	**0,14**	**0,23**	**1,05**
D. potatorum + *0.75% mechanically fibrillated CNF*	1	17,67	14,92	3,16	146,59	11312,10	12,64	1,74	10,55	59,68
	2	17,61	14,78	3,07	150,74	11150,40	15,13	1,79	10,47	59,47
	3	17,8	14,84	3,11	132,58	10090,85	14,02	1,55	10,28	57,76
	4	17,95	14,94	3,17	146,13	11496,96	12,37	1,56	10,34	57,58
	5	17,64	14,97	3,13	146,98	11034,77	13,47	1,69	10,38	58,87
Average		**17,73**	**14,89**	**3,13**	**144,60**	**11017,01**	**13,53**	**1,66**	**10,4**	**58,67**
SD		**0,14**	**0,08**	**0,04**	**6,97**	**546,20**	**1,11**	**0,11**	**0,11**	**0,96**

Table A.2 Raw data for gels with 1% (w/v) *M.pyrifera* alginate and composite gels with 1% (w/v) *M.pyrifera* alginate and different amounts of TEMPO-oxidized and mechanically fibrillated CNF[%(w/v)]. Height (h), diameter (d), weight (w), gradient, Young's modulus (E), syneresis (S), rupture strength (RS), deformation at rupture (D) and percentage of deformation at rupture (*ϵ*).

		h	*d*	*w*	*Gradient*	*E*	*S*	*RS*	*D*	*ϵ*
Alginate	**n**	**(mm)**	**(mm)**	**(g)**	**(N/m)**	**(Pa)**	**(%)**	**(kg)**	**(mm)**	**(%)**
M. pyrifera control	1	14,36	11,94	1,83	347,72	11419,25	49,41	4,20	10,33	71,96
	2	14,36	12,33	1,89	371,04	12188,32	47,75	4,49	10,36	72,12
	3	14,31	12,52	1,83	364,48	10848,50	49,41	3,41	10,07	70,39
	4	14,32	12,24	1,82	369,75	11397,15	49,69	3,52	10,14	70,82
	5	14,49	12,38	1,85	391,79	12342,09	48,86	5,04	10,55	72,80
	6	14,50	12,15	1,84	359,18	11628,78	49,13	3,89	10,59	73,05
	7	14,49	12,32	1,83	341,39	10625,90	49,41	4,09	10,32	71,20
Average		**14,40**	**12,27**	**1,84**	**363,62**	**11492,86**	**49,09**	**4,09**	**10,34**	**71,76**
SD		**0,09**	**0,18**	**0,02**	**16,60**	**633,08**	**0,65**	**0,56**	**0,19**	**1,00**
M. pyrifera + 0.15% TEMPO-oxidized CNF	1	14,84	12,63	1,93	429,05	14474,80	46,64	4,17	10,07	67,86
	2	14,97	12,53	1,92	501,11	17148,46	46,92	4,29	10,02	66,93
	3	14,79	12,47	1,91	467,33	15786,83	47,20	4,11	9,97	67,40
	4	14,77	12,53	1,91	450,78	15061,78	47,20	4,08	9,93	67,20
	5	14,68	12,59	1,89	428,59	13804,11	47,75	4,18	9,96	67,86
	6	14,88	12,49	1,89	392,84	13031,24	47,75	4,16	10,00	67,22
Average		**14,82**	**12,54**	**1,91**	**444,95**	**14884,54**	**47,24**	**4,16**	**9,99**	**67,41**
SD		**0,10**	**0,06**	**0,02**	**37,22**	**1465,66**	**0,44**	**0,07**	**0,05**	**0,38**
M. pyrifera + 0.30% TEMPO-oxidized CNF	1	15,12	12,80	2,18	489,15	20885,96	39,73	4,03	9,68	64,03
	2	15,07	12,84	2,13	431,93	17439,20	41,12	4,11	9,67	64,15
	3	15,09	12,27	2,12	467,43	20499,84	41,39	4,03	9,59	63,55
	4	15,15	12,47	2,12	450,74	19215,11	41,39	4,11	9,66	63,79
	5	15,07	12,62	2,13	430,91	18009,56	41,12	4,08	9,71	64,44
Average		**15,10**	**12,60**	**2,14**	**454,03**	**19209,93**	**40,95**	**4,07**	**9,66**	**63,99**
SD		**0,03**	**0,24**	**0,03**	**24,73**	**1504,11**	**0,69**	**0,04**	**0,04**	**0,34**
M. pyrifera + 0.50% TEMPO-oxidized CNF	1	16,15	13,97	2,58	446,22	23929,78	28,68	4,43	10,09	62,45
	2	15,87	13,91	2,40	521,95	24007,22	33,65	4,69	10,13	63,83
	3	16,13	13,82	2,45	538,58	26580,87	32,27	4,82	10,18	63,09
	4	15,81	13,50	2,39	524,89	25321,84	33,93	4,26	9,97	63,07
	5	16,19	13,96	2,51	537,30	27378,31	30,61	4,52	10,10	62,37
Average		**16,03**	**13,83**	**2,47**	**513,79**	**25443,61**	**31,83**	**4,54**	**10,09**	**62,96**
SD		**0,18**	**0,19**	**0,08**	**38,48**	**1533,47**	**2,20**	**0,22**	**0,08**	**0,59**
M. pyrifera + 0.75% TEMPO-oxidized CNF	1	16,21	14,00	2,57	660,14	35107,05	28,95	4,05	9,64	59,49
	2	16,18	13,92	2,61	745,28	41273,29	27,85	4,34	9,82	60,70
	3	16,20	13,99	2,55	623,56	32674,29	29,51	4,20	9,60	59,23
	4	16,18	13,93	2,58	651,18	35186,94	28,68	4,42	9,62	59,43
Average		**16,19**	**13,96**	**2,58**	**670,04**	**36060,39**	**28,74**	**4,25**	**9,67**	**59,71**
SD		**0,02**	**0,04**	**0,03**	**52,52**	**3665,69**	**0,69**	**0,17**	**0,10**	**0,67**
M. pyrifera + 0.15% mechanically fibrillated CNF	1	14,77	12,48	1,91	446,04	15022,97	47,20	5,16	10,36	70,15
	2	14,54	12,44	1,92	445,96	15038,00	46,92	5,17	10,45	71,88
	3	14,68	12,53	1,92	481,61	16161,63	46,92	5,89	10,70	72,88
	4	14,80	12,53	1,91	458,48	15350,14	47,20	4,94	10,37	70,06
	5	14,80	12,48	1,90	450,45	15043,53	47,47	6,21	10,68	72,16
	6	14,86	12,49	1,90	420,58	14080,32	47,47	5,55	10,56	71,05
	7	14,86	12,44	1,93	395,02	13755,38	46,64	5,37	10,53	70,89
	8	14,70	12,53	1,90	447,01	14709,93	47,47	5,68	10,60	72,12
Average		**14,75**	**12,49**	**1,91**	**443,14**	**14895,24**	**47,16**	**5,50**	**10,53**	**71,40**
SD		**0,11**	**0,04**	**0,01**	**25,70**	**743,27**	**0,31**	**0,42**	**0,13**	**1,02**
M. pyrifera + 0.30% mechanically fibrillated CNF	1	14,93	12,38	2,03	471,94	18444,16	43,88	5,18	10,55	70,64
	2	15,09	12,47	2,04	398,98	15686,87	43,60	5,33	10,24	67,85
	3	14,82	12,62	2,05	433,70	16511,82	43,33	5,08	10,18	68,67
	4	14,73	12,56	2,07	466,56	18173,52	42,77	5,60	10,29	69,86
	5	14,81	12,66	2,07	476,52	18368,75	42,77	5,37	10,26	69,30
Average		**14,88**	**12,54**	**2,05**	**449,54**	**17437,02**	**43,27**	**5,31**	**10,30**	**69,27**
SD		**0,14**	**0,11**	**0,02**	**32,89**	**1259,35**	**0,49**	**0,20**	**0,14**	**1,08**

M. pyrifera + *0.50% mechanically fibrillated CNF*	1	15,24	13,24	2,20	437,98	17942,06	39,18	5,04	10,55	69,25
	2	15,15	13,27	2,16	454,23	17750,88	40,29	4,96	10,44	68,89
	3	15,44	13,24	2,20	480,07	19924,52	39,18	5,67	10,81	70,03
	4	15,36	13,38	2,17	455,79	17927,72	40,01	4,74	10,47	68,15
	5	15,37	13,27	2,18	460,45	18594,92	39,73	5,36	10,70	69,63
	6	15,29	13,13	2,18	437,03	17933,60	39,73	5,11	10,57	69,13
	7	15,20	13,26	2,15	458,51	17837,99	40,56	5,13	10,59	69,69
Average		**15,29**	**13,26**	**2,18**	**454,86**	**18273,10**	**39,81**	**5,15**	**10,59**	**69,25**
SD		**0,10**	**0,07**	**0,02**	**14,63**	**778,56**	**0,52**	**0,30**	**0,13**	**0,62**
M. pyrifera + *0.75% mechanically fibrillated CNF*	1	15,97	13,65	2,40	575,36	27654,53	33,65	5,32	10,63	66,54
	2	15,84	13,46	2,30	443,85	19985,95	36,42	4,96	10,47	66,10
	3	15,84	13,60	2,33	545,10	24673,68	35,59	5,47	10,74	67,78
	4	15,90	13,58	2,44	522,51	26111,65	32,55	5,67	10,65	67,01
	5	15,92	13,65	2,42	473,30	23057,23	33,10	5,74	10,75	67,51
Average		**15,89**	**13,59**	**2,38**	**512,02**	**24296,61**	**34,26**	**5,43**	**10,65**	**66,99**
SD		**0,06**	**0,08**	**0,06**	**53,30**	**2950,85**	**1,66**	**0,31**	**0,11**	**0,68**

Table A.3 Raw data for gels with 1% (w/v) *L. hyperborea* stipe alginate and composite gels with 1% (w/v) *L. hyperborea* stipe alginate and different amounts of TEMPO-oxidized and mechanically fibrillated CNF[%(w/v)]. Height (h), diameter (d), weight (w), gradient, Young's modulus (E), syneresis (S), rupture strength (RS), deformation at rupture (D) and percentage of deformation at rupture (*ϵ*).

		h	*d*	*w*	*Gradient*	*E*	*S*	*RS*	*D*	*ϵ*
Alginate	**n**	**(mm)**	**(mm)**	**(g)**	**(N/m)**	**(Pa)**	**(%)**	**(kg)**	**(mm)**	**(%)**
L. hyperborea control	1	16,10	13,81	2,61	596,06	33371,28	27,85	4,26	10,17	63,19
	2	16,51	13,91	2,57	610,29	33485,65	28,95	5,21	10,63	64,37
	3	16,46	14,07	2,58	587,54	31657,98	28,68	5,76	10,88	66,08
	4	16,68	13,79	2,56	585,74	32780,79	29,23	6,25	11,17	66,96
	5	16,39	13,91	2,58	553,15	30364,95	28,68	4,98	10,47	63,85
	6	16,24	13,40	2,55	568,54	32552,29	29,51	4,21	10,04	61,82
	7	16,18	13,84	2,57	550,98	29882,98	29,01	6,36	11,14	68,84
Average		**16,37**	**13,82**	**2,57**	**583,55**	**32368,82**	**28,81**	**5,11**	**10,56**	**64,38**
SD		**0,20**	**0,21**	**0,02**	**20,21**	**1181,22**	**0,57**	**0,81**	**0,43**	**1,89**
L. hyperborea + 0.30% TEMPO-oxidized CNF	1	16,61	14,30	2,74	685,29	40685,66	24,25	4,11	9,73	58,59
	2	16,70	14,39	2,78	743,55	45119,40	23,15	4,01	9,68	57,98
	3	16,84	14,22	2,79	689,67	43527,16	22,87	3,66	9,52	56,51
	4	16,87	14,36	2,79	731,92	45377,78	22,87	3,86	9,58	56,80
	5	16,83	14,26	2,75	721,43	43961,07	23,98	4,10	9,67	57,46
	6	16,80	14,38	2,76	660,58	39801,46	23,70	3,74	9,48	56,42
	7	16,88	14,17	2,77	683,39	42916,73	23,42	3,75	9,51	56,32
	8	16,77	14,35	2,79	689,25	42538,31	22,87	3,84	9,61	57,33
Average		**16,79**	**14,30**	**2,77**	**700,64**	**42990,95**	**23,39**	**3,88**	**9,60**	**57,18**
SD		**0,09**	**0,08**	**0,02**	**28,39**	**1969,54**	**0,54**	**0,17**	**0,09**	**0,81**
L. hyperborea + 0.75% TEMPO-oxidized CNF	1	17,60	14,58	3,01	982,63	71760,87	16,79	4,63	9,82	55,78
	2	17,53	14,62	3,00	972,49	69884,51	17,06	4,83	9,88	56,34
	3	17,63	14,60	3,04	962,97	71659,60	15,96	4,64	9,90	56,15
	4	17,59	14,75	3,06	874,73	64470,85	15,41	3,76	9,37	53,25
	5	17,60	14,59	3,04	1021,43	75984,19	15,96	4,01	9,47	53,80
	6	17,68	14,59	3,12	906,75	71373,19	13,75	4,45	10,01	56,60
Average		**17,61**	**14,62**	**3,05**	**953,50**	**70855,54**	**15,82**	**4,38**	**9,74**	**55,32**
SD		**0,05**	**0,06**	**0,04**	**53,49**	**3734,82**	**1,18**	**0,41**	**0,26**	**1,43**
L. hyperborea + 0.30% mechanically fibrillated CNF	1	16,56	14,06	2,63	649,95	36664,86	27,29	4,29	10,00	60,38
	2	16,75	13,94	2,63	667,84	38765,01	27,29	4,24	9,95	59,40
	3	16,56	14,11	2,61	651,56	35942,56	27,85	4,48	10,09	60,93
	4	16,56	14,05	2,69	618,93	36578,09	25,63	4,02	9,88	59,68
	5	16,62	14,16	2,59	631,58	34189,72	28,40	4,35	10,01	60,21
	6	16,68	14,12	2,61	640,05	35513,20	27,85	4,13	9,93	59,54
	7	16,54	14,14	2,63	663,01	36934,41	27,29	4,36	10,15	61,35
	8	16,67	14,10	2,66	670,98	38756,00	26,46	4,14	9,96	59,77
Average		**16,62**	**14,09**	**2,63**	**649,24**	**36667,98**	**27,26**	**4,25**	**10,00**	**60,16**
SD		**0,08**	**0,07**	**0,03**	**18,24**	**1550,95**	**0,87**	**0,15**	**0,09**	**0,70**
L. hyperborea + 0.75% mechanically fibrillated CNF	1	17,27	14,28	2,87	921,22	62564,58	20,66	4,91	10,11	58,52
	2	17,26	14,61	2,90	971,89	64346,01	19,83	6,08	10,57	61,23
	3	17,24	14,47	2,87	842,63	55637,51	20,66	4,88	10,27	59,55
	4	17,29	14,40	2,88	971,53	65415,30	20,38	5,52	10,44	60,39
	5	17,30	14,47	2,90	894,92	60542,10	19,83	5,57	10,44	60,37
	6	17,27	14,46	2,90	864,95	58493,88	19,83	5,28	10,43	60,36
Average		**17,27**	**14,45**	**2,89**	**911,19**	**61166,56**	**20,20**	**5,38**	**10,38**	**60,07**
SD		**0,02**	**0,11**	**0,02**	**53,91**	**3693,74**	**0,42**	**0,45**	**0,16**	**0,93**

Table A.4 Raw data composite gels with 1% (w/v) *M.pyrifera* alginate and other polysaccharides [%(w/v)]. Height (h), diameter (d), weight (w), gradient, Young's modulus (E), syneresis (S), rupture strength (RS), deformation at rupture (D) and percentage of deformation at rupture (ϵ).

		h	*d*	*w*	*Gradient*	*E*	*S*	*RS*	*D*	ϵ
Alginate	**n**	**(mm)**	**(mm)**	**(g)**	**(N/m)**	**(Pa)**	**(%)**	**(kg)**	**(mm)**	**(%)**
M. pyrifera + 0.30% dextran	1	14,96	12,54	1,98	302,11	10969,70	45,26	5,33	10,84	72,47
	2	14,89	12,42	1,96	334,06	12060,22	45,82	4,87	10,65	71,52
	3	14,95	12,80	2,05	358,85	13396,93	43,33	4,63	10,58	70,78
	4	14,89	12,74	1,98	349,06	12222,34	45,26	5,35	10,94	73,49
	5	14,95	12,50	2,01	354,49	13340,72	44,43	5,12	10,76	71,98
	6	14,92	12,88	2,00	332,63	11649,98	44,71	5,08	10,81	72,42
	7	14,98	12,91	2,03	354,49	12782,70	43,88	5,11	10,78	71,93
	8	14,74	12,62	1,96	315,47	10919,64	45,82	5,10	10,73	72,81
	9	14,92	12,61	2,02	344,44	12819,37	44,20	4,98	10,65	71,35
Average		**14,91**	**12,67**	**2,00**	**337,64**	**12167,78**	**44,81**	**5,07**	**10,76**	**72,17**
SD		**0,07**	**0,17**	**0,03**	**20,49**	**966,63**	**0,90**	**0,23**	**0,11**	**0,82**
M. pyrifera + 0.75% dextran	1	15,28	13,04	2,10	322,71	12450,63	41,95	4,75	10,76	70,45
	2	15,14	13,07	2,11	315,93	12136,54	41,67	4,75	10,73	70,90
	3	15,21	13,05	2,13	337,12	13299,13	41,12	4,81	10,80	71,03
	4	15,10	13,00	2,11	327,82	12695,56	41,67	5,74	11,09	73,42
	5	15,20	13,05	2,14	312,84	12449,06	40,84	4,90	10,89	71,61
	6	15,22	13,07	2,09	316,92	12007,94	42,22	4,47	10,59	69,60
	7	15,18	13,08	2,10	317,55	12097,04	41,95	4,39	10,53	69,34
	8	15,23	12,95	2,07	300,37	11379,33	42,77	4,72	10,66	70,00
	9	15,19	13,07	2,07	323,68	11988,98	42,82	5,20	10,95	72,08
Average		**15,19**	**13,04**	**2,10**	**318,91**	**12314,40**	**41,77**	**4,81**	**10,76**	**70,79**
SD		**0,05**	**0,04**	**0,02**	**10,83**	**560,46**	**0,61**	**0,41**	**0,18**	**1,31**
M. pyrifera + 0.30% sodium hyaluronate	1	15,64	13,29	2,25	312,58	13642,01	37,80	3,98	11,99	76,68
	2	15,75	13,39	2,25	278,81	12071,22	37,80	3,65	12,36	78,50
	3	15,69	13,34	2,25	306,35	13312,36	37,80	2,44	10,51	67,00
	4	15,73	13,46	2,26	302,08	13041,95	37,52	3,94	11,99	76,24
	5	15,53	13,30	2,21	294,72	12303,28	38,90	3,44	11,22	72,26
	6	15,69	13,30	2,21	306,17	12912,95	38,90	3,56	11,57	73,72
	7	15,73	13,09	2,24	310,03	13902,97	38,08	4,45	12,41	78,87
	8	15,71	13,20	2,27	309,82	14013,64	37,25	4,04	11,88	75,60
Average		**15,68**	**13,30**	**2,24**	**302,57**	**13150,05**	**38,01**	**3,69**	**11,74**	**74,86**
SD		**0,07**	**0,11**	**0,02**	**11,10**	**710,12**	**0,60**	**0,60**	**0,63**	**3,87**
M. pyrifera + 0.75% sodium hyaluronate	1	16,79	14,20	2,73	203,04	12267,29	24,53	2,50	10,87	64,72
	2	16,96	14,52	2,86	248,51	15919,68	20,94	3,01	11,11	65,53
	3	17,06	14,34	2,80	212,03	13426,11	22,59	2,67	10,99	64,40
	4	16,79	14,43	2,69	189,91	10787,73	25,63	2,13	10,49	62,46
	5	17,10	14,68	2,79	244,15	14681,40	22,87	2,22	10,48	61,26
	6	16,89	14,44	2,75	150,25	8960,83	23,98	2,71	11,10	65,73
Average		**16,93**	**14,44**	**2,77**	**207,98**	**12673,84**	**23,42**	**2,54**	**10,84**	**64,02**
SD		**0,13**	**0,16**	**0,06**	**36,47**	**2555,03**	**1,65**	**0,33**	**0,29**	**1,78**
M. pyrifera + 0.30% xanthan	1	15,74	13,38	2,24	348,33	14960,38	38,08	2,98	9,93	63,11
	2	15,80	13,32	2,21	358,35	15174,26	38,90	3,54	10,16	64,27
	3	15,72	13,36	2,25	350,31	15206,42	37,80	3,21	10,00	63,61
	4	15,73	13,38	2,24	335,85	14415,13	38,08	2,92	9,93	63,15
	5	15,77	13,39	2,24	351,82	15116,68	38,08	3,02	9,91	62,83
	6	15,72	13,31	2,22	341,98	14560,21	38,63	3,26	10,10	64,24
	7	15,74	13,33	2,21	350,37	14757,79	38,90	3,39	10,13	64,37
	8	15,44	13,12	2,16	354,39	14438,75	40,29	3,10	9,88	64,02
Average		**15,71**	**13,32**	**2,22**	**348,92**	**14828,7**	**38,59**	**3,18**	**10,01**	**63,70**
SD		**0,11**	**0,09**	**0,03**	**7,08**	**330,06**	**0,80**	**0,21**	**0,11**	**0,61**
M. pyrifera +	1	16,68	14,13	2,66	345,62	19890,08	26,46	2,91	10,12	60,70
	2	16,39	14,07	2,60	307,53	16756,84	28,12	2,74	9,97	60,80
	3	16,45	14,00	2,65	335,32	19240,80	26,74	2,77	10,06	61,14
	4	16,59	14,05	2,70	339,14	20228,42	25,36	2,86	10,09	60,83
	5	16,58	14,01	2,65	352,82	20375,76	26,74	2,71	9,99	60,25
	6	16,65	13,91	2,66	344,92	20445,89	26,46	2,91	10,07	60,49

0.75% xanthan	7	16,37	14,00	2,68	343,87	20082,58	25,91	2,82	10,07	61,48
	8	16,57	13,9	2,65	321,40	18845,12	26,74	2,75	10,01	60,43
	9	16,55	13,94	2,62	353,70	20101,04	27,62	2,71	9,92	59,95
Average		**16,54**	**14,00**	**2,65**	**336,33**	**19483,19**	**26,57**	**2,81**	**10,05**	**60,76**
SD		**0,11**	**0,08**	**0,03**	**14,88**	**1236,50**	**0,79**	**0,08**	**0,05**	**0,40**

Table A.5 Raw data for gels with low concentration of *M.pyrifera* alginate [%(w/v)]. Height (h), diameter (d), weight (w), gradient, Young's modulus (E), syneresis (S), rupture strength (RS), deformation at rupture (D) and percentage of deformation at rupture (*ϵ*).

		h	***d***	***w***	***Gradient***	***E***	***S***	***RS***	***D***	***ϵ***
Alginate	**n**	**(mm)**	**(mm)**	**(g)**	**(N/m)**	**(Pa)**	**(%)**	**(kg)**	**(mm)**	**(%)**
0.10% M. pyrifera	1	14,34	12,79	1,30	28,24	407,26	64,06	0,03	3,60	25,08
	2	13,67	12,95	1,34	29,18	415,79	62,96	0,04	4,52	33,03
	3	13,87	12,46	1,33	25,95	399,29	63,23	0,02	3,52	25,39
	4	13,25	12,50	1,31	22,90	324,43	63,78	0,04	4,35	32,79
Average		**13,78**	**12,68**	**1,32**	**26,57**	**386,69**	**63,51**	**0,04**	**3,99**	**29,07**
SD		**0,45**	**0,24**	**0,02**	**2,80**	**42,05**	**0,50**	**0,01**	**0,51**	**4,43**
0.20% M. pyrifera	1	11,06	10,20	0,97	33,76	328,76	73,18	0,46	7,03	63,55
	2	11,13	10,12	0,98	33,77	343,10	72,91	0,60	7,42	66,62
	3	11,14	10,23	0,94	32,88	301,10	74,01	0,58	7,35	66,01
	4	11,11	10,20	0,92	32,74	288,09	74,57	0,62	7,49	67,38
	5	11,11	10,07	0,93	34,34	316,77	74,29	0,50	7,03	63,30
Average		**11,11**	**10,16**	**0,95**	**33,5**	**315,56**	**73,79**	**0,55**	**7,26**	**65,37**
SD		**0,03**	**0,07**	**0,03**	**0,67**	**21,78**	**0,72**	**0,07**	**0,22**	**1,84**
0.20% M. pyrifera + 0.75% TEMPO-oxidized CNF	1	17,81	14,33	2,93	128,93	9345,7	19,00	0,55	8,47	47,54
	2	17,95	14,38	2,92	129,43	9326,1	19,28	0,52	8,39	46,76
	3	17,76	14,40	2,89	126,32	8797,3	20,11	0,53	8,29	46,67
	4	17,94	14,30	2,95	125,20	9306,0	18,45	0,54	8,40	46,80
	5	17,85	14,33	2,89	125,59	8876,7	20,11	0,55	8,44	47,29
	6	17,65	14,04	2,84	117,70	8275,7	21,49	0,42	8,01	45,35
Average		**17,83**	**14,30**	**2,90**	**125,53**	**8987,9**	**19,74**	**0,52**	**8,33**	**46,74**
SD		**0,11**	**0,13**	**0,04**	**4,21**	**424,16**	**1,07**	**0,05**	**0,17**	**0,76**

Table A.6 Raw data for composite gels of CNF and *M.pyrifera* alginate used in for ICP-MS. Height (h), diameter (d), weight (w), gradient, Young's modulus (E), syneresis (S), rupture strength (RS), deformation at rupture (D) and percentage of deformation at rupture (*ϵ*).

		h	*d*	*w*	*Gradient*	*E*	*S*	*RS*	*D*	*ϵ*
Alginate	**n**	**(mm)**	**(mm)**	**(g)**	**(N/m)**	**(Pa)**	**(%)**	**(kg)**	**(mm)**	**(%)**
0.75% TEMPO - oxidized CNF	1	18,97	15,44	3,48	61,11	5732,97	3,80	0,10	5,98	31,54
	2	18,66	15,63	3,47	62,25	5574,24	4,07	0,09	5,45	29,19
	3	18,90	14,92	3,40	56,05	5355,99	6,01	0,05	5,60	29,65
	4	18,77	15,51	3,55	75,91	7267,55	1,86	0,09	5,47	29,15
	5	18,64	15,57	3,52	63,99	5935,27	2,69	0,12	6,11	32,77
Average		**18,79**	**15,41**	**3,48**	**63,86**	**5973,20**	**3,68**	**0,09**	**5,72**	**30,46**
SD		**0,15**	**0,29**	**0,06**	**7,36**	**754,09**	**1,57**	**0,02**	**0,30**	**1,62**
0.75% TEMPO - oxidized CNF + 0.20% M. pyrifera	1	17,81	14,33	2,93	128,93	9345,78	19,0	0,55	8,47	47,54
	2	17,95	14,38	2,92	129,43	9326,17	19,2	0,52	8,39	46,76
	3	17,76	14,40	2,89	126,32	8797,37	20,1	0,53	8,29	46,67
	4	17,94	14,30	2,95	125,20	9306,00	18,4	0,54	8,40	46,80
	5	17,85	14,33	2,89	125,59	8876,73	20,1	0,55	8,44	47,29
	6	17,65	14,04	2,84	117,70	8275,72	21,4	0,42	8,01	45,35
Average		**17,83**	**14,30**	**2,90**	**125,53**	**8987,96**	**19,7**	**0,52**	**8,33**	**46,74**
SD		**0,11**	**0,13**	**0,04**	**4,21**	**424,16**	**1,07**	**0,05**	**0,17**	**0,76**
0.75% TEMPO - oxidized CNF + 0.375% M. pyrifera	1	17,22	13,76	2,56	193,31	11217,46	29,2	1,42	9,68	56,19
	2	17,23	13,70	2,58	224,01	13326,51	28,6	1,39	9,60	55,71
	3	17,08	13,60	2,64	220,54	13818,68	27,0	1,38	9,76	57,12
	4	17,06	13,70	2,59	213,55	12676,66	28,4	1,44	9,69	56,81
	5	17,03	13,65	2,55	208,00	12035,23	29,5	1,33	9,58	56,24
	6	17,12	13,66	2,59	207,51	12434,17	28,4	1,41	9,85	57,54
Average		**17,12**	**13,68**	**2,59**	**211,15**	**12584,78**	**28,5**	**1,40**	**9,69**	**56,60**
SD		**0,08**	**0,05**	**0,03**	**10,96**	**924,70**	**0,87**	**0,04**	**0,10**	**0,68**
0.75% TEMPO - oxidized CNF + 0.75% M. pyrifera	1	16,26	13,78	2,51	423,68	22252,31	30,6	2,94	9,59	58,97
	2	16,20	13,98	2,56	445,83	23578,74	29,2	2,89	9,46	58,42
	3	16,36	13,96	2,55	417,14	22168,92	29,5	2,83	9,61	58,71
	4	16,33	13,96	2,51	431,41	22172,96	30,6	2,88	9,41	57,65
	5	16,28	13,66	2,52	440,97	23786,65	30,3	3,36	9,65	59,26
Average		**16,29**	**13,87**	**2,53**	**431,81**	**22791,92**	**30,0**	**2,98**	**9,54**	**58,60**
SD		**0,06**	**0,14**	**0,02**	**11,85**	**817,16**	**0,65**	**0,22**	**0,10**	**0,62**
0.75% TEMPO -oxidized CNF + 1.00% M. pyrifera	1	16,21	14,00	2,57	660,14	35107,05	28,9	4,05	9,64	59,49
	2	16,18	13,92	2,61	745,28	41273,29	27,8	4,34	9,82	60,70
	3	16,20	13,99	2,55	623,56	32674,29	29,5	4,20	9,60	59,23
	4	16,18	13,93	2,58	651,18	35186,94	28,6	4,42	9,62	59,43
Average		**16,19**	**13,96**	**2,58**	**670,04**	**36060,39**	**28,7**	**4,25**	**9,67**	**59,71**
SD		**0,02**	**0,04**	**0,03**	**52,52**	**3665,69**	**0,69**	**0,17**	**0,10**	**0,67**
0.375% TEMPO - oxidized CNF + 0.375% M. pyrifera	1	15,77	12,89	2,12	145,24	6031,90	41,3	1,46	9,92	62,91
	2	15,62	12,87	2,06	149,93	5841,37	43,0	1,29	9,51	60,85
	3	15,64	12,87	2,04	146,54	5606,26	43,6	1,51	9,91	63,38
	4	15,62	12,88	2,04	145,89	5565,63	43,6	1,60	9,77	62,55
	5	15,63	12,83	2,05	145,71	5660,88	43,3	1,27	9,37	59,96
	6	15,74	12,95	2,10	134,20	5407,69	41,9	1,26	9,49	60,27
Average		**15,67**	**12,88**	**2,07**	**144,59**	**5685,62**	**42,8**	**1,40**	**9,66**	**61,65**
SD		**0,07**	**0,04**	**0,03**	**5,36**	**220,33**	**0,93**	**0,14**	**0,24**	**1,47**

Table A.7 Raw data from analysis of calcium concentration [mM] done with ICP-MS on pure *M. pyrifera* alginate gels, CNF gels and CNF – alginate composites of various concentrations.

Gel type			*Calcium concentration (C_x) after x NaCl treatments, [mM]*		
M. pyr. alginate	***CNF***		***C_0***	***C_1***	***C_2***
0.75 %	-	A	87,26	14,35	5,61
		B	83,30	13,71	5,85
		C	82,82	10,42	6,38
		Mean	**84,46**	**12,83**	**5,95**
		SD	**2,43**	**2,11**	**0,39**
-	0.75 %	D	49,79	5,05	0,90
		E	49,81	5,57	1,04
		F	50,62	4,80	0,55
		Mean	**50,07**	**5,14**	**0,83**
		SD	**0,47**	**0,39**	**0,25**
0.2 %	0.75 %	G	67,85	9,01	2,33
		H	64,87	9,83	1,78
		I	62,59	10,67	1,90
		Mean	**65,10**	**9,84**	**2,00**
		SD	**2,64**	**0,83**	**0,29**
0.375 %	0.75 %	J	45,92	5,15	1,58
		K	37,67	7,89	1,95
		L	63,13	10,97	3,80
		Mean	**48,91**	**8,00**	**2,44**
		SD	**12,99**	**2,91**	**1,19**
0.75 %	0.75 %	M	66,53	14,90	5,62
		N	71,09	13,35	5,89
		O	69,44	17,65	5,96
		Mean	**69,02**	**15,30**	**5,83**
		SD	**2,31**	**2,17**	**0,18**
0.375 %	0.375 %	P	63,68	10,87	2,56
		Q	58,31	11,19	3,23
		R	63,63	10,10	5,03
		Mean	**61,87**	**10,72**	**3,61**
		SD	**3,08**	**0,56**	**1,27**

Table A.8 Weight data attained from examination of volume stability, of pure *M. pyrifera* alginate gels, CNF gels and CNF – alginate composites of various concentrations, upon NaCl treatment.

Gel type			*Weight (w_X) after x NaCl treatments, [g]*			*Weight fraction (w_X/w_0) after x NaCl treatments*		
Alginate	***CNF***		w_0	w_1	w_2	w_0/w_0	w_1/w_0	w_2/w_0
0.75 %	-	A	0,155	0,256	0,340	1	1,655	2,201
		B	0,176	0,279	0,361	1	1,591	2,055
		C	0,183	0,288	0,370	1	1,574	2,020
		Mean				**1**	**1,606**	**2,092**
		SD				**-**	**0,043**	**0,096**
-	0.75 %	D	0,583	0,513	0,485	1	0,879	0,831
		E	0,461	0,436	0,394	1	0,944	0,855
		F	0,400	0,376	0,342	1	0,941	0,855
		Mean				**1**	**0,922**	**0,847**
		SD				**-**	**0,037**	**0,014**
0.2 %	0.75 %	G	0,397	0,410	0,386	1	1,035	0,974
		H	0,314	0,329	0,287	1	1,045	0,914
		I	0,387	0,398	0,406	1	1,028	1,051
		Mean				**1**	**1,036**	**0,980**
		SD				**-**	**0,009**	**0,069**
0.375 %	0.75 %	J	0,336	0,360	0,386	1	1,069	1,146
		K	0,316	0,342	0,369	1	1,083	1,170
		L	0,305	0,339	0,370	1	1,111	1,213
		Mean				**1**	**1,088**	**1,176**
		SD				**-**	**0,021**	**0,034**
0.75 %	0.75 %	M	0,266	0,326	0,383	1	1,225	1,442
		N	0,439	0,494	0,569	1	1,125	1,296
		O	0,325	0,376	0,441	1	1,158	1,360
		Mean				**1**	**1,169**	**1,366**
		SD				**-**	**0,051**	**0,074**
0.375 %	0.375 %	P	0,243	0,285	0,308	1	1,173	1,269
		Q	0,311	0,346	0,394	1	1,114	1,269
		R	0,402	0,437	0,518	1	1,089	1,289
		Mean				**1**	**1,125**	**1,275**
		SD				**-**	**0,043**	**0,011**

D Examples of calculations

Young's modulus, corrected for weight:

$$E_{CORR.} = \frac{1000 \cdot GRADIENT \cdot HEIGHT}{\left(\frac{m_{AFTER}}{m_{BEFORE}}\right)^2 \cdot \pi \left(\frac{DIAMETER}{2}\right)^2} = \frac{1000 \cdot 347.72 N/m \cdot 14.36 mm}{\left(\frac{3.62 mm}{1.83 mm}\right)^2 \cdot \pi \left(\frac{11.94 mm}{2}\right)^2} = 11419.25 Pa$$

Syneresis:

$$S = \left(1 - \frac{m_{AFTER}}{m_{BEFORE}}\right) \cdot 100^o/_o = \left(1 - \frac{1.83 g}{3.62 g}\right) \cdot 100^o/_o = 49.41^o/_o$$

Percentage of deformation at rupture:

$$D = \left(\frac{DEFORMATION\ AT\ RUPTURE}{HEIGHT}\right) \cdot 100^o/_o = \left(\frac{10.33 mm}{14.36 mm}\right) \cdot 100^o/_o = 71.96^o/_o$$

Polymers **2017**, *9*, 378; doi:10.3390/polym9080378 www.mdpi.com/journal/polymers

E **Published Paper**

polymers

MDPI

Mechanical Properties of Composite Hydrogels of Alginate and Cellulose Nanofibrils

Olav Aarstad [1], Ellinor Bævre Heggset [2], Ina Sander Pedersen [1], Sindre Hove Bjørnøy [3], Kristin Syverud [2,4] and Berit Løkensgard Strand [1,*]

1 NOBIPOL, Department of Biotechnology and Food Sciences, NTNU Norwegian University of Science and Technology, NO-7491 Trondheim, Norway; olav.a.aarstad@ntnu.no (O.A.); inasande@stud.ntnu.no (I.S.P.)
2 RISE PFI, Nanocellulose and carbohydrate polymers, Høgskoleringen 6b, 7491 Trondheim, Norway; ellinor.heggset@rise-pfi.no (E.B.H.); kristin.syverud@rise-pfi.no (K.S.)
3 Department of Physics, NTNU Norwegian University of Science and Technology, NO-7491 Trondheim, Norway; sindre.bjornoy@ntnu.no
4 Department of Chemical Engineering, NTNU Norwegian University of Science and Technology, NO-7491 Trondheim, Norway
* Correspondence: berit.l.strand@ntnu.no; Tel.: +47-7341-2243

Received: 27 June 2017; Accepted: 17 August 2017; Published: 19 August 2017

Abstract: Alginate and cellulose nanofibrils (CNF) are attractive materials for tissue engineering and regenerative medicine. CNF gels are generally weaker and more brittle than alginate gels, while alginate gels are elastic and have high rupture strength. Alginate properties depend on their guluronan and mannuronan content and their sequence pattern and molecular weight. Likewise, CNF exists in various qualities with properties depending on, e.g., morphology and charge density. In this study combinations of three types of alginate with different composition and two types of CNF with different charge and degree of fibrillation have been studied. Assessments of the composite gels revealed that attractive properties like high rupture strength, high compressibility, high gel rigidity at small deformations (Young's modulus), and low syneresis was obtained compared to the pure gels. The effects varied with relative amounts of CNF and alginate, alginate type, and CNF quality. The largest effects were obtained by combining oxidized CNF with the alginates. Hence, by combining the two biopolymers in composite gels, it is possible to tune the rupture strength, Young's modulus, syneresis, as well as stability in physiological saline solution, which are all important properties for the use as scaffolds in tissue engineering.

Keywords: alginate; TEMPO; cellulose nanofibrils; nanocellulose; composite; hydrogels; mechanical properties

1. Introduction

Recently, composite materials of alginate and cellulose nanofibrils (CNF) have shown promising results for bioprinting and tissue engineering applications [1–3]. In particular, the shear thinning properties of CNF combined with the viscous alginate that form hydrogels with divalent cations at physiological conditions, are attractive for bioprinting [1].

Alginates are linear copolymers of 1 → 4 linked β-D-mannuronic acid (M) and α-L-guluronic acid (G). The monomers are arranged in a block-wise pattern along the chain with homopolymeric regions of M and G termed M- and G-blocks, respectively, interspaced with regions of alternating structure (MG-blocks) [4]. Alginate forms hydrogels by crosslinking with divalent cations where, particularly, the G-blocks, but also the MG-blocks, are important for the mechanical properties of the resulting gel [5,6]. Alginate hydrogels can be produced under physiological conditions [7,8]. This,

together with a low immunogenic profile [9], makes them popular materials for biomedical applications and, in particular, in tissue engineering [10]. Cellulose provides structural support in plant cell walls and can be processed as fibres or nanoscaled fibrils of cellulose, known as cellulose nanofibrils (CNF). Several procedures for preparation of CNF from cellulose pulp exist, among them 2,2,6,6-tetramethylpiperidine-1-oxyl radical (TEMPO)-mediated oxidation using sodium hypochlorite as oxidant [11]. By this, aldehyde and carboxyl groups are introduced on the surfaces of the cellulose fibrils and increase the negative charge of the fibrils. Aqueous dispersions of CNF have gel like character at low concentrations (approx. 0.5%) held together by fibril entanglement and hydrogen bonds. CNF hydrogels can be produced with cations, both monovalent and with higher valency [12], where gels with higher valency ions form stronger gels [12,13].

Due to their availability, renewability, biocompatibility, and low toxicity, both alginate and cellulose are attractive materials for a range of applications such as films, gels, and as viscosifiers. Although being suggested for tissue engineering applications, not much is known about the mechanical properties of composite gels of alginate and CNF. Composite gels of alginate and either oxidized CNC (cellulose nanocrystals) or CNF have shown increased compression strength, suggested to be the result of Ca^{2+} mediated crosslinking of the two components [14]. TEMPO-oxidized BNC (bacterial nanocellulose) have been used to improve the mechanical and chemical stability of an alginate hydrogel, and the composite gel was used for encapsulation of fibroblasts. The nanofibrous structure of the BNC was suggested to mimic the fibre structures of collagen and fibronectin found in the extracellular matrix [15–17], and fibroblast viability and proliferation was found to be higher in comparison to pure alginate gels [18]. For chondrocytes, the combination of sulfated alginate with nanocellulose were promising regarding cell viability and phenotype [2]. It has previously been shown that Young's modulus of the matrix is important for the development of stem cells into differentiated cell types/tissues [19]. Hence, the structure, chemistry, as well as the mechanical properties are of importance in tissue engineering applications. Although composite gels of CNF and alginate have been demonstrated in the literature, a systematic study of mechanical properties on combinations of different types of alginate and CNF has not yet been reported.

We hypothesize that by combining alginate and CNF, the advantageous properties of the individual constituents, i.e., the stiffness of CNF and the compressibility of alginate, could be preserved in the composite gel making it possible to tailor the mechanical properties.

2. Materials and Methods

2.1. Materials

Alginates: Alginates extracted from *Durvillea potatorum* and *Laminaria hyperborea* stipe were obtained from FMC Health and Nutrition (Sandvika, Norway), and *Macrocystis pyrifera* alginate were purchased from Sigma-Aldrich (St. Louis, MO, USA). Molecular weight and NMR parameters are given Table 1. For a detailed study on alginate fine structure see [20].

Table 1. M_w and sequence parameters in alginates used in this study [20] [1].

Alginate	M_w (kDa)	PI	F_G	F_M	F_{GG}	F_{GM}	F_{MM}	F_{MGM}	F_{GGG}	$N_{G>1}$
D. potatorum	163	1.76	0.32	0.68	0.20	0.12	0.56	0.07	0.16	6
M. pyrifera	177	1.94	0.41	0.59	0.21	0.20	0.40	0.18	0.17	5
L. hyperborea	200	2.23	0.67	0.33	0.56	0.11	0.23	0.08	0.52	13

[1] Molecular weight (M_w) and polydispersity index (PI = M_w/M_n) were determined from SEC-MALLS. Sequence parameters were calculated from ^{1}H-NMR spectra. F_G and F_M denotes the fraction of guluronic and mannuronic acid, respectively. Fractions of dimers and trimers of varying composition are denoted by two and three letters, respectively.

Nanocellulose: Never-dried bleached kraft softwood pulp fibres were used as the source material for production of two types of nanocellulose. The first type was produced using a mechanical pretreatment (beating in a Claflin mill; 1000 kWh/ton for 1 h) followed by homogenization (denoted

as mechanically-fibrillated CNF). Production of the second type (referred to as oxidized CNF) was performed using TEMPO-mediated oxidation as pretreatment, as described by Saito and colleagues [11]. NaClO (2.3 mmol per gram of cellulose) was used in the oxidation. The fibrillation was done by using a Rannie 15 type 12.56x homogenizer (APV, SPX Flow Technology, Silkeborg, Denmark) with a pressure drop of 1000 bar in each pass. Mechanically-fibrillated CNF was homogenized using five passes, the oxidized CNF using 1 pass. The concentration of the pretreated samples was 1% (*w*/*v*) before fibrillation.

The composition of carbohydrates was determined according to the standard method NREL/ TP-510-42618, using sulphuric acid hydrolysis. The composition of carbohydrate monomers produced during the hydrolysis was analysed using high-performance anion-exchange chromatography with pulsed amperometric detection (HPAEC-PAD; Dionex ICS-5000, (Thermo Fisher Scientific, Waltham, MA, USA) with a CarboPac PA1 column (Thermo Fisher Scientific, Waltham, MA, USA) and gradient elution using sodium hydroxide for elution. The carbohydrate composition of the two CNF samples is shown in Appendix A.

The intrinsic viscosity was determined as described in ISO-standard 5351:2010, using cupriethylenediamine (CED) as a solvent. The oxidized CNF was subjected to a second oxidation before the analysis. This is due to a significant amount of aldehyde groups in the oxidized samples which induce depolymerization through a β-elimination reaction [21]. In order to avoid this, a selective oxidation of the aldehyde groups was performed using sodium chlorite under acidic conditions.

The carboxylate content was determined using conductometric titration as previously described [22,23]. The equipment used was a 902 Titrando, an 856 conductivity module and Tiamo software (Metrohm). Residual fibres were quantified with a FibreTester device, as previously described by Chinga-Carrasco and colleagues [24]. The fibrillated structure and analyses of the fibre structure from atomic force microscopy (AFM) imaging with resulting characteristics of the cellulose nanofibrils have previously been described [25]. A summary of nanocellulose characteristics is shown in Appendix A.

Control polymers: Hyaluronic acid ($M_w = 8.7 \times 10^5$ Da) was a gift from Novamatrix (Norway), xanthan ($M_w = 9.6 \times 10^5$ Da) was a gift from CP Kelco (USA), and dextran ($M_w = 2.0 \times 10^6$ Da) was purchased from Pharmacia AB (Stockholm, Sweden). The molecular weight of the samples were determined using a HPLC system consisting of serially connected TSK G6000 PWxl and G5000PWxl columns (Tosoh Bioscience LLC, Tokyo, Japan) followed by a Dawn Helios II MALLS photometer and an Optilab T-rEX differential refractometer (Wyatt Technology, Santa Barbara, CA, USA). The elution buffer (0.15 M $NaNO_3$ with 1 mM EDTA, pH 6.0) was applied at a flow rate of 0.5 mL/min. Data were collected and processed using ASTRA 6.1 software. Refractive index increment values (dn/dc) used in the calculations were set to 0.148 for dextran and 0.150 for alginate, hyaluronic acid and xanthan.

2.2. Preparation of Gel Cylinders

Alginate gels were prepared by internal gelling with $CaCO_3$ and D-glucono δ-lactone (GDL) as previously described [26]. Briefly, $CaCO_3$ (56.25 mg, particle size 4 µm) suspended in 5 mL MQ water was added to 25 mL, 1.5% (*w*/*v*) of alginate solution. The mixture was degassed under vacuum suction before addition of 7.5 mL of a freshly made solution of GDL (200.36 mg). The mixture was immediately poured into 24-well tissue culture plates (16/18 mm, Costar, Cambridge, MA, USA) and left at room temperature for minimum 20 h. The gel cylinders were removed from the tissue culture plates and weight was measured on the calcium unsaturated gels before being immersed in a solution of 50 mM $CaCl_2$ and 200 mM NaCl (100 mL per gel) and left for 24 h at 4 °C for calcium saturation before syneresis and compression measurement.

Two-component gels of alginate and either xanthan, dextran or hyaluronic acid were made by a simillar procedure as for pure alginate gels. The two components were dissolved together in 25 mL MQ water, yielding a final concentration in the gelling solution of 1% (*w*/*v*) *M. pyrifera* alginate and 0.30% or 0.75% (*w*/*v*) of the other component.

Alginate—CNF composite gels were made by mixing 450 mg alginate powder with MQ water and CNF dispersion corresponding to final concentrations of 1% (*w*/*v*) alginate and 0.15–0.75% (*w*/*v*) CNF and a total volume of 30 mL. The blends were dissolved for at least 18 h under constant stirring

and homogenized for 5 min with a Vdi 12 Ultra Turrax at 11,500 rpm. Twenty-five grams of the blend was weighed out and added $CaCO_3$ and GDL as described above.

2.3. Syneresis and Gel Strength Measurements

Syneresis was determined after calcium saturation as $(W_0 - W)/W_0) \times 100$, where W_0 and W are the initial weights of the samples before calcium saturation and final weights of the calcium saturated gels, respectively. Force/deformation curves was recorded at 22 °C on a Stable Micro Systems TA-XT2 texture analyser equipped with a P/35 probe and at a compression rate of 0.1 mm/s [26]. The gels were subjected to uniaxial compression surpassing the point of rupture, where force and deformation was recorded. Young's modulus was calculated as $G \cdot (h/A)$ where G is the initial slope (N/m) of the stress deformation curve and h and A is the height and area of the gel cylinder, respectively. In order to compare Young's modulus of gels with different degree of syneresis, the relationship $E = k \cdot c^2$ was applied [27] where k is characteristic for each type of alginate, and c is the weight concentration.

2.4. Volume Stability and Calcium Binding

The weight and calcium content of pure and composite gels of *M. pyr.* alginate and oxidized CNF were measured before and after saline treatments. Gel cylinders immersed in a solution of 50 mM $CaCl_2$ and 200 mM NaCl for 24 h were cut in three approximately equal pieces, weighed and immersed separately in 40 mL of 150 mM NaCl solution at room temperature for 24 h. The gel pieces were gently removed from the solution, weighed and subjected to a second saline treatment. After weighing, the gels were added 0.5 mL of 100 mM Na-EDTA, pH = 7.0. All samples were vortexed and centrifuged
(2400 rpm, 5 min) before they were diluted 100 × in 5% HNO_3 and calcium content analysed with ICP-MS (type 8800 Triple Quadrupole ICP-MS with ASX-520 Autosampler from Agilent Technologies, Santa Clara, CA, USA). As internal standards ^{115}In and ^{89}Y were used.

2.5. Light Microscopy

Homogeneity of the gels were assessed on a Nikon Eclipse TS100 microscope (Nikon Instruments, Tokyo, Japan) by placing a drop of gelling solution between two microscopy slides and observing the gellation in the microscope using 40 × magnification.

2.6. Preparation of Aerogels for Scanning Electron Microscopy (SEM)

After the gels had been cast, the cylinders where cut, in the hydrated state, into 200 µm thick sections using a vibrating blade microtome (VT1000S, Leica Biosystems, Nussloch GmBH, Wetzlar, Germany). The sections where dehydrated in increasing concentrations of ethanol, before substitution with acetone and finally critical-point dried using liquid CO_2 (Emitech K850 critical point dryer, Quorum Technologies, Lewes, UK). The sections were mounted on aluminum stubs using carbon tape and sputter coated (208 HR, Cressington, Watford, UK) with a 5 nm layer of Pt/Pd (80/20). SEM analysis was performed with an acceleration voltage of 5 kV (S-5500 S(T)EM, Hitachi, Tokyo, Japan).

2.7. Fourier Transform Infrared Spectroscopy (FTIR) Characterization

The infrared spectra of vacuum dried samples were collected on a Bio-Rad Excalibur series FTS 3000 spectrophotometer (Bio-Rad, Hercules, CA, USA). The spectra were acquired in transmission mode on the films at a spectral range of 4000−500 cm^{-1}.

2.8. Statistical Analysis

All values are expressed as means ± standard deviations. Comparisons between groups were made using a two-sided Student's t-test and Microsoft Excel worksheet (2011). Statistical outcomes (*p*-values) are presented in Appendix B.

3. Results and Discussion

3.1. Composite Hydrogels of Alginate and CNF

Composite gels of *D. pot.*, *M. pyr.*, and *L. hyp.* alginates and CNF (mechanically-fibrillated or oxidized) saturated with calcium were measured with respect to gel rigidity (Young's modulus) and volume reduction upon gel formation (syneresis, Figure 1). Secondly, resistance to breakage and deformation at breakage was determined (Figure 2).

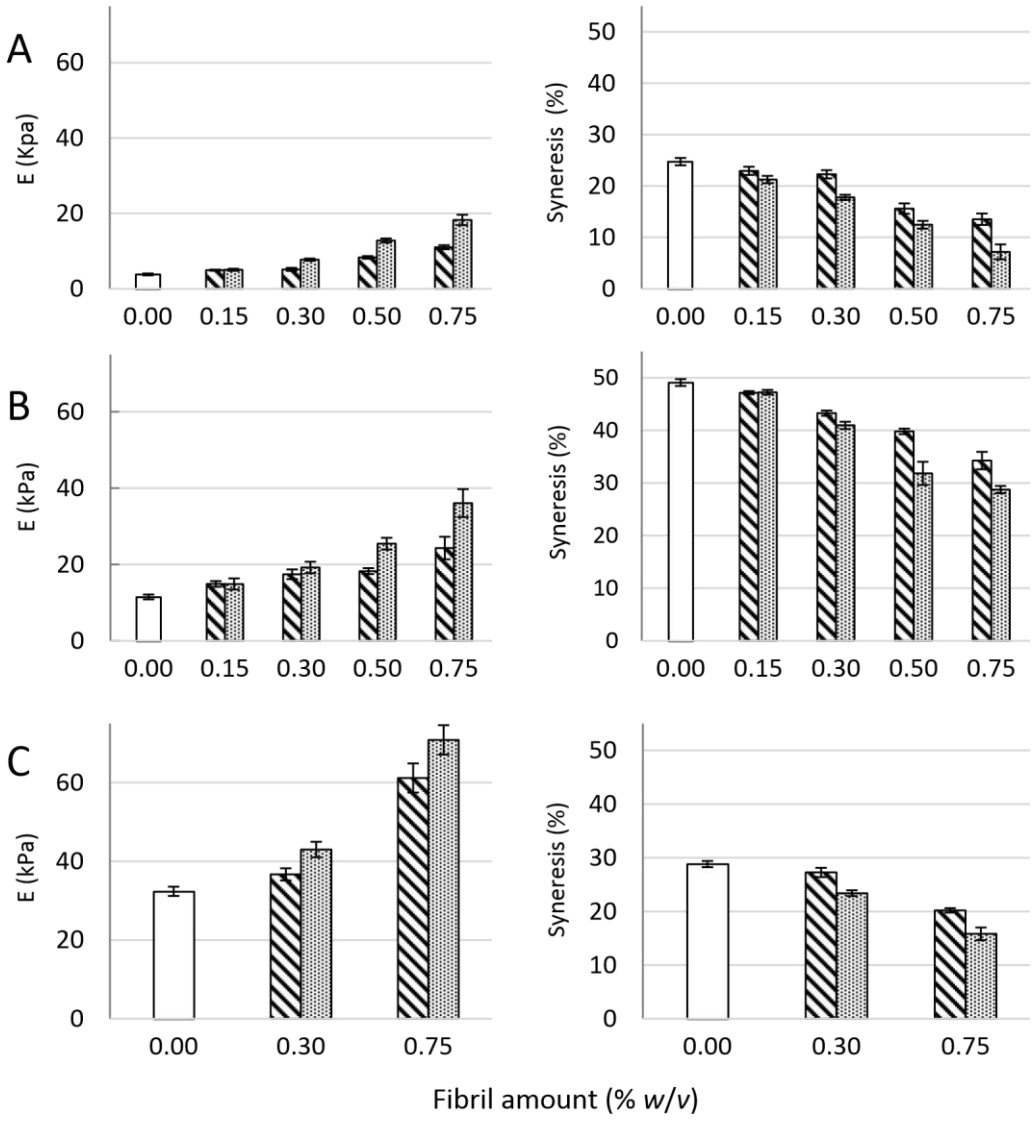

Figure 1. Young's modulus (E, left panel) and syneresis (right panel) of alginate-CNF composite Ca-gels made from 1% (*w*/*v*) *D. potatorum* (**A**), *M. pyrifera* (**B**), and *L. hyperborea* (**C**) alginates and 0–0.75% (*w*/*v*) mechanically-fibrillated (▨) and oxidized CNF (▩). Bars are means ± standard deviations, shown for n = 5–8 gels. *P*-values are presented in Tables A3 and A4 in Appendix B.

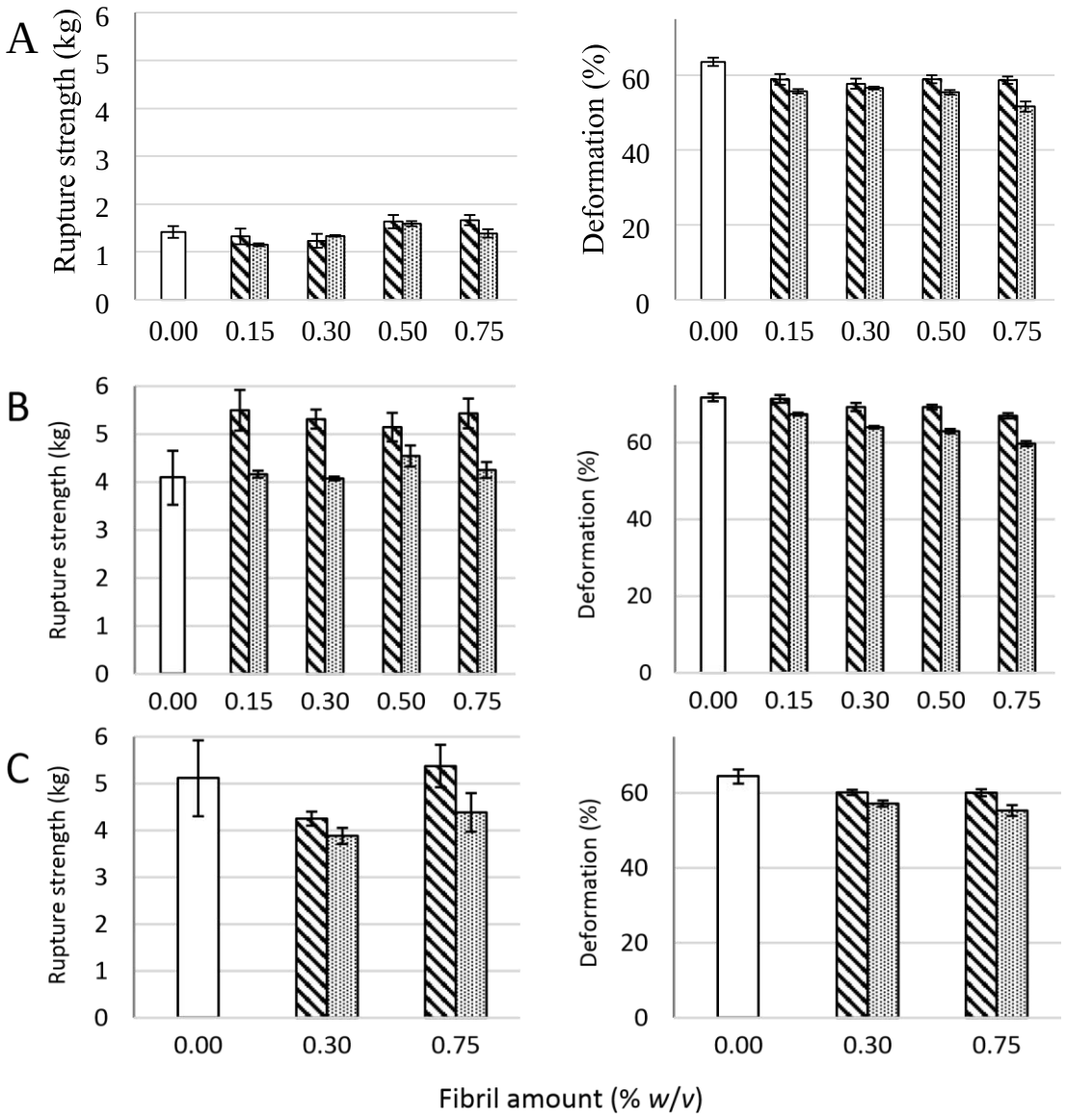

Figure 2. Rupture strength measured as the force at rupture (left panel) and compression at rupture (right panel) for *D. potatorum* (**A**), *M. pyrifera* (**B**), and *L. hyperborea* (**C**) Ca-alginate gels and mechanically-fibrillated (▨) and oxidized (▩) CNF. Bars are means +/− standard deviations, shown for n = 5–8 gels. P-values are presented in Tables A3 and A4 in Appendix B.

The composite gels of alginate and CNF showed increased Young's modulus and reduced syneresis compared to pure alginate gels. An increase in Young's modulus was observed for composite gels of both mechanically-fibrillated CNF and oxidized CNF relative to the alginate gels alone. The largest effect was seen for composite gels of oxidized CNF and alginates with intermediate to low G-content (*M. pyr.* and *D. pot.*) with a 3–5 fold increase in Young's modulus for the gels containing 0.75% (*w*/*v*) oxidized CNF relative to no addition of CNF. Additionally, for the alginate with a high G-content (*L. hyp.* stipe) that is known to form stiff gels with calcium [27], the effect of addition of CNF on Young's modulus was profound with about two times increase for the highest concentration. Syneresis was reduced for the composite gels relative to the alginate gels, meaning that the gels shrunk less after saturation with calcium when CNF was added to the hydrogels. As seen from Figure 1, the alginate gels are highly syneretic when saturated with calcium. The syneresis is known to be linked to the content of G-blocks, but indeed also to MG-blocks in the alginate [5,26], hence, the high degree of syneresis for the alginate from *M. pyr.* is as expected. Regardless of the composition of the alginate, CNF reduced the syneresis with increasing effect at increasing concentrations.

Although the reduction in syneresis was highest for the oxidized CNF—*M. pyr*. alginate composite gel (49% to 29%), the largest relative decrease was observed for *D. pot*. alginate where the syneresis was reduced from 25% to 7% with the addition of 0.75% (*w*/*v*) oxidized CNF.

No significant effect of the presence of fibrils was seen on the rupture strength of the gels, except for the increase in rupture strength for the gels of alginate from *M. pyr*. upon the addition of mechanically-fibrillated CNF (Figure 2). An overall trend was a slight reduction in the rupture strength when oxidized CNF was added to the alginate relative to the mechanically-fibrillated CNF. However, the alginate concentration is higher in the pure alginate gels than in the composite gels, due to the large differences in syneresis. The rupture strength per concentration unit alginate is, therefore, increased in the composite gels. Calcium alginate gels with a high content of G-blocks, such as the alginate from *L. hyp* stipe, are known to form strong gels due to the high numbers of crosslinks, as also reflected in the Young's modulus (Figure 1). Alginate from *M. pyr*. has a high content of MG-blocks and is known to withstand large deformation. This has been explained in terms of energy dissipating effects of collapsing MG block junction zones during deformation [28]. Surprisingly, the force at rupture increased by about 30% when mechanically-fibrillated CNF was added to this alginate gel, independently of the concentration of fibrils.

3.2. Composite Hydrogels of Oxidized CNF and Alginate

In order to better evaluate separate and combined effects of the two biopolymer components, calcium crosslinked gels with either oxidized CNF or alginate solely (0.75% (*w*/*v*)) were prepared and measured with respect to gel rigidity, syneresis, deformation, and force at rupture (Figure 3). Hydrogels of TEMPO-oxidized CNF have previously been produced with both monovalent and divalent ions [12]. Although the Young's modulus of alginate and oxidized CNF gels were similar in our study, large differences were seen for the syneresis and the rupture strength underlining the contribution of the two components to the composite system. Oxidized CNF gels displayed almost no syneresis in contrast to the highly syneretic gels from *M. pyr*. alginate. For the rupture strength, the alginate contributed with a high degree of compressibility as shown by the compression to 70% before rupture at about 4 kg force. The oxidized CNF, on the other hand, had a rupture strength of less than 0.1 kg. A dose-dependent increase in syneresis and rupture strength upon the addition of alginate to oxidized CNF was observed. The potential effect on the properties by increasing the dry weight content in the hydrogels were studied by a control containing half concentration of the two components and thus same dry matter content as in the systems of alginate and CNF alone. Additionally, here, a combined effect of the two components could be seen on the syneresis and rupture strength. A combination of 0.75% alginate with 0.75% oxidized CNF resulted in a more than four-fold increase in Young's modulus, exceeding a solely additive effect of the two separate systems. Representative force-deformation curves of composite gels of alginate and oxidized CNF is shown in Appendix D.

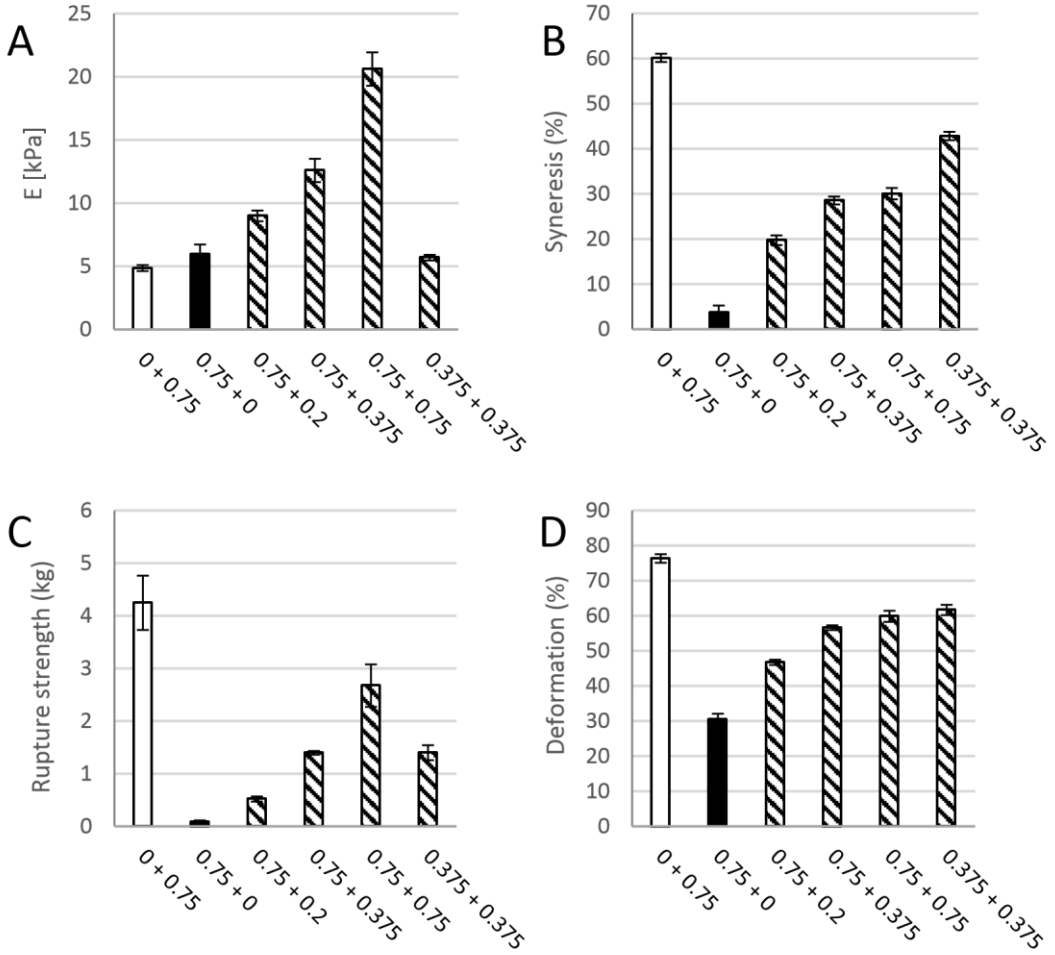

Figure 3. Young's modulus (E, (**A**)), syneresis (**B**), rupture strength (**C**) and deformation at rupture (**D**) of a pure 0.75% (*w*/*v*) *M. pyrifera* alginate gel (□), a pure (0.75% *w*/*v*) oxidized CNF gel (■), and composite gels of 0.75% (*w*/*v*) of each of the two materials (▨). Mean +/− standard deviation shown for n = 5–8 gels.

3.3. Composite Hydrogels of Alginate and Other Polysaccharides

To study more specifically the effect of addition of the long cellulose nanofibrils to alginate, control experiments using other polysaccharides in composite alginate hydrogels were conducted. Polysaccharides with approximately the same molecular weight, but different charge density and flexibility were added to calcium-alginate hydrogels of *M. pyr.* alginate to study the effect on mechanical properties. Dextran, having an α-(1,6)-linked glucose backbone with varying degree of α-(Glc-1,3) branching, is a highly-flexible polysaccharide without charges. Sodium hyaluronate is a stiffer molecule, with alternating 4-linked β-D-glucuronic acid and 3-linked *N*-acetyl-β-D-glucosamine, with negative charges due to the guluronic acid, but with no specific calcium affinity. Xanthan consists of a (1,4)-β-D-Glc main chain where every second unit is (3,1) linked to a D-Man-(1,4)-β-D-GlcA-(1,2)-α-D-Man side chain with varying degree of acetyl and pyruvate groups on the internal and terminal mannose. Xanthan has the ability to form very stiff double-stranded structures. Finally, increasing concentrations of alginate were investigated to compare the effects relative to the effects of addition of CNF on Young's modulus, syneresis, and resistance to rupture (Figure 4).

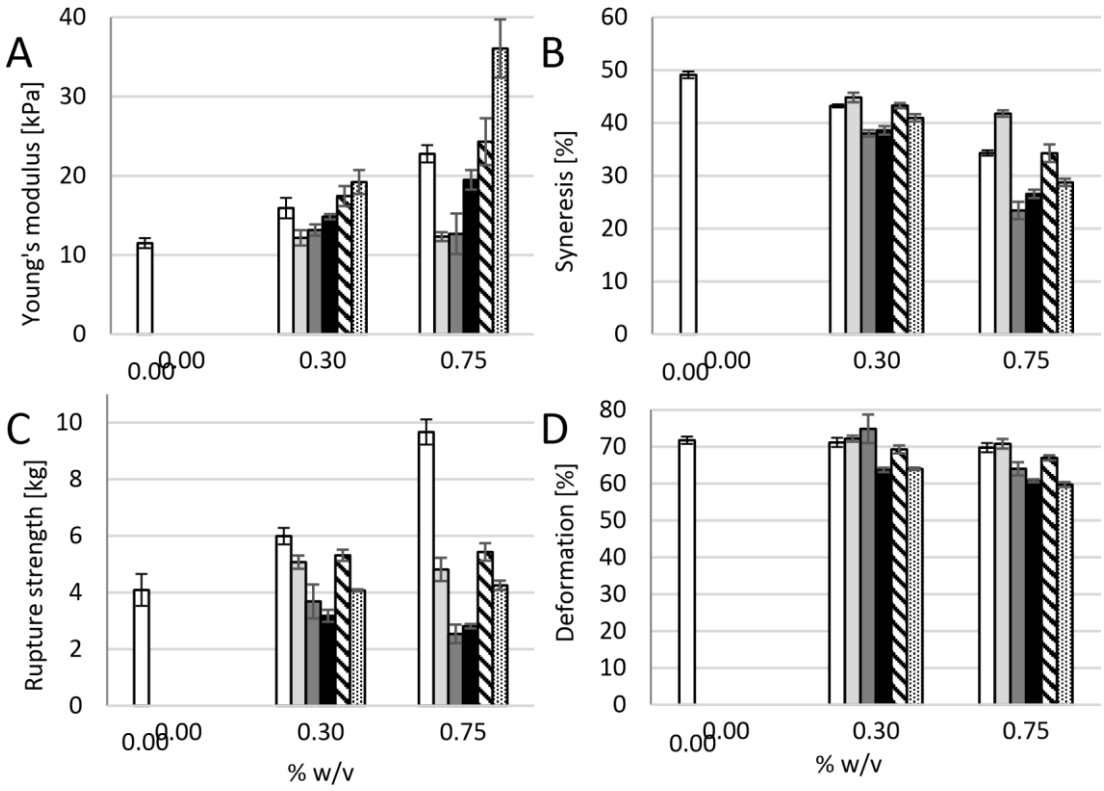

Figure 4. Young's modulus (E, (**A**)), syneresis (**B**), rupture strength (**C**), and deformation at rupture (**D**) of *M. pyrifera* alginate gels (1% *w*/*v*) with 0.30 and 0.75% (*w*/*v*) addition of *M. pyrifera* alginate (□), dextran(▨), hyaluronic acid (▩), xanthan (■), mechanically-fibrillated CNF (▧) and oxidized CNF (▦). Bars are means +/− standard deviations, shown for n = 5–9 gels. *P*-values are presented in Tables A5 and A6 in Appendix B.

Addition of dextran and sodium hyaluronate to the alginate did not affect the Young's modulus for any concentration showing that neither the increase in dry matter nor net charge by itself result in an increase in gel stiffness. A concentration-dependent increase in stiffness was seen for alginate from *M. pyr*. Although having a relatively high content of MG-blocks, the alginate from *M. pyr.* also contains a fraction of very long G-blocks [20]. Both G-blocks and MG-blocks are known to contribute to the crosslinking with calcium [5], hence, an increase in stiffness upon increase in concentration of alginate for the calcium saturated gels is as expected with increasing numbers of crosslinks per unit volume. For 0.75% (*w*/*v*) added polysaccharides, xanthan, and mechanically-fibrillated CNF gave about a doubling in the Young's modulus, compared to the pure alginate gel (1% (*w*/*v*)). Xanthan, which can be viewed as rigid rods at the length scale of a G-block junction zone, shows similarities with the addition of long G-blocks to alginate gels that results in stiffer gels with reduced syneresis [29]. The very long G-blocks have been suggested to act as reinforcement bars in the alginate hydrogel network. However, the largest increase was obtained by the addition of oxidized CNF with a 3.5 times increase in Young's modulus compared to the 1% alginate gel and also a 50% increase in Young's modulus compared to the 1.75% alginate gel for the composite gel of 1.0% alginate and 0.75% oxidized CNF. This emphasizes the combined effect of both stiffness and length of the fibres combined with the charge being important for the final stiffness of the composite gels.

In general, all the added biopolymers caused a concentration-dependent reduction in syneresis (Figure 4). Least effect was seen for the dextran, which caused slightly more syneresis than increasing the concentration of alginate. The syneresis was markedly reduced by adding xanthan and hyaluronic acid, compared to alginate alone (Figure 4). This suggests that osmotic pressure, rather than

interference with G-block junction zones, affects the degree of syneresis for these composite gels. The addition of mechanically fibrillated CNF resulted in same syneresis as for the increased alginate concentrations, however, again the oxidized CNF caused less syneresis.

The rupture strength of the alginate gels was highly influenced by the alginate concentration (Figure 4). By increasing the concentration of alginate from 1.0% to 1.75% (*w*/*v*), the rupture strength increased from 4 kg to 9 kg. None of the other additives were near this increase of rupture strength. Again, there was a slight positive effect on the rupture strength by the addition of mechanically-fibrillated CNF, and no effect was seen on the addition of oxidized CNF although a slight reduction in deformation at rupture could be observed. Hence, ionic interactions between the alginate and cellulose may be weak, although significant, for the initial resistance against compression, however, they are not comparable to the alginate crosslinking when it comes to resisting the force at high deformations. Dextran had a slight positive effect on the rupture strength, however, both hyaluronan and xanthan caused a reduction in the rupture strength.

3.4. Composite Gel Morphology and Homogeneity

Investigation of the composite gels with microscopy revealed that the cellulose was homogeneously distributed in the alginate gel that appear as transparent in the light microscope (Figure 5). No phase separation was seen either by optical microscopy or scanning electron microscopy, which further indicates a good integration between the alginate and the cellulose fibrils. The oxidized CNF has a higher (negative) charge than the fibrils in the mechanically-fibrillated quality (Table A2 in Appendix A). Additionally, the cellulose fibrils differed in size as seen in Figure 5, Appendix A Table A2, and from [25]. Although the oxidized CNF sample contains a large fraction of nanosized fibrils (optically inactive in Figure 5), it contains a major fraction of residual fibres (Figure 5, Appendix A, Table A2). It is, thus, a potential for further improvements of the mechanical properties of the composite hydrogels by increasing the yield of the fibrillation. However, the oxidized fibrils are much thinner and more homogeneous than the mechanically-fibrillated fibrils. Previous studies on composite films based on Ca^{2+} crosslinked alginate and cellulose showed increasing mechanical properties by increasing the amount of the fibrils in the biocomposite and by decreasing the fibril size. However, the introduction of negative charges on the surface of the cellulose fibrils increased the mechanical crosslinking even further [30]. Hence, this suggests that the charges, more than the size of the fibrils, influence the mechanical properties of the composite material.

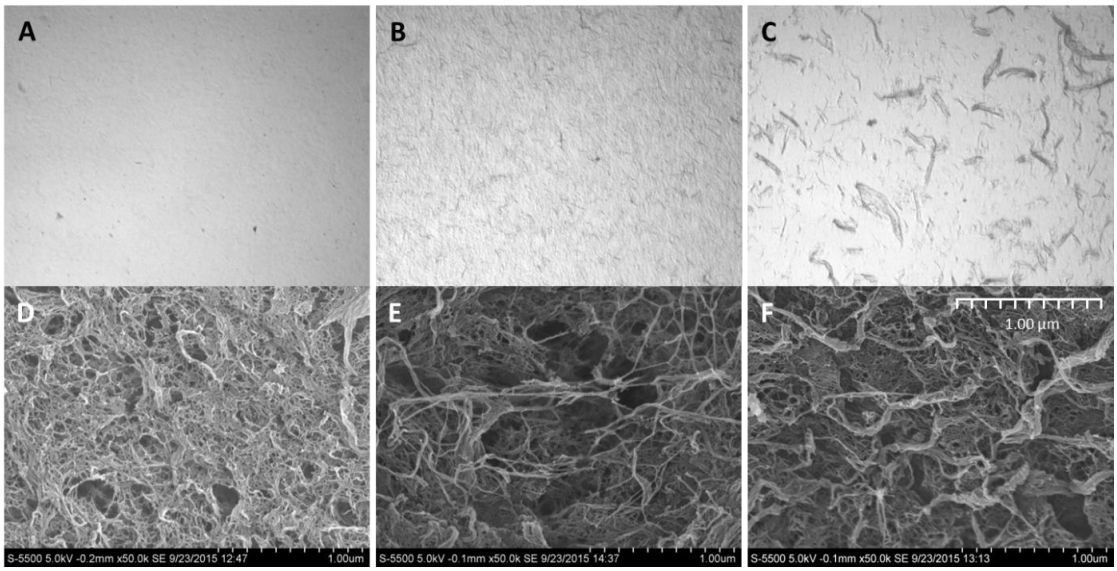

Figure 5. Microscopy of hydrogels of *M. pyrifera* alginate (1% (*w*/*v*)) (**A**), and composite gels with 0.30% mechanically fibrillated (**B**), and 0.30% oxidized CNF (**C**) at 40 × magnification. SEM images of supercritically-dried gels of the same composition (**D**–**F**).

In SEM, all the samples, including the alginate sample, show tread-like structures caused by the drying step which is necessary before SEM imaging (Figure 5). This is commonly seen for alginate hydrogels also when using supercritical drying, intended to preserve the original structure in the samples [31]. No formation of honeycomb structure, which is typically formed when freeze-drying CNF-samples, is observed [32]. A structural difference is observed upon the addition of CNF where some larger fibre structures was observed, both for the mechanically-produced and oxidized CNF. Additionally, here, for both types of cellulose fibrils, the fibrils seem to be well-integrated with the alginate with no indication of phase separation.

3.5. Volume Stability and Calcium Binding

The alginate and oxidized CNF gels were finally exposed to physiological saline solution (150 mM NaCl) to assess the volume stability and the binding of calcium in the gels (Figure 6). Surprisingly, the weak Ca-CNF gels (Figure 4) and all gels of alginate and oxidized CNF were stable during the exposure to NaCl solution. This is in contrast to the well-known swelling of Ca-alginate gels [33] recognized by the exchange of calcium ions with sodium ions and ingress of water into the gel. The stability in physiological solutions is important both for handling and in vitro studies of the biomaterial construct as well as for in vivo use. When the content of calcium was measured in the gels, an accumulation of calcium was found in the gels containing alginate for the Ca-saturated systems, with more calcium in the gels containing alginate solely than in the mixed system of same concentrations of alginate and oxidized CNF. Upon treatment with saline solution, increasing concentrations of calcium were found for increasing alginate concentrations. Similar calcium content was found in the gels containing alginate alone and alginate with oxidized CNF, pointing towards a more complex explanation of the increase in Young's modulus (Figure 1, Figure 3, and Figure 4) than calcium binding solely.

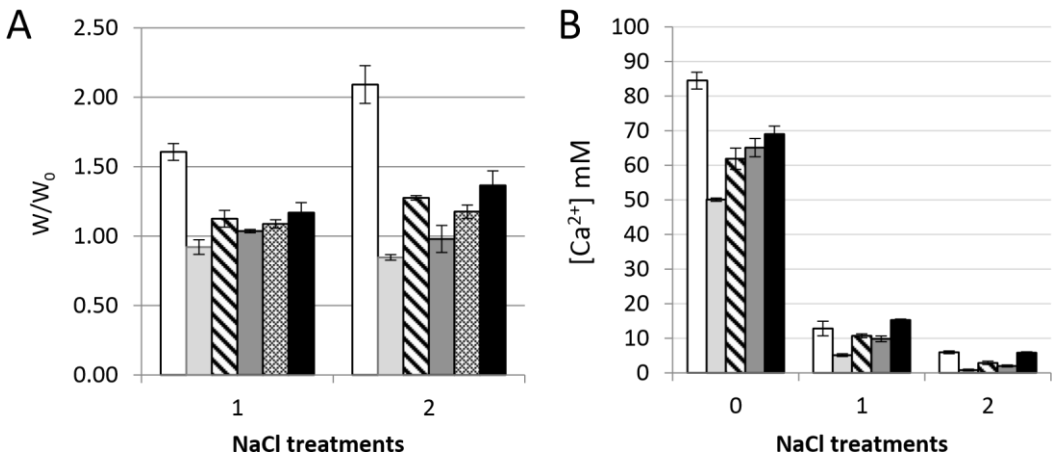

Figure 6. Calcium gels of *M. pyr*. alginate and oxidized CNF subjected to treatments with 0.9% (*w*/*v*) NaCl. Stability of gels (w/w_0, (**A**)) and calcium concentration (**B**) before and after dialysis against 150 mM NaCl solution. 0.75% (*w*/*v*) *M. pyr*. alginate (□), 0.75% (*w*/*v*) oxidized CNF (□), 0.375% (*w*/*v*) oxidized CNF + 0.375% (*w*/*v*) *M. pyr*. (▨), 0.75% (*w*/*v*) oxidized CNF + 0.2% (*w*/*v*) *M. pyr*.(▩), and 0.75% (*w*/*v*) oxidized CNF + 0.75% (*w*/*v*) *M. pyr*. (■). Mean ± standard deviation are shown for three gels.

3.6. Intermolecular Interaction Studied by FT-IR

FT-IR spectra of selected samples were obtained in an attempt to detect intermolecular interactions (Figure 7 and Appendix D). The spectra were normalized with respect to the characteristic $\nu(COO)_{asym}$ vibration band around 1600 cm^{-1}. This was done for better comparison of the wavenumber region where calcium-polymer interaction is most likely to be observed. Both calcium-saturated and –unsaturated composite gels were studied to see if the calcium content influenced the carboxylic groups, as well as to compare our results to previous observations. Calcium-unsaturated gels

contained only the calcium released from $CaCO_3$(s) as a result of the hydrolysis of GDL during gel formation, whereas the calcium saturated gels were obtained after incubation in 50 mM $CaCl_2$ + 200 mM NaCl for 24 h. As the spectra of the hydrogel composite itself are disturbed by the high water content, FTIR spectra of dried samples were obtained. Spectra of alginate powder and oxidized CNF powder were also compared with the dried CNF-alginate composite hydrogels.

It has previously been reported that the (C=O) stretching band from alginate is shifted from 1602 to 1612 cm^{-1} in oxidized CNF-alginate composite films with excess calcium removed. This has been attributed to the carboxylic groups on oxidized CNF linking alginate molecules to form a crosslinked network [34]. In the calcium-unsaturated samples we do not observe the same shift in signals. The calcium unsaturated samples gives $\nu(COO)_{asym}$ signals from 1602 to 1604 cm^{-1}, for the pure alginate gel and for composite gel of alginate and oxidized CNF, respectively. The $\nu(COO)_{asym}$ signal from *M. pyrifera* alginate powder devoid of calcium is at 1583 cm^{-1} and oxidized CNF devoid of calcium is 1606 cm^{-1}. The samples are, however, not directly comparable with [34], due to differences in sample preparation, charge density on oxidized CNF, fibril characteristics, alginate composition, and molecular weight. From our measurements, wedo not have strong evidence to support intermolecular interactions between oxidized CNF and *M. pyrifera* alginate mediated by calcium in the unsaturated calcium gels.

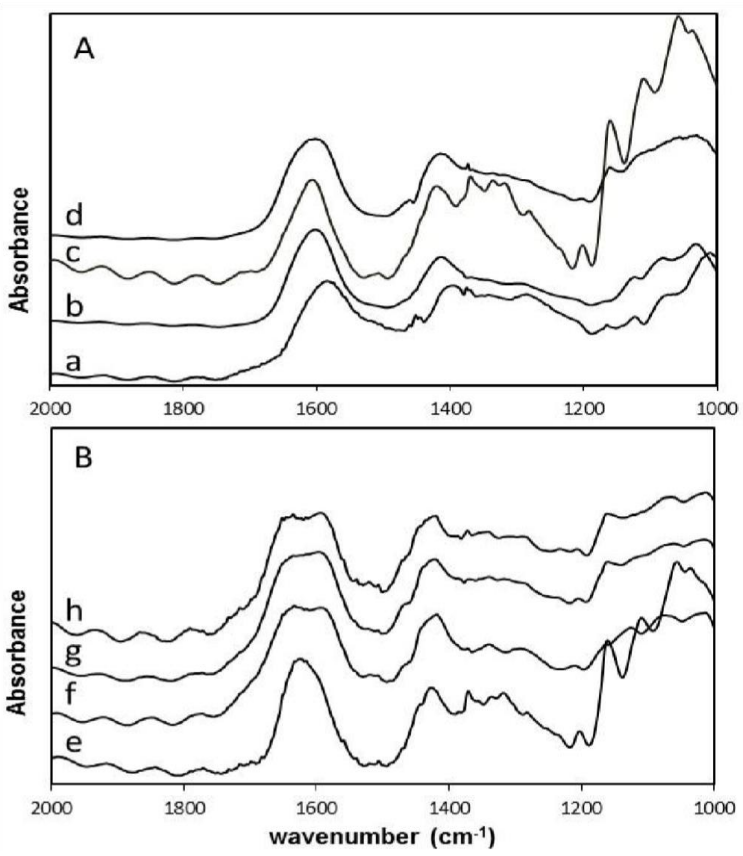

Figure 7. FT-IR spectra of freeze dried gel cylinders of 1.0% *M. pyr*. alginate and 0.75% CNF. (**A**) Calcium unsaturated samples and starting materials; (**B**) calcium saturated samples. *M. pyr.* powder, no calcium. (**a**); *M. pyr*, Ca-unsaturated (**b**); ox. CNF powder, no calcium (**c**); *M. pyr*. + ox CNF, Ca-unsaturated (**d**); Ox. CNF, Ca-saturated (**e**); *M. pyr.*, Ca-saturated (**f**); *M. Pyr.* + ox. CNF, Ca-saturated (**g**); and *M. Pyr.* + mechanically-fibrillated CNF, Ca-saturated (**h**).

The calcium saturated composite samples were strikingly different, displaying a split in the carboxyl groups (C=O) stretching band around 1600 cm^{-1}. This is not seen for the spectra of pure, calcium saturated oxidized CNF, but is observed for the pure alginate gel saturated with calcium. Our

hypothesis is that the splitting of the bands for the alginate-containing samples is due to differences in Ca^{2+} binding of carboxylic acid groups from mannuronic acid and guluronic acid. The G-block junction zones will tend to associate laterally at high calcium concentrations [35], and this may shift the signal from guluronic acid towards higher wavenumbers while the carboxylic group in mannuronic acid does not bind calcium in a specific manner and, therefore, does not shift.

As a last comment one should be careful to extrapolate results obtained on dried composite films to composite hydrogels as there will be large differences in both polymer concentration and ionic strengths. It would, therefore, be desirable to be able to study molecular interactions with methods where water interference is not an issue.

4. Conclusions

This study shows that tightly integrated composite hydrogels with tailored mechanical properties can be made from alginate and nanofibrillated cellulose in calcium saturated gels. The alginate contributes with elastic properties and increased mechanical resistance at large deformations. The cellulose nanofibrils reduces the syneresis of the alginate gels and contributes to increased resistance against compression at small deformations as seen by an increase in Young's modulus. The effect was increased using oxidized nanofibrils where composite gels also were volume stable upon saline treatments. No net increase in calcium concentration was found in the composite gels relative to the alginate gel alone. Additionally, no change in FT-IR spectra of the (C = O) stretching band was found for dried composite gels relative to dried alginate gel alone. Although no specific calcium binding event could be identified, we cannot rule out possible calcium mediated CNF-alginate or CNF-CNF interactions, as the oxidized cellulose fibrils by themselves form gels with calcium ions and as more than an additive effect on Young's modulus was seen for the combined system. The increase in Young's modulus was not seen when other relevant biopolymers were added to the alginate gel. Hence, mechanical properties of the composite hydrogels can be tailored by selecting alginates with varying block compositions and charge/concentration of cellulose fibrils. This is relevant for the use of this composite system in films and membranes in addition to the direct use of these composite hydrogels in, e.g., bioprinting and tissue engineering applications.

Acknowledgments: The authors thank Ingebjørg Leirset and Anne Marie Reitan (at RISE PFI) for skillful laboratory work. We would also like to thank Finn L. Aachman at NTNU-NT-Biotechnology for initiating the collaboration between PFI and NTNU. The work has been funded by the Research Council of Norway through the NANO2021 program, grant no. 228147-NORCEL: The Norwegian Nanocellulose Technology Platform and grant No. 221576-MARPOL: Enzymatic Modification and Upgrading of Marine Polysaccharides.

Author Contributions: Olav Aarstad, Berit Løkensgard Strand, Kristin Syverud and Ellinor Bævre Heggset conceived and designed the experiments; Ina Sander Pedersen, Olav Aarstad, and Sindre Hove Bjørnøy performed the experiments; Ina Sander Pedersen, Olav Aarstad, Sindre Hove Bjørnøy, Berit Løkensgard Strand, Ellinor Bævre Heggset, and Kristin Syverud analysed the data; Berit Løkensgard Strand, Olav Aarstad, Kristin Syverud, and Ellinor Bævre Heggset contributed with materials; and Berit Løkensgard Strand, Olav Aarstad, Ellinor Bævre Heggset and Kristin Syverud wrote the paper.

Conflicts of Interest: The authors declare no conflict of interest.

Appendix A

Table A1. Carbohydrate composition in the different CNF-samples.

Sample	Carbohydrate Composition (Weight %)				
	Glucan	**Xylan**	**Mannan**	**Arabinan**	**Galactan**
Softwood pulp	85.32	8.48	6.63	0.62	0.59
Mechanically fibrillated CNF	84.46	7.98	5.96	0.61	0.67
Oxidized CNF	66.25	6.63	2.67	0.03	0.00

The discrepancy in total monosaccharides between mechanically fibrillated CNF and oxidized CNF is due to conversion to uronic acids upon axidation in the oxidized sample, which were not quantified.

Table A2. Nanocellulose characteristics. All data, except residual fibres, are previously published in [25].

Sample	Charge Density (mmol/g)	Intrinsic Viscosity (mL/g)	Fibril Diameter (nm)	Fibril Length (μm)	Residual Fibres (%)
Mechanically fibrillated CNF	0.1	620	<100	>1	1.3
Oxidized CNF	0.9 [1]	450	<20	>1	28.5

[1] Aldehyde content was determined for the oxidized quality; 0.2 mmol/g CNF.

Appendix B

Table A3. Statistical outcomes, Figure 1: E = Young's modulus, standard deviation (SD), number of samples (*n*), and *p*-value (*p*) of samples compared to the respective pure alginate sample.

Sample	*n*	E (kPa), Mean	SD	*p* (%)	Syneresis (%), Mean	SD	*p* (%)
D. pot.	9	3.794	0.256	-	24.74	0.72	-
0.15% CNF	7	4.930	0.152	<0.01	22.95	0.79	0.08
0.30% CNF	6	5.134	0.399	<0.01	22.27	0.81	0.01
0.50% CNF	7	8.318	0.356	<0.01	15.60	1.01	<0.01
0.75% CNF	5	11.017	0.546	<0.01	13.53	1.11	<0.01
0.15% ox. CNF	7	5.036	0.272	<0.01	21.25	0.72	<0.01
0.30% ox. CNF	5	7.704	0.294	<0.01	17.78	0.50	<0.01
0.50% ox. CNF	6	12.786	0.549	<0.01	12.46	0.76	<0.01
0.75% ox. CNF	5	18.243	1.380	<0.01	7.17	1.45	<0.01
M. pyr.	7	*11.492*	*0.633*	-	*49.09*	*0.65*	-
0.15% CNF	8	14.895	0.743	<0.01	47.16	0.31	<0.01
0.30% CNF	7	17.437	1.259	<0.01	43.27	0.49	<0.01
0.50% CNF	5	18.273	0.779	<0.01	39.81	0.52	<0.01
0.75% CNF	5	24.297	2.950	<0.01	34.26	1.66	<0.01
0.15% ox. CNF	6	14.884	1.465	0.02	47.24	0.44	0.01
0.30% ox. CNF	5	19.210	1.504	<0.01	40.95	0.69	<0.01
0.50% ox. CNF	5	25.444	1.533	<0.01	31.83	2.20	<0.01
0.75% ox. CNF	5	36.060	3.666	<0.01	28.74	0.69	<0.01
L. hyp.	7	32.369	1.181	-	28.81	0.57	-
0.30% CNF	8	36.668	1.551	<0.01	27.26	0.87	<0.01
0.75% CNF	6	61.167	3.694	<0.01	20.20	0.42	<0.01
0.30% ox. CNF	8	42.991	1.970	<0.01	23.39	0.54	<0.01
0.75% ox. CNF	6	70.956	3.735	<0.01	15.82	1.18	<0.01

Table A4. Statistical outcomes, Figure 2: Rupture strength (mean), deformation (mean) standard deviation (SD), number of samples (*n*), and *p*-value (*p*) of samples compared to the respective pure alginate sample.

Sample	*n*	Rupture Strength (kg), Mean	SD	*p* (%)	Deformation (%), Mean	SD	*p* (%)
D. pot.	9	1.42	0.12	-	63.55	1.13	-
0.15% CNF	7	1.32	0.17	22.7	58.89	1.45	<0.01
0.30% CNF	6	1.23	0.14	2.45	57.70	1.39	<0.01
0.50% CNF	7	1.63	0.14	0.79	58.92	1.05	<0.01
0.75% CNF	5	1.66	0.11	0.35	58.67	0.96	<0.01
0.15% ox. CNF	7	1.15	0.03	0.02	55.70	0.60	<0.01
0.30% ox. CNF	5	1.35	0.02	19.1	56.56	0.35	<0.01
0.50% ox. CNF	6	1.59	0.05	0.79	55.44	0.61	<0.01
0.75% ox. CNF	5	1.39	0.09	66.3	51.63	1.35	<0.01
M. pyr.	*7*	4.09	0.56	-	71.76	1.09	-
0.15% CNF	8	5.50	0.42	0.03	71.40	1.02	50.3
0.30% CNF	7	5.31	0.20	0.03	69.27	1.08	0.11
0.50% CNF	5	5.15	0.30	0.35	69.25	0.62	0.06
0.75% CNF	5	5.43	0.31	0.07	66.99	0.68	<0.01
0.15% ox. CNF	6	4.16	0.07	75.4	67.41	0.38	<0.01
0.30% ox. CNF	5	4.07	0.04	95.2	63.99	0.34	<0.01
0.50% ox. CNF	5	4.54	0.22	12.1	62.96	0.59	<0.01
0.75% ox. CNF	5	4.25	0.17	55.0	59.71	0.67	<0.01
L. hyp.	7	5.11	0.81	-	64.38	1.89	-
0.30% CNF	8	4.25	0.15	<0.01	60.16	0.70	<0.01
0.75% CNF	6	5.38	0.45	<0.01	60.07	0.93	<0.01
0.30% ox. CNF	8	3.88	0.17	<0.01	57.18	0.81	<0.01
0.75% ox. CNF	6	4.38	0.41	<0.01	55.32	1.43	<0.01

Table A5. Statistical outcomes, Figure 4A,B: E = Young's modulus, standard deviation (SD), number of samples (*n*), and *p*-value (*p*) of samples compared to the 1.0% alginate sample for control polymers. *P*-values for CNF (*) are comparisons to the respective dry weight concentrations of alginate (1.30% and 1.75%).

Sample	*n*	E (kPa)	SD	*p* (%)	Syneresis (%)	SD	*p* (%)
1.0% M.pyr.	7	11.493	633	-	49.09	0.65	-
0.30% M.pyr.	8	15.916	1.285	<0.01	43.22	0.29	<0.01
0.30% dextran	9	12.168	0.967	14.2	44.81	0.90	<0.01
0.30% hyaluronan	8	13.150	0.710	0.08	38.01	0.60	<0.01
0.30% xanthan	8	14.829	0.330	<0.01	38.59	0.80	<0.01
0.75% M.pyr.	8	22.773	1.092	<0.01	34.31	0.51	<0.01
0.75% dextran	9	12.314	0.560	2.05	41.77	0.61	<0.01
0.75% hyaluronan	9	12.674	2.555	26.3	23.42	1.65	<0.01
0.75% xanthan	9	19.483	1.237	<0.01	26.57	0.79	<0.01
*0.30% CNF**	7	17.437	1.259	4.37	43.27	0.49	81.9
*0.30% ox. CNF**	5	19.210	1.504	0.18	40.95	0.69	<0.01
*0.75% CNF**	5	24.297	2.950	20.7	34.26	1.66	94.0
*0.75% ox. CNF**	5	36.060	3.666	<0.01	28.74	0.69	<0.01

Table A6. Statistical outcomes, Figure 4C,D: Statistical outcomes, Figure 4: E = Young's modulus, standard deviation (SD), number of samples (*n*), and *p*-value (*p*) of samples compared to the 1.0% alginate sample for other polymers CNF. *P*-values for CNF (*) are comparisons to the respective dry weight concentrations of alginate (1.30% and 1.75%).

Sample	***n***	**Rupture Strength (kg), Mean**	**SD**	***p* (%)**	**Deformation (%), Mean**	**SD**	***p* (%)**
1.0% M.pyr.	7	4.09	0.56	-	71.76	1.00	-
0.30% M.pyr.	8	5.99	0.29	<0.01	71.17	1.25	34.0
0.30% dextran	9	5.07	0.23	0.08	72.17	0.82	38.3
0.30% hyaluronan	8	3.69	0.60	21.0	74.86	3.87	6.76
0.30% xanthan	8	3.18	0.21	0.16	63.70	0.61	<0.01
0.75% M.pyr.	8	9.67	0.44	<0.01	69.74	1.24	0.64
0.75% dextran	9	4.81	0.41	1.37	70.79	1.31	13.6
0.75% hyaluronan	9	2.54	0.33	<0.01	64.02	1.78	<0.01
0.75% xanthan	9	2.81	0.08	<0.01	60.76	0.40	<0.01
*0.30% CNF**	7	5.31	0.20	0.04	69.27	1.08	1.06
0.30% ox. CNF*	5	4.07	0.04	<0.01	63.99	0.34	<0.01
0.75% CNF*	5	5.43	0.31	<0.01	66.99	0.68	0.015
0.75% ox. CNF*	5	4.25	0.17	<0.01	59.71	0.67	<0.01

Appendix C

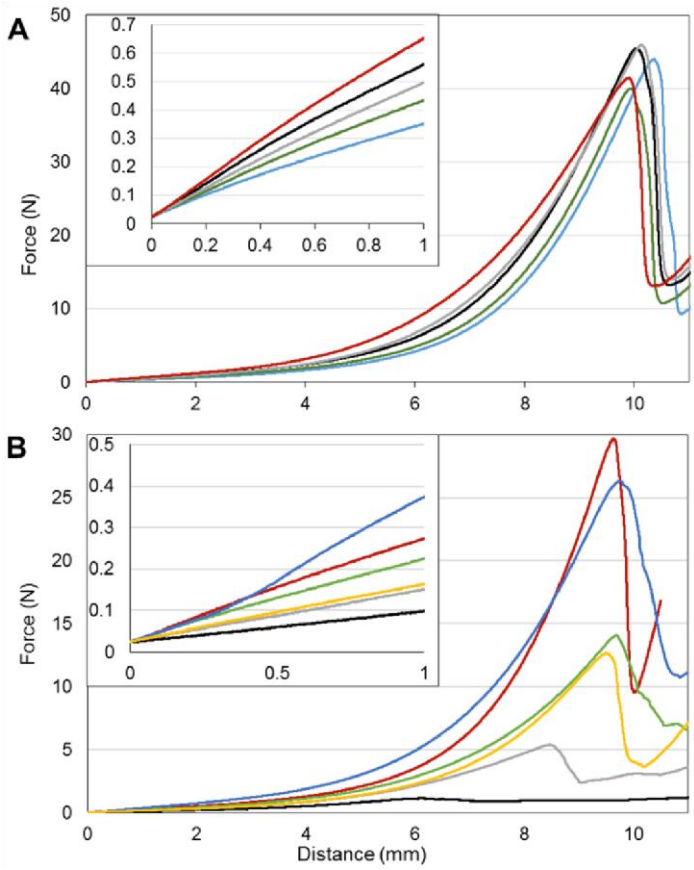

Figure A1. Stress-deformation curves of gel cylinders presented in Figures 1B and 2B (**A**) and Figure 3 (**B**). The inserted picture shows the initial compression where the gels display elastic behaviour. Young's modulus is calculated from 0.1 to 0.3 mm. (A) 1% (*w*/*v*) *M. pyr*. (—), 1% (*w*/*v*) *M. pyr*. + 0.15% (*w*/*v*) ox. CNF (—), 1% (*w*/*v*) *M. pyr*. + 0.30% (*w*/*v*) ox. CNF (—), 1% (*w*/*v*) *M. pyr* + 0.50% (*w*/*v*) ox. CNF (—) and 1% (*w*/*v*) *M. pyr* + 0.75% (*w*/*v*) ox. CNF (—); (B) 0.75% (*w*/*v*) *M. pyr* (—), 0.75% (*w*/*v*) ox. CNF (—), 0.375% (*w*/*v*) ox. CNF + 0.375% (*w*/*v*) *M. pyr* (—), 0.75% (*w*/*v*) ox. CNF + 0.2% (*w*/*v*) *M. pyr* (—), 0.75% (*w*/*v*) ox. CNF + 0.375% (*w*/*v*) *M. pyr* (—) and 0.75% (*w*/*v*) ox. CNF + 0.75% (*w*/*v*) *M. pyr* (—).

Appendix D

Table A7. FTIR peaks for $\nu(COO)_{asym}$ (cm^{-1}) for samples shown in Figure 7.

	Sample	Calcium Saturated Gel	ν(COO)asym (cm^{-1})
a	*M. pyr*. powder, no calcium	pristine	1583
b	1.0% (*w*/*v*) *M. pyr*	no	1602
c	ox. CNF, no calcium	pristine	1606
d	1% (*w*/*v*) *M. pyr* + 0.75% (*w*/*v*) ox. CNF	no	1604
e	0.75% (*w*/*v*) ox. CNF	yes	1624
f	1.0% (*w*/*v*) *M. pyr.*	yes	1589/1633 *
g	1.0% (*w*/*v*) *M. pyr*. + 0.75% (*w*/*v*) ox. CNF	yes	1593/1635 *
h	1.0% (*w*/*v*) *M. Pyr*. + 0.75% (*w*/*v*) mechanically fibrillated CNF	yes	1591/1639 *

* Two unresolved signals centered around 1620 cm^{-1}.

References

1. Markstedt, K.; Mantas, A.; Tournier, I.; Martinez Avila, H.; Haegg, D.; Gatenholm, P. 3D bioprinting human chondrocytes with nanocellulose-alginate bioink for cartilage tissue engineering applications. *Biomacromolecules* **2015**, *16*, 1489–1496. [CrossRef] [PubMed]
2. Muller, M.; öztürk, E.; Zenobi-Wong, M.; Arlov, O.; Gatenholm, P. Alginate sulfate-nanocellulose bioinks for cartilage bioprinting applications. *Ann. Biomed. Eng.* **2017**, *45*, 210–223. [CrossRef] [PubMed]
3. Nguyen, D.; Enejder, A.; Nguyen, D.; Forsman, A.; Ekholm, J.; Nimkingratana, P.; Brantsing, C.; Lindahl, A.; Simonsson, S.; Hagg, D.A.; et al. Cartilage tissue engineering by the 3d bioprinting of ips cells in a nanocellulose/alginate bioink. *Sci. Rep.* **2017**, *7*, 658. [CrossRef] [PubMed]
4. Haug, A.; Larsen, B.; Smidsrõd, O. Studies on the sequence of uronic acid residues in alginic acid. *Acta Chem. Scand.* **1967**, *21*, 691–704. [CrossRef]
5. Donati, I.; Holtan, S.; Morch, Y.A.; Borgogna, M.; Dentini, M.; Skjak-Braek, G. New hypothesis on the role of alternating sequences in calcium-alginate gels. *Biomacromolecules.* **2005**, *6*, 1031–1040. [CrossRef] [PubMed]
6. Grant, G.T.; Morris, E.R.; Rees, D.A.; Smith, P.J.C.; Thom, D. Biological interactions between polysaccharides and divalent cations—Egg-box model. *FEBS Lett.* **1973**, *32*, 195–198. [CrossRef]
7. Draget, K.I.; Ostgaard, K.; Smidsrod, O. Homogeneous alginate gels—A technical approach. *Carbohydr. Polym.* **1990**, *14*, 159–178. [CrossRef]
8. Martinsen, A.; Skjak-Braek, G.; Smidrsod, O. Alginate as immobilization material: I. Correlation between chemical and physical properties of alginate gel beads. *Biotechnol. Bioeng.* **1989**, *33*, 79–89. [CrossRef] [PubMed]
9. Rokstad, A.M.; Brekke, O.L.; Steinkjer, B.; Ryan, L.; Kollarikova, G.; Strand, B.L.; Skjak-Braek, G.; Lacik, I.; Espevik, T.; Mollnes, T.E. Alginate microbeads are complement compatible, in contrast to polycation containing microcapsules, as revealed in a human whole blood model. *Acta Biomater.* **2011**, *7*, 2566–2578. [CrossRef] [PubMed]
10. Lee, K.Y.; Mooney, D.J. Alginate: Properties and biomedical applications. *Prog. Polym. Sci.* **2012**, *37*, 227–258. [CrossRef] [PubMed]
11. Saito, T.; Nishiyama, Y.; Putaux, J.L.; Vignon, M.; Isogai, A. Homogeneous suspensions of individualized microfibrils from tempo-catalyzed oxidation of native cellulose. *Biomacromolecules* **2006**, *7*, 1687–1691. [CrossRef] [PubMed]
12. Dong, H.; Snyder, J.F.; Williams, K.S.; Andzelm, J.W. Cation-induced hydrogels of cellulose nanofibrils with tunable moduli. *Biomacromolecules* **2013**, *14*, 3338–3345. [CrossRef] [PubMed]
13. Zander, N.E.; Dong, H.; Steele, J.; Grant, J.T. Metal cation cross-linked nanocellulose hydrogels as tissue engineering substrates. *ACS Appl. Mater. Interfaces* **2014**, *6*, 18502–18510. [CrossRef] [PubMed]
14. Lin, N.; Huang, J.; Dufresne, A. Preparation, properties and applications of polysaccharide nanocrystals in advanced functional nanomaterials: A review. *Nanoscale* **2012**, *4*, 3274–3294. [CrossRef] [PubMed]
15. Depan, D.; Misra, R.D.K. The interplay between nanostructured carbon-grafted chitosan scaffolds and protein adsorption on the cellular response of osteoblasts: Structure-function property relationship. *Acta Biomater.* **2013**, *9*, 6084–6094. [CrossRef] [PubMed]
16. Yim, E.K.; Leong, K.W. Significance of synthetic nanostructures in dictating cellular response. *Nanomed. Nanotechnol. Biol. Med.* **2005**, *1*, 10–21. [CrossRef] [PubMed]
17. Zhang, L.J.; Webster, T.J. Nanotechnology and nanomaterials: Promises for improved tissue regeneration. *Nano Today* **2009**, *4*, 66–80. [CrossRef]
18. Park, M.; Lee, D.; Hyun, J. Nanocellulose-alginate hydrogel for cell encapsulation. *Carbohydr. Polym.* **2015**, *116*, 223–228. [CrossRef] [PubMed]
19. Engler, A.J.; Sen, S.; Sweeney, H.L.; Discher, D.E. Matrix elasticity directs stem cell lineage specification. *Cell* **2006**, *126*, 677–689. [CrossRef] [PubMed]
20. Aarstad, O.; Tøndervik, A.; Sletta, H.; Skjåk-Bræk, G. Alginate sequencing: An analysis of block distribution in alginates using specific alginate degrading enzymes. *Biomacromolecules* **2012**, *13*, 106–116. [CrossRef] [PubMed]

21. Shinoda, R.; Saito, T.; Okita, Y.; Isogai, A. Relationship between length and degree of polymerization of tempo-oxidized cellulose nanofibrils. *Biomacromolecules* **2012**, *13*, 842–849. [CrossRef] [PubMed]
22. Araki, J.; Wada, M.; Kuga, S. Steric stabilization of a cellulose microcrystal suspension by poly(ethylene glycol) grafting. *Langmuir* **2001**, *17*, 21–27. [CrossRef]
23. Saito, T.; Isogai, A. Tempo-mediated oxidation of native cellulose. The effect of oxidation conditions on chemical and crystal structures of the water-insoluble fractions. *Biomacromolecules* **2004**, *5*, 1983–1989. [CrossRef] [PubMed]
24. Chinga-Carrasco, G.; Averianova, N.; Kondalenko, O.; Garaeva, M.; Petrov, V.; Leinsvang, B.; Karlsen, T. The effect of residual fibres on the micro-topography of cellulose nanopaper. *Micron* **2014**, *56*, 80–84. [CrossRef] [PubMed]
25. Heggset, E.B.; Chinga-Carrasco, G.; Syverud, K. Temperature stability of nanocellulose dispersions. *Carbohydr. Polym.* **2017**, *157*, 114–121. [CrossRef] [PubMed]
26. Mørch, Y.A.; Holtan, S.; Donati, I.; Strand, B.L.; Skjåk-Bræk, G. Mechanical properties of c-5 epimerized alginates. *Biomacromolecules* **2008**, *9*, 2360–2368. [CrossRef] [PubMed]
27. Smidsrød, O.; Haug, A. Properties of poly(1,4-hexuronates) in the gel state. Ii. Comparison of gels of different chemical composition. *Acta Chem. Scand.* **1972**, *26*, 79–88.
28. Donati, I.; Mørch, Y.A.; Strand, B.L.; Skjåk-Bræk, G.; Paoletti, S. Effect of elongation of alternating sequences on swelling behavior and large deformation properties of natural alginate gels. *J. Phys. Chem.* **2009**, *113*, 12916–12922. [CrossRef] [PubMed]
29. Aarstad, O.; Strand, B.L.; Klepp-Andersen, L.M.; Skjak-Braek, G. Analysis of G-block distributions and their impact on gel properties of in vitro epimerized mannuronan. *Biomacromolecules* **2013**, *14*, 3409–3416. [CrossRef] [PubMed]
30. Sirvio, J.A.; Kolehmainen, A.; Liimatainen, H.; Niinimaki, J.; Hormi, O.E.O. Biocomposite cellulose-alginate films: Promising packaging materials. *Food Chem.* **2014**, *151*, 343–351. [CrossRef] [PubMed]
31. Xie, M.; Olderøy, M.Ø.; Zhang, Z.; Andreassen, J.-P.; Strand, B.L.; Sikorski, P. Biocomposites prepared by alkaline phosphatase mediated mineralization of alginate microbeads. *RSC Adv.* **2012**, *2*, 1457–1465. [CrossRef]
32. Syverud, K.; Pettersen, S.R.; Draget, K.; Chinga-Carrasco, G. Controlling the elastic modulus of cellulose nanofibril hydrogels-scaffolds with potential in tissue engineering. *Cellulose* **2015**, *22*, 473–481. [CrossRef]
33. Mørch, Y.A.; Donati, I.; Strand, B.L.; Skjåk-Bræk, G. Effect of Ca^{2+}, Ba^{2+}, and Sr^{2+} on alginate microbeads. *Biomacromolecules* **2006**, *7*, 1471–1480. [CrossRef] [PubMed]
34. Lin, N.; Bruzzese, C.; Dufresne, A. Tempo-oxidized nanocellulose participating as crosslinking aid for alginate-based sponges. *Appl. Mater. Interfaces* **2012**, *4*, 4948–4959. [CrossRef] [PubMed]
35. Stokke, B.T.; Draget, K.I.; Smidsrød, O.; Yuguchi, Y.; Urakawa, H.; Kajiwara, K. Small-angle X-ray scattering and rheological characterization of algiate gels. 1. Ca-alginate gels. *Macromolecules* **2000**, *33*, 1853–1863. [CrossRef]